Chapter 12

Past Antarctic ice sheet dynamics (PAIS) and implications for future sea-level change

Florence Colleoni[1], Laura De Santis[1], Tim R. Naish[2], Robert M. DeConto[3], Carlota Escutia[4], Paolo Stocchi[5,12], Gabriele Uenzelmann-Neben[6], Katharina Hochmuth[7], Claus-Dieter Hillenbrand[8], Tina van de Flierdt[9], Lara F. Pérez[8], German Leitchenkov[10,11], Francesca Sangiorgi[12], Stewart Jamieson[13], Michael J. Bentley[13], David J. Wilson[14] and the PAIS community*

[1]National Institute of Oceanography and Applied Geophysics – OGS, Sgonico, Italy, [2]Antarctic Research Centre, Victoria University of Wellington, Wellington, New Zealand, [3]Department of Geosciences, University of Massachusetts, Amherst, Amherst, MA, United States, [4]Andalusian Institute of Earth Sciences, CSIC and Universidad de Granada, Armilla, Spain, [5]NIOZ - Royal Netherlands Institute for Sea Research, Coastal Systems Department (TX), and Utrecht University, Den Burg, the Netherlands, [6]Alfred Wegener Institute Helmholtz Center for Polar and Marine Research, Bremerhaven, Germany, [7]School of Geography, Geology and the Environment, University of Leicester, Leicester, United Kingdom, [8]British Antarctic Survey, Cambridge, United Kingdom, [9]Department of Earth Science and Engineering, Imperial College London, London, United Kingdom, [10]Institute for Geology and Mineral Resources of the World Ocean, St. Petersburg, Russia, [11]Institute of Earth Sciences, St. Petersburg State University, St. Petersburg, Russia, [12]Laboratory of Palaeobotany and Palynology, Department of Earth Sciences, Marine Palynology and Paleoceanography, Utrecht University, Utrecht, The Netherlands, [13]Department of Geography, Durham University, Durham, United Kingdom, [14]Institute of Earth and Planetary Sciences, University College London and Birkbeck, University of London, London, United Kingdom

12.1 Research focus of the PAIS programme

Ice sheet and sea-level reconstructions from the past 'warmer-than-present' climates of the last 34 million years provide powerful insights into the long-term response of the polar ice sheets to climate changes projected for the

*List of authors is shown before the references.

Antarctic Climate Evolution. DOI: https://doi.org/10.1016/B978-0-12-819109-5.00010-4

21st century and onward. Proximal geological evidence shows the onset of large-scale Antarctic glaciations occurred around the Eocene/Oligocene Transition at approximately 34 Ma (EOT, e.g. Barrett, 1989; Coxall et al., 2005; Escutia et al., 2011; Galeotti et al., 2016, 2021 (this volume); Hambrey et al., 1991; Passchier et al., 2013, 2016). Since then, the Antarctic Ice Sheet (AIS) evolution and variability, recorded in the direct geological archives, have been widely compared with the benthic oxygen isotope proxy records of deep-water temperature and global ice volume from far-field deep ocean locations (e.g. De Vleeschouwer et al., 2017; Zachos et al., 2001). Together, they suggest fluctuations in ice volume and ice sheet extent that can be driven by changes in atmospheric CO_2 level and astronomical forcing (Galeotti et al., 2016; Hansen et al., 2015; Levy et al., 2019; Naish et al., 2001, 2009a; Pälike et al., 2006; Patterson et al., 2014). Looking at the broad picture, the EOT really marked the transition into an ice house world (Miller et al., 1991; 2020b; Westerhold et al., 2020). As the initial cryosphere evolved, only one pole, the South Pole, hosted a continental-size ice sheet. Geological evidence from the Arctic revealed that small ice-sheets or ice caps may have formed in the Northern high latitudes as early as the Eocene (e.g. Eldrett et al 2007; Tripati and Darby, 2018). Then, along with the gradual decrease in atmospheric CO_2 level (Fig. 12.1A), Greenland glaciated from the Late Miocene, rapidly followed by episodic and extensive glaciations of most of the high-latitude Arctic margins, after the onset of Northern Hemisphere glaciations 2.7 Ma (e.g. Thiede et al., 2011).

During the past 34 million years, changes in global climate and polar ice volume have been paced by orbital forcing – the Milankovitch cycles. These regular glacial–interglacial cycles, which are amplified by internal Earth system feedbacks, occur on a background of secular change over millions of years driven by global plate tectonics and the carbon cycle (Fig. 12.1). Rapid stepwise transitions between climate states (e.g. EOT) correspond to thresholds in the Earth system often linked to a combination of tectonic reorganisation, atmospheric greenhouse gas composition and extreme astronomical forcing (Levy et al., 2019; Wilson et al., 2021; Zachos et al., 2001, 2008). Our knowledge of the evolution of the AIS and its influence on global climate is now widely documented by proximal ice and sediment core records (e.g. Barrett, 2007; Bereiter et al., 2015; Escutia et al., 2019; EPICA Community Members, 2006; Levy et al., 2019; McKay et al., 2016).

The circum-Antarctic seismic stratigraphic records of the continental margins reveal erosive unconformities indicative of at least six main periods of massive AIS advances (e.g. Bart and De Santis, 2012; Brancolini et al., 1995a, 1995b; Cooper et al., 1999, 2011; De Santis et al., 1999; Donda et al., 2007; Gohl et al., 2013; Gulick et al., 2017; Kristoffersen and Jokat, 2008; Larter et al., 1997; Lindeque et al., 2016; Steinhauff and Webb, 1987). Not all the unconformities have been dated but Hochmuth et al. (2019, 2020) recently provided the first attempt of pan-Antarctic correlation of the various regional

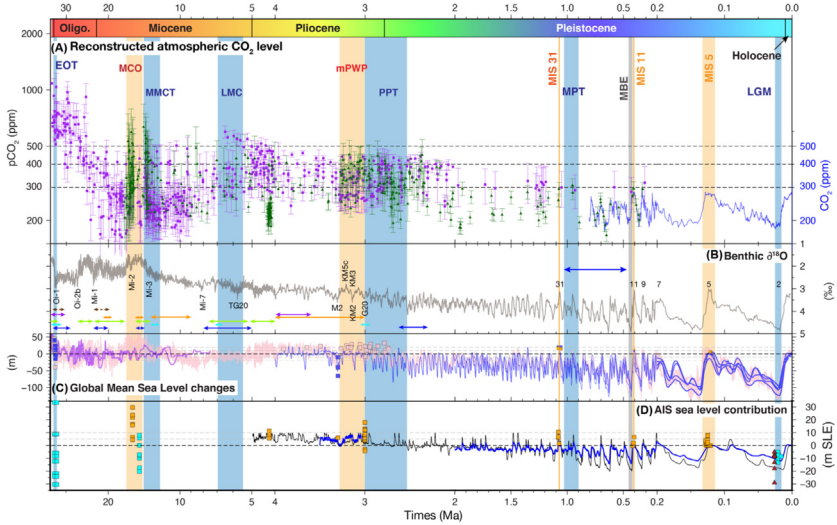

FIGURE 12.1 Proxies and simulations synthesis over the past 34 million years. Note that the time scale is logarithmic. (A) Reconstructed atmospheric p[CO_2] levels are based on alkenone (Badger et al., 2013a, 2013b; Pagani et al., 2005, 2010, 2011; Seki et al., 2010; Super et al., 2018; Zhang et al., 2013) and on boron measurements (Bartoli et al., 2011; Foster et al., 2012; Greenop et al., 2014; Honisch et al., 2009; Martinez-Boti et al., 2015). Late Pleistocene atmospheric CO_2 levels are based on the Antarctic ice core composite record from Bereiter et al. (2015); (B) Deep sea benthic $\delta^{18}O$ record from Zachos et al. (2001a, 2008). Marine isotope stages (glacials and interglacials) discussed or named in the chapter are indicated and based on Miller et al. (1991) for the Oligocene and Miocene, on Haywood et al. (2016) for the Pliocene and on Lisiecki and Raymo (2005) for the Pleistocene. Note that marine isotopes stages EOT-1 (~34.46−33.9 Ma) and EOT-2 (33.7 Ma) are not indicated. Seismic stratigraphic unconformities from different Antarctic sectors are reported with arrows, based on Hochmuth et al. (2020) and references therein (Ross Sea: dark blue; Wilkes Land: green; Weddell Sea: cyan; Amundsen Sea: orange; Cosmonaut Sea: brown; Prydz Bay: purple); (C) Reconstructed (pink, purple) and simulated (blue) global mean sea level changes (GMSL). Proxy-based reconstructions: benthic $\delta^{18}O$ (Miller et al., 2020a) from EOT to present, backstripped sequence stratigraphy from New Jersey from EOT until the Late Miocene (Kominz et al., 2008; Miller et al., 2005). For the EOT (pink solid squares): Bohaty et al. (2012); Hauptvogel and Passchier (2012); Katz et al. (2008), Lear et al. (2008); Miller et al. (2009); Pekar and Christie-Blick (2008); Pekar et al. (2002); Stocchi et al. (2013). For the Pliocene: converted benthic $\delta^{18}O$ record from Dumitru et al. (2019) until the PPT. Pink squares correspond to reconstructed Pliocene highstands (Dumitru et al., 2019; Dwyer and Chandler, 2009; Kulpecz et al., 2009; Miller et al., 2012; Naish and Wilson, 2009b; Sosdian and Rosenthal, 2009; Wardlaw and Quinn, 1991; Winnick and Caves, 2015) and to M2 glaciation (Dwyer and Chandler, 2009; Miller et al., 2005; Naish and Wilson, 2009b). For Pleistocene: sea level reconstructions are taken from Hearty et al. (2020); Sandstrom et al. (2021) for MIS 31 (uncorrected from GIA and dynamic topography) and from Raymo and Mitrovica (2012) and Roberts et al. (2012) for MIS 11. For the last 400 kyrs, reconstructed curves of sea level changes are from Waelbroeck et al. (2002) and from Rohling et al. (2009). For MIS5, palaeoshorelines data are from the compilation in Dutton et al. (2015) and references therein. Simulated GMSL changes are from Bintanja et al. (2005), de Boer et al. (2015) and Stap et al. (2017), and from Raymo et al. (2006) for MIS 31 (blue squares); (D) Simulated

(*Continued*)

seismic unconformities (Fig. 12.1B). These seismic unconformities likely correspond to: early Antarctic glaciations after the EOT (e.g. Galeotti et al., 2016), a transient glaciation at Oligocene-Miocene boundary ~23–21 Ma (e.g. Naish et al., 2001, 2021, this volume; summarised in Wilson and Luyendyk, 2009), ice sheet re-advance at the end of the Mid-Miocene Climatic Optimum (MCO) about 15.8–14.2 Ma (e.g. Levy et al., 2016), the cooling and expansion of the East Antarctic Ice Sheet (EAIS) at the Middle Miocene Climate Transition (MMCT) ~13.8 Ma (e.g. Levy et al., 2016; Lewis et al., 2007; 2008; Pierce et al., 2017), cooling after a period of warmth known as the Late Miocene Cooling ~8–5 Ma (LMC) (Gulick et al., 2017; Herbert et al., 2016; McKay et al., 2009) and cooling and expansion of marine-based ice during the Plio-Pleistocene Transition (PPT) 3–2.5 Ma (McKay et al., 2012a; Naish et al., 2009a; Patterson et al., 2014) and possibly to the Mid-Pleistocene Transition ~1 Ma (e.g. O'Brien et al., 2007). These periods evidenced by positive excursions in the deep sea benthic $\delta^{18}O$ isotope records (Fig. 12.1B) correspond to episodes of global cooling and ice volume growth periods, generally associated with a decline in atmospheric CO_2 below

◀ Antarctic ice sheet melting contributions (metre Sea Level Equivalent, m SLE) to GMSL changes are from ice sheet simulations (squares and curves) and from Glacio-isostatic-Adjustment simulations (dark red triangles). Note that some of the reported simulated ice volumes do not refer to volumes above floatation. For the EOT: DeConto and Pollard (2003), Gasson et al (2014), Ladant et al. (2014), Liakka et al. (2014), Pollard and DeConto (2005), Wilson et al. (2013). For the Miocene: Colleoni et al. (2018b), Gasson et al. (2016), Langebroek et al. (2009), Stap et al. (2019). For Early Pliocene: Pollard and DeConto (2009, transient and black line), Golledge et al. (2017a, orange squares). For mPWP to Late Pliocene: de Boer et al. (2013, transient blue line), Pollard and DeConto (2009, transient black line). Orange squares come from Tan et al. (2017) for M2 glaciation and remaining symbols are for the mPWP considering Austermann et al. (2015), de Boer et al. (2015), DeConto and Pollard (2016), Dolan et al. (2018), Gasson et al. (2015), Pollard and DeConto (2012), Yan et al. (2016). When simulations were run with averaged mPWP climatic conditions, orange squares are indicatively plotted at 3 Ma. For the entire Pleistocene: blue line – de Boer et al. (2014) and black line – Pollard and DeConto (2009). For MIS 31: Beltran et al. (2020), de Boer et al. (2017a), DeConto et al. (2012). For MIS 11: Mas e Braga et al. (2021), Sutter et al. (2019), Tigchelaar et al. (2018). For MIS 5: Colleoni et al. (2018b), de Boer et al. (2015), DeConto and Pollard (2016), Goelzer et al. (2016), Huybrechts (2002), Pollard and DeConto (2012), Quiquet et al. (2018), Sutter et al. (2016), Sutter et al. (2019), Tigchelaar et al. (2018). For LGM based on ice sheet simulations: Brigg et al. (2014), Colleoni et al. (2018b), de Boer et al. (2013), Golledge et al. (2012), Golledge et al. (2014), Mackintosh et al. (2011), Pollard et al. (2016), Philippon et al. (2006), Quiquet et al. (2018), Sutter et al. (2019). For LGM based on glacio-isostatic adjustment simulations: Argus et al. (2014), Gomez et al. (2013), Ivins and James (2005), Ivins et al. (2013), Lambeck et al. (2014), Peltier (2004), Whitehouse et al. (2012b). Cold periods of interest in this chapter are indicated with blue bars: *EOT*, Eocene-Oligocene Transition; *MMCT*, Mid-Miocene Climatic Transition; *LMC*, Late Miocene Cooling; *PPT*, Plio-Pleistocene Transition; *MPT*, Mid-Pleistocene Transition; *MBE*, mid-Brunhes Event; *LGM*, Last Glacial Maximum. Warm periods mentioned in this chapter are indicated with orange bars: *MCO*, Mid-Miocene Climatic Optimum; *mPWP*, mid-Pliocene Warm Period, MIS 31, MIS 11, MIS 5. Please refer to the online version of this figure for enhanced resolution and magnification.

a threshold (Fig. 12.1A) for triggering the expansion of terrestrial and/or marine-based ice and/or the onset of perennial sea-ice.

Between these cooling periods, multi-proxy global climatic reconstructions and proximal Antarctic geological climate and ice sheet reconstructions provide evidence for intense and/or brief warm periods during which:

- atmospheric CO_2 levels, surface temperatures and global sea level rose well above present-day levels during the MCO (17−15 Ma) and the middle Pliocene Warm Period (mPWP, 3.3−3 Ma) (see Miller et al., 2012 for a review); both periods were characterised by CO_2 concentrations higher than 400 ppm and up to 800 ppm for some specific intervals of the MCO (see Fig. 12.1A and references therein).
- atmospheric CO_2 levels were near pre-industrial levels, i.e. around 300 ppm but were associated with warmer global surface temperatures and higher sea-levels than today during the 'super interglacials' of the Pleistocene. This was likely driven by astronomical forcing. Examples include marine isotope stage (MIS) 31 (1.081−1.062 Ma), and specific warm Late Pleistocene interglacials such as MIS 11 (425−395 ka) and MIS 5e (130−116 ka) (e.g. Dutton et al., 2015; Miller et al., 2020b).

These past warm periods are policy-relevant as they provide accessible examples of how the AIS responded to warmer-than-present global temperatures, comparable to those projected for the coming decades to centuries (IPCC AR5, 2013; IPCC SROCC, 2019). However, using these past warm periods to inform our understanding of the AIS sensitivity under different atmospheric CO_2 levels remains a challenge, in part because Earth system boundary conditions were subtly different than today, and the duration and intensity of these past warm periods was highly variable (e.g. Bracegirdle et al., 2019; Colleoni et al., 2018a; DeConto and Pollard, 2016; Dutton et al., 2015; Noble et al., 2020).

For example, the duration of those past warm periods differs from about 2 million years for the MCO, approximately 300 thousand years for the mPWP to a few millennia for some Pleistocene interglacials. Thus, an approach focusing on specific MCO and mPWP glacial-interglacial cycles and interglacials (with similarities to our present interglacial) is being developed. For example, the Pliocene Model Intercomparison Project community is focussing its ongoing mPWP model-data comparison on the M2-KM5c (3.264−3.205 Ma) and KM5c-KM2 (3.205−3.130 Ma) intervals (Fig. 12.1B) (Haywood et al., 2016). By using more appropriate forcing and boundary conditions for climate model simulations, discrepancies between models and data generally decrease (e.g. Otto-Bliesner et al., 2017).

In most simulations of future ice sheet evolution, model projections typically extend only until the policy horizon of CE (Common Era) 2100. However, some ice sheet models have run projections out as far as CE 2500 (e.g. Clark et al., 2016; DeConto and Pollard, 2016; Golledge et al., 2015).

The recent IPCC special report on 'Ocean and Cryosphere in a Changing Climate' (IPCC ROCC, 2019) utilises these projections and the results of a structured expert judgement approach (Bamber et al., 2019) to present projections to CE 2300, that to some extent account for the long-term thermodynamical response of the Greenland and Antarctic ice sheets and related instabilities (e.g. DeConto and Pollard, 2016; Golledge et al., 2015). Palaeoclimatic changes are often considered at timescales of tens of millennia to millennia and, in a few archives, at sub-millennial timescale. At such timescales, past reconstructions can inform long-term projections over a few millennia (see Golledge et al., 2020 for a review), but some refinements at sub-millennial timescales to investigate some abrupt events of the near past are necessary to reconcile with the projections.

During past warm periods global paleogeography, paleotopography and paleobathymetry can differ substantially from today. Periods prior to the Plio-Pleistocene Transition (3.0−2.5 Ma) were characterised by a very different continental and oceanic configuration that yielded changes in the proportion of emerged lands and their locations. This affected surface elevation, oceanic gateways and bathymetry, which in turn impacted ocean and atmospheric circulation (e.g. Dowsett et al., 2016; Herold et al., 2008; Huang et al., 2017; Kennedy et al., 2015; von der Heydt et al., 2016), on global mean sea level changes (e.g. Miller et al., 2020b) and on heat transport compared to modern conditions. The Antarctic continent and its surface elevation have also evolved throughout the Cenozoic, with important consequences for ice sheet behaviour (e.g. Colleoni et al., 2018b; Paxman et al., 2020). Thus, direct comparison between the past and future AIS sensitivity to high levels of atmospheric greenhouse gases is not straightforward.

Most of the efforts of the PAIS programme, and its predecessor, the Antarctic Climate Evolution (ACE) programme, focused on the past warm periods (e.g. MCO, mPWP, warm interglacials of the Pleisotcene) (Fig. 12.1). More specifically, ice sheet and climate simulations of the MCO emerged during the PAIS programme lifetime. Within its programme, PAIS promoted collaborative work within six specific sub-committees that addressed the following topics for almost all of the warm periods listed above:

- Paleoclimate records from the Antarctic Margin and Southern Ocean (PRAMSO);
- Paleotopographic-Paleobathymetric Reconstructions;
- Subglacial Geophysics;
- Ice Cores and Marine Core Synthesis;
- Recent Ice Sheet Reconstructions;
- Deep-Time Ice Sheet Reconstructions.

Scientific advances related to each of these topics are extensively described in the previous chapters of this book. Many research projects that were initiated within the ACE programme concluded during the PAIS

programme. Many of their findings continue to have a significant impact on the community of Antarctic researchers and well beyond. In the following sections, we highlight some of the key findings that have advanced our understanding of the Antarctic Ice Sheet dynamics, instabilities and thresholds during past warm periods. We conclude with a discussion of the PAIS legacy, and highlight emerging issues, knowledge gaps, needs and challenges to be addressed within the next decade by the observational and modelling communities.

12.2 Importance of evolving topography, bathymetry, erosion and pinning points

Ice−sheet−ocean−bedrock interactions are of major importance for understanding the dynamics of the AIS (Colleoni et al., 2018a; Mengel and Levermann, 2014; Paxman et al., 2020; Whitehouse et al., 2019). Surface and basal boundary conditions determine the characteristics and regime of the ice flow. At the base of a terrestrial or marine-based ice sheet, the geothermal heat flux, the morphology as well as the nature of the bed (hard rock or soft sediments), affect the sliding of the ice, generate heat and yield basal meltwater. When the ice sheet advances, it erodes its bed and carries sediment. Eroded material is released into ice shelf cavities and onto the continental shelf at the grounding zone where the ice sheet floats, disconnecting from its bed. Some of this glacigenic detritus finds its way via glacial troughs and via channels across the continental slope and rise and ultimately to the abyssal plain. Some eroded material is also carried by icebergs and deposited offshore as Iceberg Rafted Debris (IBRD). These sediments, preserved in a wide range of marine environments, provide a valuable archive of past ice sheet dynamics and coeval oceanic and atmospheric conditions.

The AIS substantially expanded $\sim$34 Ma and since then has advanced and retreated numerous times (see Galeotti et al., 2016). As a result, the morphology of the bed below the ice sheet evolved considerably. Seismic stratigraphic records from the Antarctic continental margins (e.g. Cooper et al., 1991; De Santis et al.; 1999; Eittreim et al., 1995; Gohl et al., 2013; Huang and Jokat, 2016; Whitehead et al., 2006) clearly show that the shallow continental shelves have been prograding northward through time. Sediment isopach (thickness) reconstructions indicate that much of the sediments have accumulated, and accreted, along the Antarctic continental slope and rise (see references in Hochmuth and Gohl, 2019; Hochmuth et al., 2020 for circum-Antarctic review and reconstructions), implying that a large volume of material has been eroded and removed from inland regions since the onset of continental glaciation (e.g. Hochmuth et al., 2020; Paxman et al., 2019; Wilson et al., 2012).

The most recent circum-Antarctic reconstructions show that the morphology of the bed has changed substantially over the past 34 million years (Fig. 12.2). At the EOT, most of the West and East Antarctic sectors that are currently below sea level were instead above sea level (Paxman et al., 2019; Wilson et al., 2012) (Fig. 12.2). With time, tectonic subsidence and erosion caused those sectors to deepen below sea level. These reconstructions have significant implications for the understanding of the evolution of the AIS and for its ice flow. It is, indeed, much easier to grow an ice sheet on a terrestrial surface than on a submarine bed. On such a restored and emergent topography, simulated Antarctic glaciations at the EOT produce a total ice volume greater than today and similar to that of the Last Glacial Maximum (LGM, ~21 ka) (Ladant et al., 2014; Wilson et al., 2013), even though atmospheric CO_2 levels were much higher than today, ranging from around 780–560 ppm (Fig. 12.1A). At the EOT, the ice sheet did not expand across the continental shelves, because the ocean temperatures were too warm (e.g. Bjill et al., 2018; DeConto et al., 2007). In fact, geological evidence from the Antarctic Peninsula documents a faunal turnover from species adapted to temperate waters (+5°C) to species adapted to cold waters through the EOT (Buono et al., 2019; Kriwet et al., 2016) (see from Galeotti et al., 2021, this volume).

Continental shelf evolution was critical for advances of the AIS across the marine realm after the EOT (e.g. Paxman et al., 2020). The evolution of the shallow continental shelves around Antarctica was connected to the evolution of the topography in the continent's interior. Various reconstructions (Brancolini et al., 1995a, 1995b; Cooper et al., 1991; Eittreim et al., 1995; Hochmuth et al., 2020; Huang and Jokat, 2016; Paxman et al., 2019) suggest that in most of the sectors, the continental shelf edge was located further south than today (Fig. 12.2) and then prograded seaward over time (e.g. Cooper et al., 1991; De Santis et al., 1999; Huang et al., 2014). The stratigraphic records combined with existing Antarctic deep drilling sites suggest that the majority of the continental margin expansion occurred prior to the Pliocene (De Santis et al., 1995, 1999, Hochmuth and Gohl, 2019; McKay et al., 2021), although in some sectors (e.g. Amundsen Sea, Gohl et al., 2013; Prydz Bay, O'Brien et al., 2007; Wilkes Land, Escutia et al., 2011), progradation of the margin was still important throughout the Pliocene (see from McKay et al., 2021, this volume). The Middle to Late Miocene was a period of transition during which the Antarctic ice sheet margin advanced into a cooling ocean, grounding on the continental shelf (Levy et al., 2021, this volume). This is also when prominent marine-based sectors of the AIS developed (e.g., Uenzelmann-Neben, 2019), especially in West Antarctica (Bart, 2003). Numerical ice sheet simulations using new Antarctic Mid-Miocene palaeogeographies, showed that during this period, the AIS became increasingly sensitive to oceanic conditions (Colleoni et al., 2018b), resulting in large glacial-interglacial changes in ice volume (Gasson et al., 2016).

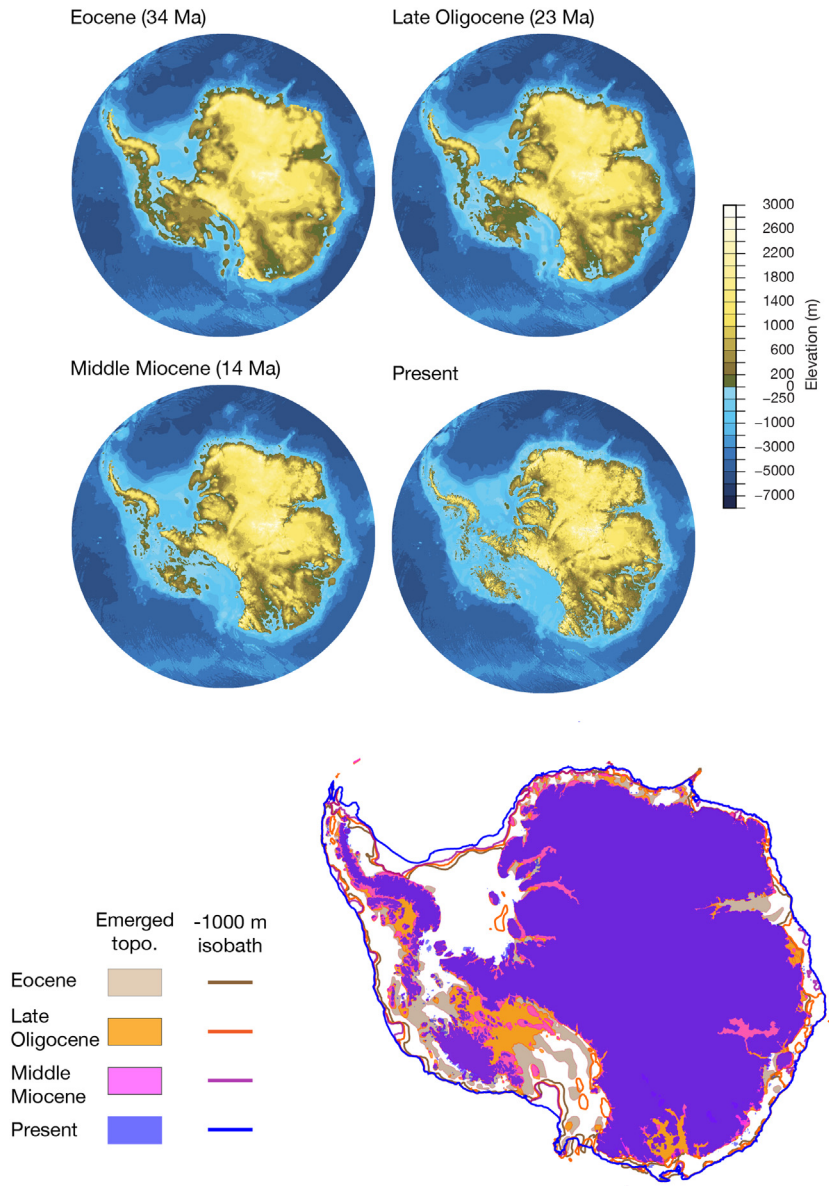

FIGURE 12.2 Top: Pan-Antarctic isostatically-relaxed palaeogeographic reconstructions from Paxman et al. (2019) for the Eocene (34 Ma), the Late Oligocene (23 Ma), the Middle Miocene (14 Ma) and BEDMAP2 for modern pan-Antarctic geography (Fretwell et al., 2013). Bottom: superimposed Eocene (brown), Late Oligocene (orange), Middle Miocene (pink) and modern (blue) emerged topography. Isobath at − 1000 m for each time slices is also indicated.

From the Pliocene onward, the Antarctic continental margin evolved very little. Erosion of the continental interior appears to have been less influential on the ice sheet since the Pliocene than during the earlier Oligocene and Miocene (Naish et al., 2021, this volume), and the terrestrial ice sheet became more stable (Gulick et al., 2017; Kim et al., 2018; McKay et al., 2012a; Passchier et al., 2011). However, fluctuations of marine-based ice in deep subglacial basins still occurred, especially when atmospheric CO_2 was between 400 and 300 ppm, during the early and middle Pliocene between 5 and 3 Ma (Bertram et al., 2018; Cook et al., 2013, 2014; Hansen et al., 2015; Levy et al., 2021, this volume; Naish et al., 2009a; Patterson et al., 2014; Pollard and DeConto, 2009; Reinardy et al., 2015). The relative stability of the terrestrial AIS is further supported by a recent study of cosmogenic nuclide concentrations (e.g. in situ ^{10}Be) in a sediment core from the Ross Sea (ANDRILL Site AND-1B), which suggests minimal retreat of the EAIS onto land during the last 8 million years (Shakun et al., 2018).

Another important aspect of the continental margin evolution is that its orientation or slope gradually changed from seaward dipping until the Early Pliocene, to landward dipping as it is now (Cooper et al., 1991; De Santis et al., 1999) (Fig. 12.3A). This change was caused by the numerous ice sheet advances and retreats and associated erosion and deposition of sediments. In turn, changes in the bed morphology then fed back on the ice sheet dynamics. Thus, since the Pliocene, the bed of the AIS marine-based sectors has generally been characterised by retrograde slopes, which favoured the potential of Marine Ice Sheet Instability (MISI) (Colleoni et al., 2018b; Jamieson et al., 2012; McKay et al., 2016). Prior to the Late Miocene, climatic conditions were generally warm, the continental shelves were less expanded in most of the Antarctic sectors and did not present strong retrograde slope. Consequently, the ice sheet could retreat easily during warm climate episodes with strong surface and oceanic melt (e.g. Gasson et al 2016; Levy et al., 2016). At the end of the Miocene, the climate gradually cooled, which favoured terrestrial EAIS stability, but as the retrograde bed slope began to form instabilities and fast AIS grounding line retreat in the marine-based sectors during phases of prolonged or exceptional warmth became more important (Blackburn et al., 2020; Colleoni et al., 2018b; Cook et al., 2013; DeConto and Pollard, 2016; DeConto et al., 2012; Golledge et al., 2017a; Levy et al., 2019; Naish et al., 2009a; Pollard and DeConto, 2009; Pollard et al., 2015).

Fast retreat of the grounding line can, however, be slowed down or stopped by the occurrence of pinning points at the bed that provide a buttressing backstress that resists seaward ice flow (Mengel and Levermann, 2014). Pinning points or pinning areas can take different forms. Ice rises, for example, form when an ice shelf anchors on a pre-existing bathymetric high, stabilising the flow (Matsuoka et al., 2015) (Fig. 12.3B). They can be tectonic structures or volcanic islands. Today, several ice rises are visible from the

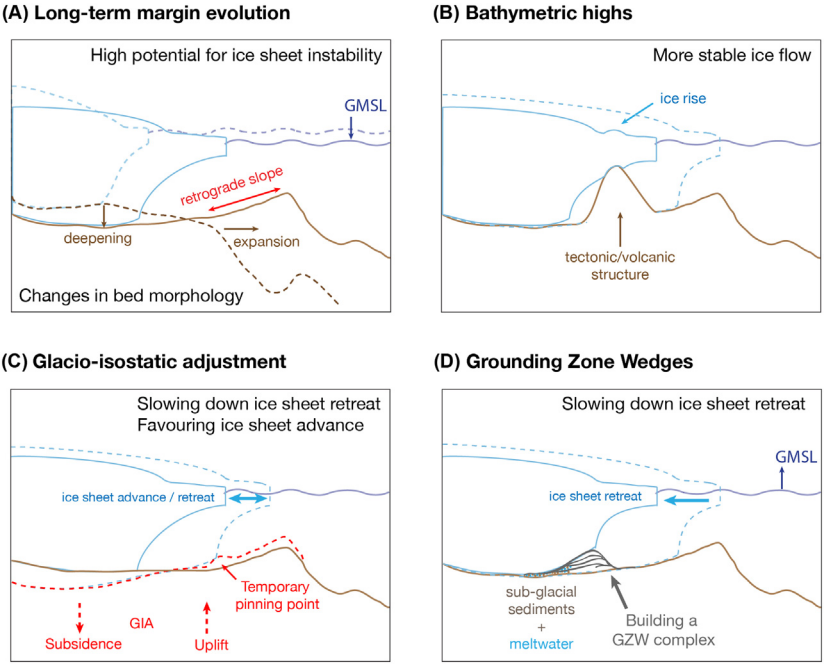

FIGURE 12.3 Schematics of the different ways by which an ice sheet can anchor on the bed. A: Long-term margin evolution; B: bathymetric highs; C: Glacio-isostatic adjustment; D: Grounding Zone wedges. *GMSL*, global mean sea level; *GZW*, grounding zone wedge; *GIA*, glacio-isostatic adjustment.

surface, for example, in the Ross Sea embayment (e.g. Roosevelt Island, Crary Ice Rise, Franklin Islands and Ross Island) and in the Weddell Sea embayment (e.g., Berkner Island). Halberstadt et al. (2016) and Simkins et al. (2018) suggest that the retreat of the grounding line during the last deglaciation was slower in the western Ross Sea than in the eastern Ross Sea, which is characterised by a smoother bed.

Pinning points can also form temporarily due to the uplift of the bed as a result of glacio-isostatic adjustment (GIA) during ice sheet retreat and unloading of the crust (e.g. Whitehouse, 2018; Fig. 12.3C). Numerical simulations show that ignoring GIA during ice sheet advances result in smaller, less extended ice sheets than would occur if GIA was accounted for, because GIA creates pinning opportunities (e.g., Colleoni et al., 2018b). Kingslake et al. (2018) showed that during the early Holocene, the West Antarctic Ice Sheet (WAIS) in both the Weddell Sea and the Ross Sea may have temporarily retreated beyond its present-day grounding line position. It subsequently re-advanced potentially due to uplift of the bed due to GIA (Bradley et al., 2015) and the occurrence of relief (e.g. Bungenstock Ice Rise, Weddell Sea)

on which the ice shelf could pin. Similarly, high-resolution bathymetry acquired from a ridge under the Pine Island Glacier Ice Shelf has revealed geomorphological features that may be consistent with a retreat of Pine Island Glacier inland from its present position earlier during the Holocene and a subsequent re-advance to its early 20th Century position (Graham et al., 2013). These pinning points can be subsequently eroded or can simply 'resorb' after glacio-isostatic adjustment of the bed.

Finally, the ice sheet can build its own pinning points by accumulating sediments in grounding zone wedges (GZW) during deglaciations, which slows its retreat (e.g. Alley et al., 2007; Horgan et al., 2013; Fig. 12.3D). An example of this effect was outlined in Bart et al. (2017, 2018), who analysed a complex of GZWs that formed during the last deglaciation in the Whales Deep basin (Eastern Ross Sea). Proxy analyses and dating of sediment cores revealed that the first four GZWs were built during the first ~5000 years of a gradual 75-km southward ice sheet retreat, between ~17 and ~12.3 ka. They were characterised by low sedimentation rates (i.e., the GZWs are very thin) and sediment compositions indicate that the grounding line was pinned on those GZWs, whilst an extensive ice shelf formed during the retreat. The last three GZWs accumulated, with a clear aggradation sequence, in about 800 years between 12.3 and 11.5 ka, implying that the grounding line was not retreating during this brief interval. These GZWs were characterised by very high sedimentation rates and were thus relatively thick compared to the older ones. Sediment compositions seaward of those three GZWs indicate that the ice shelf broke up at the very beginning of this time interval and never reformed, and that the grounding line remained pinned successively on top of those last three GZWs. After building the uppermost GZW, the grounding line stepped back by about 100 km within a few decades, resulting in a very brief, massive ice discharge of about 0.1 mm sea level equivalent (SLE, Bart and Tulaczyk, 2020). Similar mechanisms and sequences have been inferred from the analysis of Pine Island Bay continental shelf multi-beam and marine seismic data from the Amundsen Sea Embayment shelf (Jakobsson et al., 2011, 2012; Klages et al., 2015; Uenzelmann-Neben et al., 2007). Data show that the ice stream retreat was paused due to the building of GZWs during the last deglaciation. GZWs can also build as a consequence of ice sheet retreat in a narrow trough in which lateral edges serve as a pinning zone that slows down the retreat. Livingstone et al. (2013) and Jamieson et al. (2012, 2014) mapped a series of GZWs in a paleo-ice stream trough in Marguerite Bay (Antarctic Peninsula). Numerical simulations have shown that ice stream retreat rates slowed as the grounding line passed the laterally narrow parts of the trough. If a constant sedimentation rate was assumed, GZWs could form, thus further slowing the retreat.

The presence or absence of pinning points influences ice sheet dynamics. The estimated rates of sea level change during past periods may have been affected by potential pauses or changes in the rate of AIS (or other ice

sheets) advances or retreats, due to ice-bed interactions. These variations may become highly relevant, especially for the interpretation of sea level reconstructions since the LGM, or simulated ice volume changes at the sub-millennial scale (Bart et al., 2018, Kingslake et al., 2018; Klages et al., 2017). However, the erosion of potential paleo-pinning points, during the numerous phases of expansion of the AIS, makes it difficult to know the role of pinning points on past ice sheet variability at sub-millennial time scales in reconstructions older than the LGM. Therefore, pinning points are generally not resolved in paleo-ice sheet simulations, where bed topography cannot be reconstructed with sufficient accuracy or resolution ($<$5 km). Moreover, shallow ice approximation ice sheet models frequently used for paleo-ice sheet simulations need a smoothing of the bed morphology in order to enable numerical convergence in areas where the morphology is too steep for the applicability of the hydrostatic approximation. For example, the Parallel Ice Sheet Model (PISM, Bueler and Brown, 2009) proposes different levels of smoothing of the bed, and this model is frequently used within the PISM paleo-community (e.g. Albrecht et al., 2020, Golledge et al., 2012). Full-Stokes ice sheet models, in which no hydrostatic approximation is applied, do not require bed smoothing since the physics accounts for both horizontal and vertical shear of the ice flow. However, full-Stokes models are too computationally demanding and are still not usable for most paleoclimate applications (Colleoni et al., 2018a and references therein). Given that most paleogeographic reconstructions (e.g. Hochmuth et al., 2020; Paxman et al., 2019) are very coarse in spatial resolution and highly uncertain in terms of detail, bed smoothing in ice sheet simulations resulting in the loss of local pinning points is generally of lesser importance than the biased controls on ice sheet dynamics induced by uncertain bed morphologies (e.g. Gasson et al., 2015).

12.3 Reconstructions of Southern Ocean sea and air surface temperature gradients

Equator-to-pole surface temperature gradients influence Earth's latitudinal heat distribution. Reconstructions of meridional temperature gradients since the Late Cretaceous clearly show a gradual steepening during the transition from greenhouse to icehouse conditions as the polar regions cooled and ice sheets developed (e.g. Zhang et al., 2019). Reconstructions also show the emergence of oceanic fronts in the sub-tropics and high latitudes, especially in the Northern Hemisphere (e.g. Zhang et al., 2019). The development of the Southern Ocean frontal system is of importance for reconstructing past AISs. The Antarctic Polar Front (APF) is a region marked by elevated current speeds and strong horizontal gradients in seawater density, temperature and salinity. It is currently located at approximately 50°S in the Atlantic and Indian sectors, and around 60°S in the Pacific sector. During warm periods,

proxies imply a substantial southward shift of the APF associated with a significant reduction in sea ice extent (e.g. Bjill et al., 2018; Carter et al., 2021, this volume; Chadwick et al., 2020; Evangelinos et al., 2020; Salabarnada et al., 2018; Sangiorgi et al., 2018; Taylor-Silva and Riesselman, 2018). Conversely, during cold periods, the APF shifted northward accompanied by a large expansion of the sea ice cover (Gersonde et al., 2005; Kemp et al., 2010; McKay et al., 2012a).

Fewer sediment cores have been recovered in the Southern Ocean high latitudes than in the Northern Hemisphere high latitudes. South of 50°S, sea surface temperature (SST) proxy reconstructions are rare (Fig. 12.4). The ACE programme and more recently the PAIS programme increased the number of SST and Sea Water Temperature (SWT) measurements at 0−200 m depths from the Southern Ocean's Antarctic margin. SST and SWT records are now available for the MCO from the continental shelf site ANDRILL AND-2A (Western Ross Sea, Levy et al., 2016) and from the continental rise at Integrated Ocean Drilling Program (IODP) Site U1356 (Adélie Land margin, Hartman et al., 2018; Sangiorgi et al., 2018). Mid- to late-Pliocene SST records are available from ANDRILL-1B sediment core (Ross Sea shelf, McKay et al., 2012a) and from other cores on the continental rise and abyssal plains from the Indian sectors (see Dowsett et al., 2013 for an SST compilation). MIS 31 SST records are available from continental rise sites such as Ocean Drilling Program (ODP) Site 1101 (Antarctic Peninsula, Beltran et al., 2020) and IODP Site U1361 (Adélie Land margin, Beltran et al., 2020) and from site ODP Site 1094, (south of APF, South Atlantic sector, Beltran et al., 2020). For MIS 11 and MIS 5e, no Antarctic continental margins SST records are available so far. However, recent International Ocean Discovery Program (IODP) Expedition 374 to the Ross Sea (McKay et al., 2019), IODP Expedition 379 to the Amundsen Sea (Gohl et al., 2019) and expedition INS2017_V01 on the Sabrina Coast (Armand et al., 2018; O'Brien et al., 2020) have recovered highly expanded sedimentary sections from the continental rise. This promises upcoming high-resolution SST records for Pleistocene interglacials, filling a gap where ice proximal SST information have been missing.

A comparison between MCO and mPWP global meridional proxy-based SST gradients highlights the difference between the two periods in the Southern Hemisphere and how much the global climate state has evolved between 17 and 3 Ma (Fig. 12.4A). During the MCO, the air surface temperature gradient strengthened between 30°S to 40°S, as in the Northern Hemisphere, suggesting that the sub-tropical marine frontal system was well developed. The meridional SST and SWT gradients were much weaker than today and a summer warming of 16°C to 22°C (± 5°C) compared to today was observed in geochemical proxies at around 60−65°S on the East Antarctic continental rise (Hartman et al., 2018; Sangiorgi et al., 2018) and a warming of about 2°C to 12°C (± 5°C) compared to today was recorded in

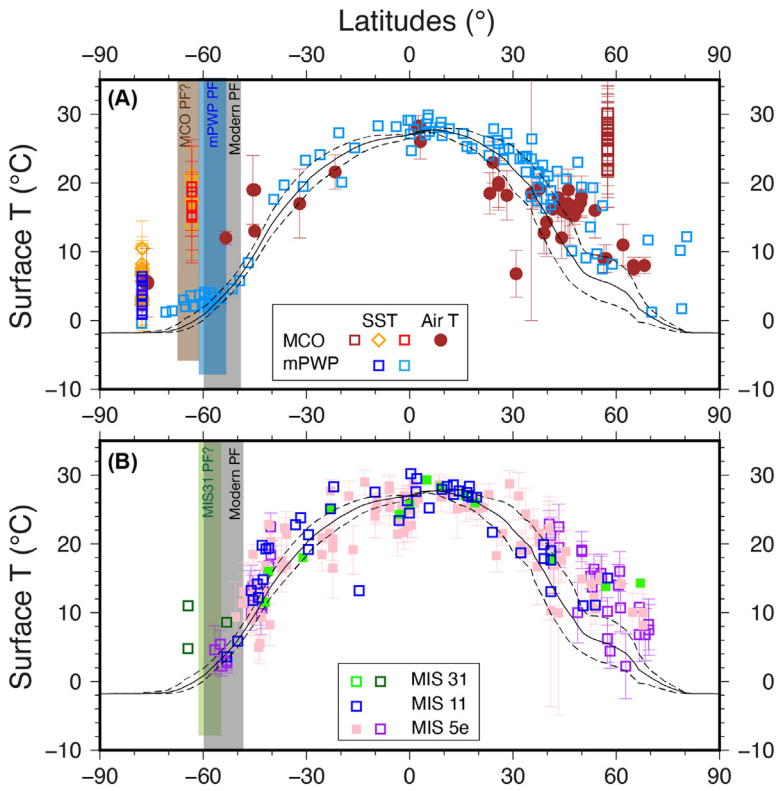

FIGURE 12.4 Proxy compilation of reconstructed meridional sea surface temperatures (SST) for the MCO and the mPWP (A), MIS 31, MIS 11 and MIS 5 (B). Note that vertical colour bars correspond to our interpretation of approximated location of the zonally-averaged circum-Antarctic Polar Front. Due to the paucity of global data for the MCO we include Mean Air Temperature (MAT, brown solid circles) from the Goldner et al. (2014) compilation. SST records for the MCO are from the Super et al. (2020) BAYSPAR calibration of TEX_{86} for North Atlantic ODP Site 982 (brown open squares), from Levy et al. (2016) TEX_{86} Ross Sea SWT 0–200 m depth and Adélie Land margin (Sangiorgi et al., 2018; orange open diamonds) and from Hartman et al. (2018) for TEX_{86} BAYSPAR calibrated Adélie Land margin (red open squares). MAT and SST proxies for the mPWP are from the Dowsett et al. (2012) global compilation (light blue open squares) and the McKay et al. (2012b) TEX_{86} Ross Sea SST record (dark blue open squares). SST proxies for MIS 31 are from the Justino et al. (2017) for global compilation (light green solid squares) and Beltran et al. (2020) for the Antarctic Peninsula, Weddell Sea and Adélie Land margin SST records (dark green open squares). SST proxies for MIS 11 are from Justino et al. (2017). SST proxies for MIS 5 are from Capron et al. (2014) (solid pink squares) and Hoffman et al. (2017) (open purple squares), both at 125 ka. Black continuous (mean annual) and dashed lines (boreal and austral summers) correspond to pre-industrial HadlSST reconstruction from Rayner et al. (2003). Note that many of the SST proxies plotted here from the various compilations tend to be more representative of boreal or austral summer conditions rather than of mean annual conditions.

the Ross Sea (Levy et al., 2016, Sangiorgi et al., 2018) indicating a total absence, or rare occurrences, of sea ice during this period. The mPWP was characterised by a meridional SST gradient weaker than today (e.g. Brierley et al., 2009; Haywood et al., 2013) and with a significant Arctic amplification, while the warming anomaly was more subdued in the high southern latitudes (Fig. 12.4A). South of 55°S, East Antarctic continental rise summer SSTs were warmer than today by about 4°C to 6°C on the East Antarctic continental rise and by up to 7°C on the Ross Sea continental shelf (McKay et al., 2012a), indicative of a highly reduced, if not absent, summer sea ice cover in some sectors.

During both the MCO and the mPWP, the APF was probably more contracted towards high latitudes in all sectors around Antarctica (Sangiorgi et al., 2018; Taylor-Silva and Riesselman, 2018). The mPWP presents a meridional SST gradient steeper than during the MCO and it is possible that the APF might not have reached latitudes as poleward as during the MCO. The contrast between the mPWP and MCO meridional SST gradient south of 40°S suggests that the gradient probably steepened during the Late Miocene (Herbert et al., 2016). However, in some sectors of the Antarctic margin, there is strong evidence for warmer conditions during the Early Pliocene compared to the mPWP, i.e. sea-ice reduction and warming west of the Antarctic Peninsula (e.g. Escutia et al., 2009; Hillenbrand and Ehrmann, 2005) and in Prydz Bay (Whitehead et al., 2005) (see also Chapter 9 by Levy et al., 2021, this volume). This was accompanied by a poleward shift of the APF (Bart and Iwai, 2012; Escutia et al., 2009; Whitehead and Bohaty, 2003).

During the Pleistocene, MIS 31, MIS 11 and MIS 5e meridional SST gradients highlight the strong impact of precessional astronomical forcing, with SSTs warmer than today especially in the Northern Hemisphere mid-to-high latitudes (Fig. 12.4B). All three interglacials present SST gradients quite similar to today in the equatorial to sub-tropical latitudinal bands. The discrepancies between them emerge for latitudes poleward of 50°S. For MIS 31, alkenone and long chain diol analysis on sediment cores reveal an SST warming of 4°C to 12°C on the Adélie Land margins and the Antarctic Peninsula (Beltran et al., 2020). Proxies suggest reduced or even absent winter and summer sea ice in the Ross Sea and offshore Adélie Land margin; information is missing for other Antarctic sectors (see references for Fig. 12.6D). The abrupt appearance of foraminiferal oozes and bioclastic limestone in the Ross Sea and coccolith-bearing sediments in Prydz Bay during MIS 31 (Bohaty et al., 1998; Scherer et al., 2003; Villa et al., 2008, 2012) indicates a significant southward migration of the APF. In terms of the SST gradient, MIS 31 shows more similarities with the mPWP in the Southern Hemisphere than with the more recent Late Pleistocene interglacials.

No SST or SWT proxies south of 60°S are available for MIS 11, and thus it is difficult to assess the magnitude of a potential warming closer to

the Antarctic margins. Interpretation of diatom and geochemical changes could help to estimate SST or SWT from the Wilkes Subglacial Basin and the Ross Sea margins (see Wilson et al., 2021 for references). North of 40°S, tropical to subtropical MIS 11 SSTs were warmer than modern by about 1°C−4°C, and between 50°S and 60°S only a 1°C−2°C warming above modern is recorded (Kunz-Pirrung et al., 2002). Apart from just a single exception, no SST reconstructions are available for MIS 5e south of 60°S (Capron et al., 2014; Chadwick et al., 2020; Hoffman et al., 2017) and the reconstructed SSTs north of 60°S are similar to those of MIS 11 (Fig. 12.4B). It is hence difficult to assess the magnitude of surface and ice proximal sub-surface ocean warming during MIS 5e. Capron et al. (2014) report warmer than present-day conditions that occurred for a longer time interval in southern high latitudes than in northern high latitudes. They also report an earlier MIS 5e warming in the Southern Ocean starting from 130 ka compared with the Northern high latitudes and synchronous with Antarctic ice core records. Moreover, Chadwick et al. (2020) showed that the sea-ice minima and SST maxima were reached at slightly different times in three Southern Ocean sectors. During both MIS 11 and MIS 5e, the few existing records indicate a seasonally sea ice covered ocean (Chadwick et al., 2020; Escutia et al., 2011; Kunz-Pirrung et al., 2002; Wilson et al., 2018; Wolff et al., 2006). Ice core analyses by Wolff et al. (2006) suggested, on the basis of sea-ice proxies in the EPICA Dome C ice core, that winter sea ice was largely reduced during MIS 5e and MIS 11 in the Indian sector of Antarctica, and that summer sea ice was likely absent. In addition, similar proxy analyses on the EPICA DML ice core from Dronning Maud Land indicate a sea ice reduction in the Atlantic sector during MIS 5e (Schüpbach et al., 2013).

12.4 Extent of major Antarctic glaciations

This section focuses on glaciations that occurred during the Eocene-Oligocene Transition (EOT, ∼34 Ma) (Galeotti et al., 2021, this volume; Galeotti et al., 2016), during the Mid-Miocene Climatic Transition (MMCT, 14.5−13.5 Ma) (Levy et al., 2021, this volume), the M2 glaciation (3.312−3.264 Ma) preceding the mPWP, and the Last Glacial Maximum (LGM, ∼21 ka) (see Levy et al., 2021; Siegert et al., 2021, this volume).

The EOT was characterised by the development of a continental ice sheet on Antarctica (Barrett, 1989; Hambrey et al., 1991; Wise et al., 1992; Zachos et al., 1992) as atmospheric CO_2 concentrations level fell (e.g. DeConto and Pollard, 2003) and the Southern Ocean cooled (e.g., Bijl et al., 2013) as a result of the opening of ocean gateways (e.g. Kennett, 1977) (Fig. 12.1). Across the EOT, deep-see temperatures cooled by 3°C to 5°C (e.g. Liu et al., 2018) as a consequence of decreasing CO_2 levels (Pagani et al., 2005). Sedimentary cycles from a drill core in the western Ross Sea

provided the first direct evidence of orbitally controlled glacial cycles between 34 million and 31 million years ago (Galeotti et al., 2016). Initially, under atmospheric CO_2 levels of ≥ 600 ppm, a smaller AIS, restricted to the terrestrial continent, was highly responsive to local insolation forcing. The establishment of the Antarctic Ice Sheet (AIS) was associated with an approximately +1.5 per mil increase in deep-water marine oxygen isotope values ($\delta^{18}O$) beginning at ~34 million years ago (Ma) and peaking at ~33.6 Ma (Bohaty et al., 2012; Coxall et al., 2005), with two positive $\delta^{18}O$ steps separated by ~200,000 years (Fig. 12.1B). The first positive step in the isotope data primarily reflects a temperature decrease (Lear et al., 2008) (EOT-1, ~34.46–33.9 Ma); the second one has been interpreted as the onset of a prolonged interval of maximum ice extent at ~33.6–33.7 Ma (EOT-2) (Liu et al., 2009). Stratigraphic unconformities identified from the continental margins of Antarctica (Fig. 12.1B, e.g. Cooper et al., 2004; De Santis et al., 1995; Eittreim et al., 1995; Escutia et al., 2005; Gohl et al., 2013; Gulick et al., 2017; Uenzelmann-Neben and Gohl, 2014; Whitehead et al., 2006) presumably correspond to one of these $\delta^{18}O$ excursions.

Galeotti et al. (2016) suggest that a continental-scale AIS with frequent calving at the coastline did not form until ~32.8 million years ago, coincident with the earliest time when atmospheric CO_2 levels fell below ~600 ppm. The atmospheric CO_2 threshold for the onset of large-scale Antarctic glaciations remains, however, uncertain and varies between 900 and 560 ppm in numerical climate and ice sheet simulations (DeConto and Pollard, 2003; Gasson et al., 2014; Ladant et al., 2014, Liakka et al., 2014). Liakka et al. (2014) showed that when accounting for vegetation-albedo feedbacks, large-scale Antarctic glaciations occurred when atmospheric CO_2 dropped between 1120 and 560 ppm. Ladant et al. (2014) simulated a first Antarctic expansion at EOT-1 associated with a first sea level drop of about 10 m (atmospheric CO_2 set to 900 ppm) and a second one coinciding with early Oligocene glaciation Oi-1 (33.4–33.0 Ma, Miller et al.,1991; Zachos and Kump, 2005) of about 63 m (atmospheric CO_2 set to 700 ppm). Sequence boundary and ice volume proxies suggest that the extent of the AIS gradually increased across the EOT and expanded to either near-modern dimensions (Miller et al., 2008; 2020a) or as much as 25% larger than at present day (Katz et al., 2008; Wilson et al., 2013). Numerical ice sheet modelling studies show a large range of ice volumes across the EOT. Simulated glaciations lead to sea level fall clustered around 10 m SLE and 25 m SLE relative to present AIS volume (DeConto and Pollard, 2003; Gasson et al., 2014; Ladant et al., 2014; Liakka et al., 2014; Pollard and DeConto, 2005; Wilson et al., 2013) (Fig. 12.1D), which corresponds to a total simulated AIS volume up to 83 m SLE. This is broadly in agreement with sea level falls up to 70 m estimated from low-latitude shallow-marine sequences (e.g. Cramer et al., 2011) (Fig. 12.1C). Both DeConto and Pollard (2003) and Ladant et al. (2014) simulated large isolated ice caps over East

Antarctic highlands presumably during EOT-1, that ultimately coalesced during Oi-1 (Fig. 12.5). This is supported by the geological evidence of glacimarine deposits in the Wilkes Land continental shelf and rise since 33.6 Ma (Escutia et al., 2005, 2011) and by glacial sediment transport to the continental slope of the Prydz Bay margin since ~35 Ma (O'Brien et al., 2004). No ice grounded on the continental shelf at this time (Fig. 12.5, e.g. Barrett, 1989, 2007), and the continental shelf edge was located further South than present for most of the Antarctic margin (Fig. 12.2). See chapter 7 by Galeotti et al. (2021) for more details about the EOT.

The Mid-Miocene Climatic Transition (MMCT, ~14.8–13.5 Ma) is a period of global cooling following the extreme warmth of the Mid-Miocene Climatic Optimum (MCO). The onset of global climatic cooling at ~14.8 Ma marks the start of the MMCT (Böhme, 2003; Flower and Kennett, 1993; Holbourn et al., 2014; Shevenell et al., 2008). Disconformities in the ANDRILL AND-2A record (Levy et al., 2016) and across the Ross Sea (De Santis et al., 1999), pulsed deposition of ice-rafted debris offshore Prydz Bay and the Adélie Land margin (Pierce et al., 2017) together with an increase in sea ice indicators in

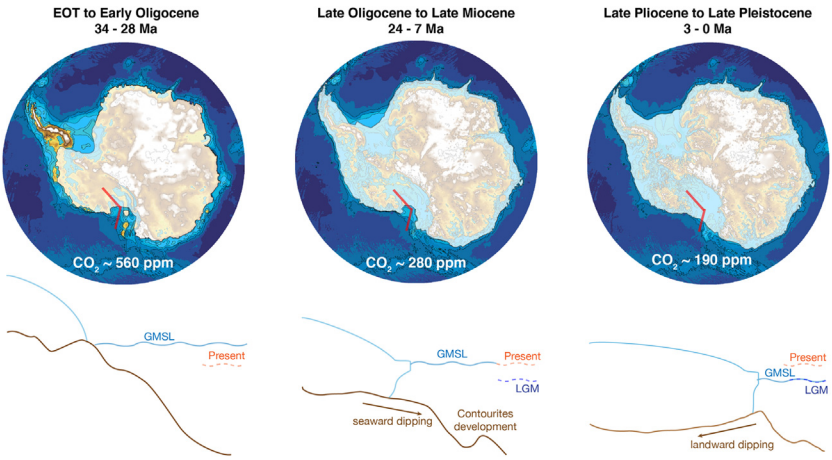

FIGURE 12.5 Simulated Antarctic ice sheet extent during past glaciations of different intervals. EOT to Early Oligocene (34–28 Ma): extent adapted from simulations by Ladant et al. (2014) with prescribed atmospheric CO_2 concentrations of 700–560 ppm. Late Oligocene to Late Miocene (24–7 Ma): extent adapted from simulations by Gasson et al. (2016) and Colleoni et al. (2018b) prescribing with an atmospheric CO_2 level of 280 ppm. Late Pliocene to Late Pleistocene (3 Ma to 0): extent adapted from Colleoni et al. (2018b) with prescribed atmospheric CO_2 values of 190 ppm. Paleotopographies and bathymetries are from Paxman et al. (2019). Note that ice shelves are not represented on the panels. Schematics below each circum-Antarctic view correspond to an idealised transect along the red lines indicated on the Antarctic maps above. Those schematics illustrate the evolution of the continental margin through time, with corresponding global mean sea level variations (GMSL, see Fig. 12.1C) referred to present sea level (dashed orange line) and Last Glacial Maximum sea level (LGM, 21 ka, dashed blue line).

the Ross Sea and off East Antarctica (Levy et al., 2016; Sangiorgi et al., 2018) and major turnover in Southern Ocean diatom species (Crampton et al., 2016) suggest marine ice sheet advances across the Ross Sea during glacial intervals for the first time since the onset of the MCO (for more detail see Levy et al., 2021, this volume) (Fig. 12.5). Ice sheet advance in the Wilkes Land margin is recorded by erosion of older sediments from the shelf (Escutia et al., 2011) and an increase in dinocyst assemblages from the seasonal sea ice zone south of the APF (Sangiorgi et al., 2018). Additionally, less well-dated erosional unconformities in the Weddell Sea (e.g. Huang et al., 2014), Amundsen Sea (e.g. Lindeque et al., 2016; Uenzelmann-Neben and Gohl, 2012), Bellingshausen Sea-Antarctic Peninsula (e.g. Rebesco et al., 2006; Uenzelmann-Neben, 2006), Sabrina Coast (Gulick et al., 2017) and Prydz Bay (e.g. Whitehead et al., 2006), are attributed to MMCT marine-based ice expansion, and together imply that both the EAIS and the WAIS expanded onto the continental shelf at this time (for more detail see Levy et al., 2021). An increase in glacial-interglacial amplitude in the far-field $\delta^{18}O$ data suggests that the AIS expanded further during successively, gradually colder glacial phases. This interval of increased glacial expansion culminated in a major step in the $\delta^{18}O$ record at 13.9 Ma (Fig. 12.1B). During the MMCT, Southern Ocean SSTs cooled by about 6°C (Holbourn et al., 2007; Sangiorgi et al., 2018). Bottom water temperatures generally cooled by 2°C to 3°C (Cramer et al., 2011; Lear et al., 2015; Shevenell et al., 2008) and global sea level may have dropped by as much as 50 m (Miller et al., 2020a), hinting at the possibility of some ice expansion in the Northern Hemisphere (DeConto et al., 2008). Summer temperatures in the Trans-Antarctic Mountains declined by >8°C (Denton and Sugden, 2005) and this cooling has been linked with a shift from temperate climate and wet-based glaciation with a dynamic ice sheet to cold climate and predominantly dry glaciation style with a more stable terrestrial ice sheet under modern-like Antarctic polar climatic conditions (Lewis and Ashworth, 2016; Lewis et al., 2008; Sugden and Denton, 2004).

The largest benthic foraminifera $\delta^{18}O$ shift during this period is of about 1.3‰ (e.g. Holbourn et al., 2013), partly corresponding to an estimated sea level drop of 35−40 m from interglacial to glacial. Interestingly, numerical ice sheet models can only simulate such a large interglacial-to-glacial amplitude in ice volume (Colleoni et al., 2018a; Gasson et al., 2016) when using a reconstructed Mid-Miocene paleogeography (e.g. Paxman et al., 2019). Backstripped sea level data (Kominz et al., 2008; Miller et al., 2005) and calibrated benthic $\delta^{18}O$ sea level changes (Miller et al., 2020a) revealed potential sea level falls up to 10−20 m below the present-day mean sea level during the MMCT (Fig. 12.1C), implying a greatly expanded AIS, perhaps up to 30% larger than today. The compilation of simulated Antarctic ice volume contributions to global mean sea level for this cold period ranges between +10 and −20 m SLE relative to present (Colleoni et al., 2018a; Gasson et al., 2016) (Fig. 12.1D, cyan squares). See Chapter 9 by Levy et al. (2021), this volume for more details about the MMCT.

The Mid-Pliocene M2 glaciation (**~3.312–3.264 Ma**) corresponds to a large transient increase in the deep-sea benthic $\delta^{18}O$ records (Fig. 12.1B) with a cooling of at least 3.5°C preceding the peak of M2 (Karas et al., 2020) and an atmospheric CO_2 level reduction of about 320–343 ppm (de La Vega et al., 2020). A compilation of climate proxy data suggests that during this glaciation, Greenland mountain glaciers expanded (Jansen et al., 2000; Thiede et al., 2011) and that other ice caps also grew in the Northern Hemisphere (De Schepper et al., 2014; Tan et al., 2017). In fact, this glaciation marks the end of global warmth of the early Pliocene (5.5–3.3 Ma) and the beginning of a step-wise transition towards bipolar cooling that culminated in continental-scale Northern Hemisphere glaciations ~2.7 Ma. Numerous sedimentary hiatuses, including the M2 glaciation, are observed in the AND-1B sediment record (western Ross Sea, Naish et al., 2009a) during the Mid to Late Pliocene. Continental margin morphology appears to have allowed the AIS to advance to the shelf edge during the M2 glaciation in the Ross Sea (e.g. Kim et al, 2018; McKay et al., 2012a, 2019), Prydz Bay (O'Brien et al., 2007), Sabrina Coast (Gulick et al., 2017), Wilkes Land (De Santis et al., 2003; Eittreim et al., 1995; Escutia et al., 1997) and the Antarctic Peninsula and Amundsen Sea (Gohl et al., 2013; Rebesco et al., 2006). The glacio-eustatic sea level drop of this period is represented by a major erosional sequence boundary on the New Jersey shelf (Miller et al., 2005) and global sea level fall of about 30 m (Grant et al., 2019; Miller et al., 2012, 2020a; Naish and Wilson, 2009b) (Fig. 12.1C). Based on the review of circum-Antarctic evidence of grounding events and sequence stratigraphy, Bart (2001) suggested an Antarctic ice volume larger than today and almost as large as during the LGM, implying the existence of relatively small Northern Hemisphere ice sheets. In contrast, the compilation of simulated Antarctic ice volume, likely underestimates the ice sheet expansion during this glaciation (Fig. 12.1D) and, instead, yields a global mean sea level rise up to 5 m above present-day mean sea level (De Boer et al., 2017a; Pollard and DeConto, 2009; Tan et al., 2017).

The Last Glacial Maximum (LGM, ~19–23 ka) is the most recent glaciation, and as such, is the best documented. Ice core records have shown that the atmospheric CO_2 levels dropped to about 185 ppm (Lüthi et al., 2008). Global climatic reconstructions revealed that the global mean temperature dropped by about 4°C to 7°C (e.g. Schneider von Deimling et al., 2006; Tierney et al., 2020) compared to present. Marine benthic and planktic foraminifera recorded a clear $\delta^{18}O$ increase (Imbrie et al., 1984; Lisiecki and Raymo, 2005), observable concomitantly to all past cold glacial periods (Imbrie et al., 1984, SPECMAP stack; Lisiecki and Raymo, 2005, LR04 stack; Westerhold et al., 2020, CENOGRID; Zachos et al., 2008, Fig. 12.1B). Calibrated conversions of the $\delta^{18}O$ record or dated paleo coral reefs suggest a global mean sea level drop ranging between 80 and 130 m relative to present (Fig. 12.1C) (e.g. Bard et al., 1990; Shackleton, 2000;

Waelbroeck et al., 2002), with a cluster between 110 and 130 m below present-day mean sea level. Diatoms and radiolarians show that the sea ice cover was larger than today. Winter sea ice cover shifted northward by about 5−10° (e.g. Benz et al., 2016; Gersonde et al., 2005) and the summer sea ice edge, although more uncertain, might have been located around 60.5°S (Green et al., 2020 and references therein). Compilation of climate proxies suggests a potential strengthening and equatorward shift of the Southern Hemisphere westerlies (e.g. Konrad et al., 2014; Lamy et al., 2014; Struve et al., 2020), which remains debated (e.g. Kim et al., 2018; Lamy et al., 2019; Sime et al., 2016).

There is persuasive evidence from the geological record to indicate that the AIS was larger than present around the time of the global sea level low-stand at ~20 ka, although the extent of this expansion is well constrained at only a few sites around the continental margin (Whitehouse, 2018). Both marine and terrestrial geological data indicate that at the LGM, the AIS almost extended to the continental-shelf break in most sectors (Anderson et al., 2002, 2014; Arndt et al., 2017; Bart et al., 2018; Eittreim et al., 1995; Hillenbrand et al., 2012, 2014; Mackintosh et al., 2014; The RAISED Consortium et al., 2014) (Fig. 12.5), as during many previous Pleistocene glaciations (e.g. Escutia et al., 2003). However, the AIS did not advance up to the continental shelf edge in Prydz Bay (Mackintosh et al., 2014; O'Brien et al., 2007; Wu et al., 2021), in the Western Ross Sea (Halberstadt et al., 2016; Prothro et al., 2018) and in parts of the Amundsen Sea (e.g. Klages et al., 2017; Larter et al., 2014). Furthermore, the scenario for ice advance in the Weddell Sea embayment remains uncertain (Nichols et al., 2019; The RAISED Consortium et al., 2014; Whitehouse et al., 2017). Ice sheet expansion during the LGM led to a thickening of the AIS of several hundreds of metres in the margins of almost all sectors, especially around West Antarctica as supported by exposure data (see Siegert et al., 2021, this volume). On the Antarctic plateau, ice core $\delta^{18}O$ isotope records suggest that the elevation increased 270−660 m between the LGM and present-day (Werner et al., 2018). Over West Antarctica, the increase in elevation during the LGM is up to 850−1800 m (Werner et al., 2018).

The relatively small number of proximal geological records on AIS extent and thickness during the LGM prevents an accurate constraint on LGM ice volume. Distal, deep ocean benthic foraminifera $\delta^{18}O$ records may provide overall ice volume estimates but do not allow disentangling contributions from individual ice sheets at the LGM (Simms et al., 2019, and references therein; Clark and Tarasov, 2014). Ice sheet modelling is one of the possible approaches to simulate the volume of the AIS at the LGM. Such modelling suggested an increase in ice volume of 5.9−19.2 m of sea level equivalent (SLE) (Bentley, 1999; Huybrechts, 2002) in the late 1990 and early 2000s. With the improvement of ice sheet models and climate forcing,

the range of AIS contributions to sea level change at LGM has narrowed to about −5 to −12 m SLE (e.g. Briggs et al., 2014; Golledge et al., 2012; Gomez et al., 2013; Huybrechts, 2002; Maris et al., 2014; Quiquet et al., 2018, Sutter et al., 2019), with a cluster around −7 to −8 m SLE (Fig. 12.1D). Another approach is to infer AIS thickness by means of glacial-hydro isostatic adjustment (GIA) models, which describe the viscous response of the solid Earth to past changes in surface loading by ice and water (Whitehouse, 2018). This approach has also been used in combination with ice sheet modelling (e.g. Whitehouse et al., 2012b) and/or by making use of constraints on ice thickness from reconstructions based on exposure age dating, as well as satellite observations of current uplift (Argus et al., 2014; Ivins et al., 2013; Whitehouse et al., 2012b). Estimates from GIA modelling for the AIS contribution to global mean sea level amount to −5 to −30 m SLE with most of the contributions smaller than −13 m SLE (Fig. 12.1D). Older studies had estimated large sea level contributions generally above 15 m (e.g. Bassett et al., 2007; Huybrechts, 2002; Nakada et al., 2000; Peltier and Fairbanks, 2006; Philippon et al., 2006), but more recent modelling studies and reconstructions have refined these estimates to below 13.5 m (Argus et al., 2014; Briggs et al., 2014; Gomez et al., 2013; Mackintosh et al., 2011; Whitehouse et al., 2012a) with an average contribution of about −10 m SLE (e.g. Simms et al., 2019 and references therein).

Despite these improvements, AIS contributions to sea level changes at the LGM remain poorly constrained (Simms et al., 2019, and references therein; Clark and Tarasov, 2014) and this has global consequences on the assessment of past, present and future sea level changes. Land ice retreat in both hemispheres during the last deglaciation has produced a residual GIA signal that still affects present-day sea level changes measurements (Martín-Español et al., 2016). This residual signal is estimated from modelled reconstructions of global land ice thickness changes, and spatio-temporal deglaciation history (e.g. ICE-5G to ICE 7G, GLAC-1, ANU; Lambeck and Chappell, 2001; Lambeck et al., 2002; Peltier, 2004; Peltier et al., 2015; Roy and Peltier, 2018; Tarasov and Peltier, 2002, 2003). To date, there is no consensus on AIS volumes at the LGM and through the last deglaciation. A compilation of cosmogenic exposure ages from low-elevation sites shows that the AIS substantially thinned throughout the Holocene, but mainly after the Melt Water Pulse 1A (MWP-1A) (Small et al., 2019). The RAISED Consortium et al. (2014) provided partial pan-Antarctic grounding line positions at ∼15, 10 and 5 ka. In the deglaciation scenarios ICE-6G and ICE-7G (Peltier et al., 2015; Roy and Peltier, 2018), the AIS extent at the LGM has been set up to its present-day extent, but with grounded ice filling the embayments currently occupied by the Ross Ice Shelf, by the Ronne-Filchner Ice Shelf and by the Amery Ice Shelf. This surely affects the calculation of GIA and its residual signal and, as such, the assessment of

post-glacial and present-day land ice contribution to on-going sea level changes (Martín-Español et al., 2016).

At regional scale, the inclusion of realistic, spatially variable relative sea-level forcing through coupled simulations of 3D ice-sheet and GIA-modulated sea-level change results in a stabilising effect on marine-grounded ice sheet dynamics (Gomez et al., 2010). The grounding line, in fact, advances or retreats in response to the regional ice fluctuation. The latter triggers viscoelastic solid Earth rebound as well as a change of the local geoid height in response to the variation of the gravitational pull (e.g. Stocchi et al., 2013). In particular, the predicted increase in the volume of the WAIS during the last glacial cycle is smaller in the coupled simulations due to negative feedbacks associated with an increase in near-field water depth. The latter stems from the combination of ice-driven solid Earth subsidence and counterintuitive local sea-level rise caused by the gravitational attraction of the growing ice sheet's mass (De Boer et al., 2014b, 2017b; Gomez et al., 2013; Konrad et al., 2014). At global scale, Gomez et al. (2020) showed that the retreat of Northern Hemisphere ice sheets during the last deglaciation and associated sea level rise directly impacts the dynamical behaviour of the AIS and conditions its own retreat. Modelled AIS sensitivity on different paleobathymetries since the Mid-Miocene shows that the position of the AIS advance on the continental shelf depends on glacio-isostatic adjustment (generating pinning points, see Section 12.2) and on the timing and magnitude of global mean sea level changes (Colleoni et al., 2018b; Gomez et al., 2020; Paxman et al., 2020). A similar relationship between the AIS stability and global mean sea level changes has recently been inferred from a North Atlantic deep-ocean benthic $\delta^{18}O$ record of the Plio-Pleistocene Transition and the early Pleistocene (Jakob et al., 2020). Based on a range of Mg/Ca paleothermometer calibrations, the sea level record suggests that the gradual expansion of the Northern Hemisphere ice sheets, and the consequent substantial lowering of global mean sea level, led to an increasing stability of the marine-based sectors of the EAIS (Jakob et al., 2020). Other studies also highlight the sensitivity of the marine-based sectors of the AIS to rapid sea level rise at millennial to sub-millennial time-scales, such as the impact of rapid sea level rise during the various meltwater pulses episodes of past deglaciations (e.g. Golledge et al., 2014; Petrini et al., 2018; Turney et al., 2020; and Siegert et al., 2021, this volume).

12.5 Antarctic ice sheet response to past climate warmings

Assessing the AIS behaviour during past periods warmer than today can inform on the magnitude and timing of past and future sea level changes, as well as on various mechanisms triggering ice sheet retreats that can vary through time (i.e. atmospheric and/or oceanic warming). At millennial to

sub-millennial scales, the crossing of tipping points caused by Earth's climate system feedbacks can cause rapid ice sheet retreats. One example is ocean warming triggering MISI. Because the global climatic state has been constantly evolving, the conditions necessary to cross these tipping points have also evolved. To highlight this aspect, several policy-relevant warm periods in the geologic past have been analysed, based on a few climatic and glaciological indicators synthesised in Fig. 12.6. Note that except for the sea ice (Fig. 12.6D), all the other variables are expressed as anomaly relative to their present-day value (20^{th} Century for MAT and SST).

The compilation of global mean sea level changes and simulated Antarctic contributions shown in Fig. 12.1 and synthesised in Fig. 12.6E is exhaustive and illustrates a key research focus of the paleo polar community over recent decades. We do not discard computed estimates of AIS contribution to global mean sea level change that could appear out of the range of data. Instead, we consider such values as part of the uncertainties associated with uncertain physics and boundary conditions. References for all compiled data and simulated ice volumes are provided in the caption of Fig. 12.1.

The Mid-Miocene Climatic Optimum (MCO, 17−14.8 Ma). The MCO presents an interesting analogue for assessment of climate projected for the next decades to centuries (Steinthorsdottir et al., 2020). At that time, Antarctica hosted the only existing continental-size ice sheet. Geological proxy data indicate atmospheric CO_2 concentrations generally varied between 300 and 600 ppm on glacial-interglacial (orbital) time scales during much of the MCO (Foster et al., 2012; Greenop et al., 2014), but it may have reached values as high as 840 ppm (Retallack, 2009) (Fig. 12.1A). The limited existing geological proxies of terrestrial Antarctic temperature, from the Ross Sea (Warny et al., 2009) and off Adélie Land (Sangiorgi et al., 2018), indicate a surface air temperature warming of approximately 14°C−25°C relative to today. Comparison with the global mean annual temperature (MAT) clearly emphasises strong polar amplification occurred during the MCO (Goldner et al., 2014). SWT and SST reconstructions from the Ross Sea (ANDRILL-2A, Levy et al., 2016) and from the Adélie Land margins (Hartman et al., 2018, Sangiorgi et al., 2018) also support this polar amplification (Fig. 12.6C). On the continental rise (paleo latitude 53°S, Sangiorgi et al., 2018), a 5°C−10°C SWT warming (likely summer) was recorded, but on the continental shelf (∼77°S) this estimated warming was even larger, reaching 10°C−20°C through the MCO.

Together, far-field data and modelling experiments suggest a highly dynamic ice sheet during the MCO. The AIS was mostly responsive to eccentricity-modulated precession affecting local insolation and leading to widespread inland retreat of the land-terminating ice sheet on glacial-interglacial timescales (e.g. Holbourn et al., 2013). Levy et al. (2019) suggested glacial to interglacial ice volume fluctuations were of about 30−46 m

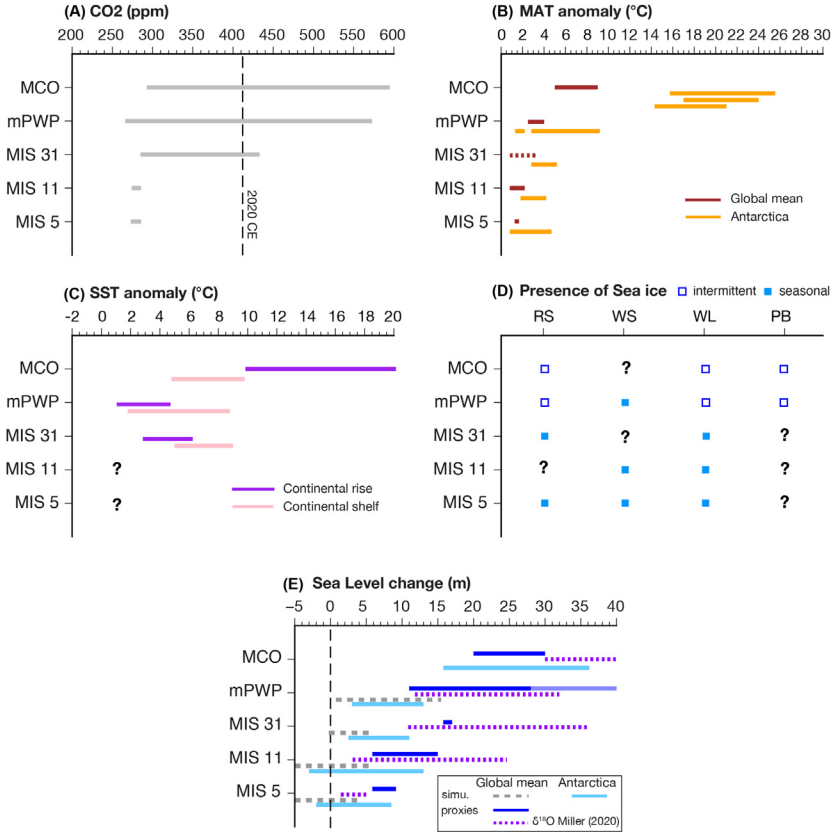

FIGURE 12.6 Main climatic indicators of each warm period considered in the chapter (A–D) and associated simulated range of Antarctic contributions to global mean sea level changes (E). Each panel shows ranges of climatic proxies or simulated quantities at the global scale and for Antarctica relative to their present-day value. Note that for each range (global or Antarctic), minimum and maximum uncertainties of the represented proxies are given. (A) Atmospheric CO_2 levels, see Fig. 12.1A for references. (B) Global mean annual temperature (MAT, °C) anomaly relative to 20th Century average: MCO – Goldner et al. (2014); mPWP – Salzmann et al. (2013) terrestrial proxies (see their Table S3b) and Dowsett et al. (2012) for SST compilation; MIS 31 – Justino et al (2019) averaged SST compilation also accounting for Beltran et al. (2020) Antarctic margin proxy-based SST. Note there are no northern high-latitude MAT or SST reconstructions. Proxies in the northern high latitudes suggest sea ice free conditions (Detlef et al., 2018) as during the mPWP. Given the high similarities with the mPWP SST gradient (Fig. 12.4), MIS 31 global MAT is tentatively extended to mean mPWP MAT (dashed line); MIS 11 – Lang and Wolff (2011) and MIS 5 – Turney and Jones (2010); MAT (°C) anomalies for the Antarctic region (including ice core records) are relative to 1990 at the closest weather station to the sediment cores location: MCO – Warny et al. (2009), mPWP – Haywood et al. (2020), Passchier et al. (2011), MIS 31 – Scherer et al. (2008), MIS 11 – Jouzel et al. (2007), MIS 5 – Jouzel et al. (2007), Lang and Wolff (2011). (C) Sea surface temperature (SST, °C) anomaly relative to present value at each core location: continental shelf values (pink) are from

(*Continued*)

SLE for a $\delta^{18}O$ shift of about 0.88%, which was successfully simulated by Gasson et al. (2016) and Colleoni et al. (2018a) using idealised (but representative) mid-Miocene boundary conditions. Geological records recovered adjacent to the EAIS suggest it advanced and retreated many times through the TAM during the MCO (Hauptvogel and Passchier, 2012) but did not advance far beyond the coastline during glacial intervals (Levy et al., 2016). The cored interval spanning ~17–15 Ma at Integrated Ocean Discovery Program (IODP) Site U1521 (McKay et al., 2019) consists of diatom-rich mudstone and diatomite, which also indicates ice distal environments in the Ross Sea through the MCO. Sediments collected at IODP Site U1356, off the coast of the Adélie Land margin (East Antarctica), suggest open-water conditions at the site throughout the MCO (Sangiorgi et al., 2018). Modelling studies suggest the Wilkes Subglacial Basin remained free of grounded ice during warm interglacial episodes through the early to mid-Miocene (Colleoni et al., 2018a; Gasson et al., 2016; Paxman et al., 2020) but it is unclear whether grounded ice advanced across the region during glacial intervals prior to the MMCT (Pierce et al., 2017). Mg/Ca calibrated sea level and sequence boundary estimates suggest global mean sea level (GMSL) rise ranging from +20 to +30 m above present (Kominz et al., 2008; Miller et al., 2005) (Fig. 12.6E). The compilation of simulated AIS contributions to GMSL vary between +15 and +35 m SLE (Colleoni et al., 2018b; Gasson et al., 2016; Langebroek et al., 2009; Stap et al., 2019)

◀ Cape Roberts or ANDRILL sites: MCO – Sangiorgi et al. (2018) are sea water temperatures (0–200 m depth), mPWP – McKay et al. (2009), MIS 31 – Scherer et al. (2008). SST records from continental slope and rise (purple) are from: MCO – Sangiorgi et al. (2018) sea water temperature (0–200 m depth), Hartman et al. (2018), mPWP – Dowsett et al. (2012) compilation of proxies below 60°S, MIS 31 – Beltran et al. (2020). Note that many of the SST proxies could be representative of boreal or austral summer conditions rather than annual mean. (D) Proxies for presence/absence of sea ice are shown for different Antarctic sectors, RS (Ross Sea), WS (Weddell Sea), WL (Wilkes Land margin), PB (Prydz Bay). Open blue squares indicate episodic sea ice cover during the period, solid blue squares indicate seasonal sea ice (mostly no sea ice during austral summer) and question marks correspond to the absence of information for the sector. For MCO – Hannah (2006), Levy et al. (2016), Sangiorgi et al. (2018); for mPWP – Burckle et al. (1990), McKay et al. (2012a), Taylor-Silva and Riesselman (2018), Whitehead et al. (2005) for MIS 31 – Bohaty et al. (1998), Beltran et al. (2020), Scherer et al. (2008), Villa et al. (2008); for MIS 11 – Escutia et al. (2011), Kunz-Pirrung et al. (2002), Wilson et al. (2018), Wolff et al. (2006) for MIS 5 – Hartman et al. (2016), Konfirst et al. (2012), Kunz-Pirrung et al. (2002), Presti et al. (2011), Wilson et al. (2018), Wolff et al. (2006). (E) Ranges for global mean sea level changes (GMSL) relative to today from data (dark blue) and models (dotted grey). For mPWP, the proxies indicate a sea level rise up to 40 m above present, indicated by the transparent blue line. For MIS 31, GMSL data are uncorrected from GIA and dynamical topography. Simulated ranges of Antarctic Ice Sheet melting contributions are shown in light blue. A range from recent GMSL reconstructions based on benthic $\delta^{18}O$ records from Miller et al. (2020a) is shown with a dotted purple line. See Fig 12.1C and D and the main text for references.

(Fig. 12.6E). Such a large range mostly results from the use of different ice sheet models, different bed topographies and bathymetries, and different climate forcing in the mid-Miocene experiments. The range of potential Antarctic ice sheet GMSL contribution reduced to +16−17 m in Gasson et al. (2016), and Colleoni et al. (2018b) using an idealised Mid-Miocene paleotopography similar to that of Paxman et al. (2019), and a prescribed atmospheric CO_2 of 500 ppm. See Chapter 9 by Levy et al. (2021) for more details on this period.

The mid-Pliocene Warm Period (mPWP, 3.3−3 Ma) is considered as one of the most geologically accessible and relevant examples of climate change driven by atmospheric CO_2 levels equivalent to present-day (Haywood et al., 2016; Masson-Delmotte et al., 2013; Naish and Zwartz, 2012). Atmospheric CO_2 levels ranged between 300 and 450 ppm and global mean temperature was about 2°C−3°C warmer than present during the warmest interglacials (Masson-Delmotte et al., 2013) (Fig. 12.6A and B). One of the striking characteristics of the mPWP is that the SST proxy compilations reveal a meridional temperature gradient weaker than today (Fig. 12.4) characterised by expansion of tropical to sub-tropical bands, no boreal and reduced austral summer sea-ice and, thus, a strong northern and southern polar amplification (e.g. Haywood et al., 2020; Lunt et al., 2012). Modelling shows that such SST patterns reflected a weaker Hadley circulation than today (Brierley et al., 2009; Haywood et al., 2020). In the Southern high-latitudes, the coastal Antarctic region was up to 6°C warmer than today (e.g. McKay et al., 2012a; compilation in Dowsett et al., 2012) (Fig. 12.6B) mostly due to the fact that summer sea-ice, and the ice sheet, had retreated and the APF had contracted to more southern latitudes (Taylor-Silva and Riesselman, 2018). Evidence documents episodic sea ice in the Ross Sea, and offshore Adélie Land and in Prydz Bay (e.g. McKay et al., 2012a; compilation in Dowsett et al., 2012) (Fig. 12.6D). Seasonal sea ice was likely present in the Weddell Sea (Burckle et al., 1990). Reconstructed SSTs show a pan-Antarctic warming of up to 5°C on the continental slope and rise (Escutia et al., 2009; Whitehead and Bohaty, 2003). SSTs also show a warming up to 6°C in the Ross Sea (McKay et al., 2009) (Fig. 12.6C), which was likely caused by the sea-ice albedo feedback, and decreasing local albedo due to the retreat of coastal land ice.

GMSL reconstructions from (paleo-shorelines and sequence stratigraphy) indicate a sea level rise between about 15 to 28 m (Dumitru et al., 2019; Dwyer and Chandler, 2009; Kulpecz et al., 2009; Miller et al., 2012, 2020a; Naish and Wilson, 2009b; Sosdian and Rosenthal, 2009; Wardlaw and Quinn, 1991; Winnick and Caves, 2015), whereas Mg/Ca paleothermometry calibration of benthic $\delta^{18}O$ records suggest a GMSL up to 40 m above present (Fig. 12.6E). GMSL changes based solely on benthic $\delta^{18}O$ records, however, yield large uncertainties (±15 m) (e.g. Raymo et al., 2018). GMSL change amplitudes larger than 30 m above present can only

be explained by melting the terrestrial sectors of the AIS, but retreat of the EAIS in the Ross Sea since 8 Ma appears unlikely because a recent study found extremely low concentrations of cosmogenic ^{10}Be and ^{26}Al isotopes in the ANDRILL AND-1B marine sediment core (Shakun et al., 2018). In addition, many of these peak GMSL estimates (e.g. Hearty et al., 2020; Miller et al., 2012) have not been corrected for regional deviations due to tectonics, glacio-isostatic adjustment and dynamic topography (Dumitru et al., 2019; Raymo et al., 2011; Rovere et al., 2015). A reassessment of Grant et al. (2019) based on far-field data implies GMSL during the warmest mid-Pliocene interglacial was no higher than 21 m (Grant and Naish, 2021, this volume). This new estimate is very close to the average of 20 m above present provided by sea level reconstructions based on sequence stratigraphy and paleo-shore lines.

The compilation of simulated Antarctic ice sheet contributions to GMSL ranges from ~+3 to +15 m SLE (Austermann et al., 2015; De Boer et al., 2015, 2017a, 2017b; DeConto and Pollard, 2016; Dolan et al., 2018; Gasson et al., 2015; Pollard and DeConto, 2009, 2012; Yan et al., 2016) (Fig. 12.6E). Although there is no observational evidence of a potential melting from the Greenland Ice Sheet so far, recent transient numerical simulations suggest that Greenland ice sheet loss could have contributed up to about 6 m SLE to GMSL rise (De Boer et al., 2017a, 2017b). Based on this estimate, the lower bound GMSL rise (+15 m) implies a contribution of the AIS no larger than 9 m SLE. Considering the upper bound of GMSL rise of about +20 to +28 m above present, the maximum contribution of the AIS thus ranges between +15 and +22 m SLE, implying melting of the WAIS and all marine-based sectors of the EAIS (e.g. DeConto and Pollard, 2016; Golledge et al., 2017a, 2017b). ANDRILL AND-1B in the Ross Sea recorded numerous occurrences of open-marine conditions suggesting frequent retreats of the Ross Ice Shelf during the mPWP (Naish et al., 2009a, 2009b). Provenance of fine-grained detritus offshore the Wilkes Subglacial Basin and ice-rafted debris offshore the Aurora Subglacial Basin and Prydz Bay was attributed to the retreat of marine-based sectors of the EAIS (Bertram et al., 2018; Cook et al., 2013, 2014; Whitehead et al., 2006). Similar circum-Antarctic retreat of the marine-based sectors was simulated for one of the Early Pliocene interglacials (Golledge et al., 2017a, 2017b), supported by sedimentological and geological evidence of circum-Antarctic warming events during that period (e.g. Escutia et al 2009; McKay et al., 2012a; Whitehead and Bohaty, 2003). See Chapter 9 by Levy et al. (2021), this volume for more details on this period.

Marine Isotope Stage 31 (MIS 31, 1.081−1.062 Ma) is a prominent mid-Pleistocene interglacial categorised as 'super interglacial' based on the expanded lacustrine sediment record from Lake El'gygytgyn in Siberia (Melles et al., 2012). It corresponded with exceptionally high eccentricity and obliquity values inducing particularly intense high-

latitude summers. The level of atmospheric CO_2 is not well known for this interval but ranges from 300 to 420 ppm (Honisch et al., 2009) (Fig. 12.6A). A circum-Antarctic warming has been inferred from sediment core analysis in the Ross Sea (Naish et al., 2009a, 2009b; Scherer et al., 2008), in Prydz Bay (Villa et al., 2008), on the Adélie Land margin and in the Antarctic Peninsula (Beltran et al., 2020). In particular, the presence of diatoms in the Cape Roberts sediment record (Scherer et al., 2008) suggests a 3°C−5°C warming of upper ocean temperatures compared to today, with seasonally open-ocean conditions (no summer sea ice) (Fig. 12.6D). For the Adélie Land margin and the Antarctic Peninsula, Beltran et al. (2020) reconstructed summer SSTs that on average were 3°C to 6°C warmer than today (Fig. 12.6C). Similar warm conditions are recorded in the Ross Sea at ANDRILL AND-1B as indicated by seasonal open-ocean conditions (Fig. 12.6D), suggesting a retreat of the Ross Ice Shelf (McKay et al., 2012b; Naish et al., 2009a, 2009b). GMSL rise during MIS 31 is relatively poorly constrained from far-field records. Sea-level indicators preserved in coastal cliffs of the Northern Cape Province of South Africa and from Cape Range, Western Australia, suggest highstands not higher than 15−16.5 m above present mean sea level (Hearty et al., 2020; Sandstrom et al., 2021). Note that those estimates are not corrected for GIA, dynamic topography and local tectonic. Far-field evidences of four consecutive Middle Pleistocene Transition sea-level highstands between MIS 31 and MIS 35 were identified in a speleothem record from a western Sicily cave (Mediterranean Sea) (Stocchi et al., 2017). The peculiarity of this marine cave is that it was last flooded between MIS 35 and MIS 31 and has been tectonically uplifted to higher elevations afterward. Among several GIA-modulated relative sea level scenarios, only those accounting for a significant AIS retreat up to about 25 m SLE at MIS 31 and 35 are capable to flood the marine Sicilian cave. The compilation of simulated AIS melting contribution to GMSL ranges from 2 to 10 m SLE (Beltran et al., 2020; de Boer et al., 2013; DeConto et al., 2012) (Fig. 12.6E). The upper bound of this range is in agreement with far-field, though uncorrected, sea level changes and indicates a large WAIS retreat, with a modest contribution from East Antarctic marine-based sectors. In fact, mineralogical provenance from IBRD from ODP Site 1090 (South Atlantic) and ODP Site 1165 (Prydz Bay) revealed that the EAIS retreated significantly over MIS 31 and particularly in the Prydz Bay region. However, other sectors of the EAIS were still characterised by active marine margins (Teitler et al., 2015). Beltran et al. (2020) suggested that the AIS retreat was caused by a stronger advection of Circumpolar Deep Water (CDW) resulting from the changes of the westerlies (subpolar jet). Such a process was also inferred from changes in the geochemical composition of Holocene foraminifera shells from the Amundsen Sea and the aeolian dust from a

West Antarctic ice core record. (Hillenbrand et al., 2017). See also chapter 11 by Wilson et al. (2021) for more details on this period.

Marine Isotope Stage 11 (MIS 11, 425−375 ka) occurred close to the Mid-Brunhes Event (Fig. 12.1). It is the Late Pleistocene warm stage considered as one of the closest analogues to our future because astronomical forcing of a few time slices within MIS 11 are very similar to today (Loutre and Berger, 2003). MIS 11 is also the oldest middle Pleistocene interglacial categorised as a 'super interglacial' based on lacustrine sediment records from the Lake El'gygytgyn in Siberia (Melles et al., 2012). Global mean air temperature was 1.5°C−3°C higher compared to modern temperatures (Fig. 12.6B) although atmospheric CO_2 levels were only around 280 ppm (comparable to pre-industrial levels) (Fig. 12.6A). On the Antarctic plateau, the surface air temperature increased was 2°C−3°C greater than today (Jouzel et al., 2007; Uemura et al., 2018). A polar amplification occurred during that period but was reduced compared to MIS 31 or older warm periods. MIS 11 is not really an intense or brief interglacial such as MIS 5e (130−116 ka, see below); its major characteristic is its longer duration of ∼50,000 years (Tzedakis et al., 2012), which may have been key to substantial ice sheet melting (Irvali et al., 2020). Reconstructed SSTs were not much warmer than modern temperatures (e.g. Becquey and Gersonde, 2002, 2003a, 2003b; Hodell et al., 2000; King and Howard, 2000). In fact, geological evidence supports the idea that a modest but sustained warming was at the origin of ice sheet retreat in the Wilkes Subglacial Basin during MIS 11 (Blackburn et al., 2020; Wilson et al., 2018). Recent modelling studies show that the WAIS and part of the EAIS retreat could occur with a limited warming of 0.4°C if applied for a duration of 4000 years (Mas e Braga et al., 2021). As with other past intervals, the absence of ice proximal oceanic temperature reconstructions is one of the critical gaps to constrain ice sheet simulations of this interval. Reconstructed GMSL suggest a rise of about 13 m above present sea level (Raymo and Mitrovica, 2012; Roberts et al., 2012) and up to 20 m during MIS 11 (Brigham-Grette, 1999; Hearty et al., 1999; Kindler and Hearty, 2000). Such a range implies the complete melting of both the Greenland Ice Sheet and the WAIS, which would account for about 12 m SLE, leaving about 8 m SLE from the EAIS (e.g. Lythe and Vaughan, 2001; Warrick et al., 1996). Mas e Braga et al. (2021) recently simulated a contribution from the WAIS around 4.3−4.5 m SLE and a contribution from the EAIS ranging from 2.3 to 3.7 m SLE. Sedimentological analyses from Erik Drift, Southeast Greenland reveal that most of South Greenland deglaciated during MIS 11 (Reyes et al., 2014). The compilation of simulated AIS contributions to GMSL ranges from ∼−3 to +13 m SLE (Mas e Braga et al., 2021; Sutter et al., 2019; Tigchelaar et al., 2018) (Fig. 12.6E) and in absence of further geological constraints, it is difficult to refine this range. See Chapter 11 by Wilson et al. (2021) for more details on this period.

Marine Isotope Stage 5e or Last Interglacial (LIG, 130−116 ka) was the most recent interglacial with temperatures warmer than today. It has long been considered as an analogue for future climatic changes (Jansen et al., 2007). However, at the peak of the LIG, the astronomical forcing differed too much from the present-day to be a true analogue (Ganopolski and Robinson, 2011). Nevertheless, the LIG presents a very useful time period for understanding the Earth System response (e.g. internal feedbacks in the climate system) to the Paris Agreement temperature targets (e.g. IPCC 1.5°C Special Report). Atmospheric CO_2 concentration was low (Fig. 12.6A), and reconstructed global mean temperature is estimated to have been about 0.5°C−2°C higher than today (Hoffman et al., 2017; Masson-Delmotte et al., 2013) (Fig. 12.6B). The East Antarctic plateau recorded a warming up to 5.5°C at ~128.6 ka followed by a plateau around 2°C (Jouzel et al., 2007; Petit et al., 1999; Watanabe et al, 2003). A polar amplification thus occurred during this period (Capron et al., 2017) and was broadly of the same magnitude as during MIS 11. Antarctic continental margin sediment records imply seasonal sea ice in most of the sensitive marine-based sectors (e.g. Konfirst et al., 2012; Presti et al., 2011) (Fig. 12.6D). GMSL rise is estimated to about 5.9 to 9.3 m above present level from paleo-shorelines (Dutton et al., 2015 and ref. therein) and up to almost 20 m based on calibration of benthic and planktonic $\delta^{18}O$ records (Rohling et al., 2009; Waelbroeck et al., 2002) (Fig. 12.6D), also involving some Greenland Ice Sheet mass loss. However, ice core constraints and modelling studies suggest that the contribution from Greenland was likely only about 2−3 m (Dahl-Jensen et al., 2013), implying a significant meltwater contribution from Antarctica, although also a Greenland Ice Sheet contribution of up to 5.1 m SLE has been suggested (Yan et al., 2016). The compilation of simulated AIS melting contributions to GMSL ranges from about −2 to +8 m SLE (Fig. 12.6E) (e.g. Colleoni et al., 2018b; de Boer et al., 2015; DeConto and Pollard, 2016; Goelzer et al., 2016; Huybrechts, 2002; Pollard and DeConto, 2012; Quiquet et al., 2018; Sutter et al., 2016, 2019; Tigchelaar et al., 2018; compilation in De Boer et al., 2019). Antarctic ice core records of $\delta^{18}O$, considered as a proxy for local ice volume changes, have been analysed in an attempt to better constrain the individual contribution of Antarctica to GMSL. Based on these analyses, numerical climate and ice sheet simulations suggest that part of the $\delta^{18}O$ signal could be explained by sea ice reduction rather than ice sheet retreat (e.g. Holloway et al., 2016). In the absence of ice proximal ocean temperature reconstructions, as for other Late Pleistocene interglacials, it is very difficult to constrain the magnitude and timing of the AIS retreat during this interval. The magnitude of oceanic warming required to trigger a large retreat of the marine-based sectors at that time varies between models from +2°C to +3°C relative to pre-industrial temperature (e.g. DeConto and Pollard, 2016; Sutter et al., 2016; Turney et al., 2020). However, Turney

et al. (2020) also showed that with a modest ocean warming of 0.4°C, the major ice shelves could disintegrate within 600 years. While continental margin sediments offshore from the Wilkes Subglacial Basin suggested a reduction of this marine-based sector of the EAIS during MIS 5e (Wilson et al., 2018), geological evidence from the WAIS is contradictory and suggests either that no major ice sheet retreat occurred (e.g. Clark et al., 2020; Hillenbrand et al., 2002, 2009; Spector et al., 2018) or that considerable retreat took place (e.g. Turney et al., 2020). See Chapter 11 by Wilson et al. (2021) for more details on this period.

12.6 Antarctica and global teleconnections: the bipolar seesaw

Inter-hemispheric heat transport, the so-called bipolar see-saw (Stocker and Johnsen, 2003), is another key process affecting AIS evolution. It regulates oceanic and atmospheric temperatures at sub-millennial to millennial time scales. The bipolar see-saw mechanism was hypothesised by Stocker (1998) on the basis of observed asynchronous changes in ice core records between Greenland and Antarctica for some of the Dansgaard/Oeschger events that occurred during the last glacial cycle (Blunier et al., 1998). Stocker and Johnsen (2003) hypothesised that iceberg melting and meltwater discharges close to the North Atlantic convection sites caused a substantial weakening of the Atlantic Meridional Oceanic Circulation (AMOC). Such a slowdown could have induced a gradual heat transfer to the South, with a lag of a few centuries to millenia, thus explaining the asynchronous temperature changes between Greenland and Antarctic ice core records during the last glacial period (EPICA Community Members, 2006, Pedro et al., 2018). Recent findings confirm that cooling of the Antarctic Cold Reversal is synchronous with the Bølling–Allerød warming in the Northern Hemisphere 14,600 years ago (Stenni et al., 2011). The Bølling–Allerød is coincident with the occurrence of meltwater pulse 1A (MWP-1A) that caused a rapid sea level rise of about 9–20 m (e.g. Deschamps et al., 2012; Lambeck et al.,2014; Liu et al., 2016; Peltier et al., 2015) at a rate of 4 m/100 yr (e.g. Carlson and Clark, 2012; Deschamps et al., 2012; Peltier and Fairbanks, 2006). Although some studies have considered the AIS as a potential contributor to MWP-1A (e.g. Clark et al., 1996; Bassett et al., 2007; Golledge et al., 2014; Weaver et al., 2003), most geological and glaciological studies argue against a large Antarctic contribution (e.g. Bentley et al., 2010; Licht, 2004; Spector et al., 2017; The RAISED Consortium et al., 2014). However, IBRD records from 'Iceberg Alley' in the Scotia Sea may record the occurrence of eight events between 20 and 9 ka, including the MWP-1A (e.g. Weber et al., 2014). Etourneau et al. (2019) showed that a 0.3°C to 1.5°C increase in subsurface ocean temperature (50–400 m) in the northeastern Antarctic Peninsula

drove a major collapse and recession of the regional ice shelf during both the instrumental period and the last 9000 years. Modelling studies support the idea of responsive marine-based sectors of the AIS at millennial time scales, driven by oceanic melting rather than by atmospheric forcing triggering fast ice sheet instabilities (e.g. Blasco et al., 2019; Golledge et al., 2014; Lowry et al., 2019).

Meltwater sources of such millennial oscillations are poorly constrained, however (e.g. Clark et al., 2002; Liu et al., 2016; Peltier, 2005). This limits our understanding of the causes of the events, i.e. warm water advection to the grounding line (e.g. Golledge et al., 2014) bipolar seesaw caused by melting Northern Hemisphere ice sheets (e.g. Menviel et al., 2011), abrupt global mean sea level rise (e.g. Clark et al., 2002; Golledge et al., 2014; Gomez et al., 2020), atmospheric forcing (e.g. WAIS Divide Project Members, 2015) or feedbacks within the climate system. Past, present and future meltwater-climate feedbacks have been widely studied and there is an extensive literature on modelling the global climate response to freshwater discharge from ice sheets (e.g. Böning et al., 2016; Bronselaer et al., 2018; Golledge et al., 2019; Roche et al., 2014; Sadai et al., 2020; Stammer, 2008). Results from these studies highlight the role of altered inter-hemispheric heat transport on the global climate both in the past and in the future. Different mechanisms respond to the freshwater at different timescales but the overall feedback loop spans the millennial scale (Turney et al., 2020). The sequence of those feedback loops is illustrated in Fig. 12.7 and is based on two recent contributions, i.e., Turney et al. (2020) for the LIG (130−116 ka), and Golledge et al. (2019) for projected climate changes until CE 2100 following RCP 8.5 emission scenario.

Turney et al. (2020) reported evidence of substantial ice discharge across the Weddell Sea sector during the LIG based on a blue-ice core record. Substantiated with climate and ice sheet simulations, they suggest that the ice discharge (and subsequent multi-metre global mean sea level rise) was caused by a millennial-scale oceanic warming following freshwater discharge in the Northern high latitudes (Heinrich event 11 at ∼135−130 ka) and a weakening of the AMOC (Böhm et al., 2015). This mechanism corresponds to the bipolar see-saw. Turney et al. (2020) identified a loop of positive ice-sheet-climate feedback that further amplified the warming close to the Antarctic margin. Grant et al. (2014) identified two main meltwater pulses, one at 139 ka pre-dating Heinrich event 11 (135 ± 1 and 130 ± 2 ka) and one occurring at about 133 ka during this Heinrich event. Marino et al. (2015) found that Heinrich event 11 coincided with a rapid sea-level rise mostly explained by Northern hemisphere ice sheet deglaciation. The occurrence of this meltwater pulse supports the positive feedback described in Turney et al. (2020) and potentially explains the delayed timing of the AIS contribution to the GMSL highstand at the LIG. A delay of a few thousand years is supported by the idealised modelling study by Blasco et al. (2019), suggesting

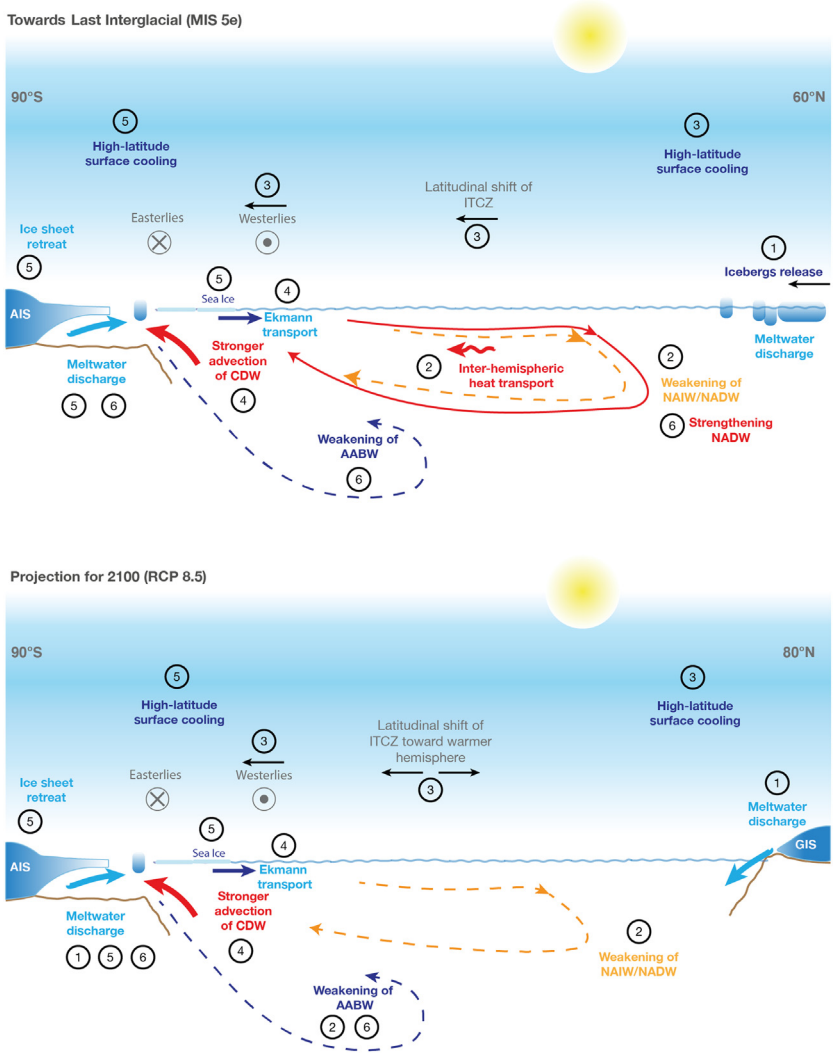

FIGURE 12.7 Cartoons for the impact of freshwater release and associated feedback loops at the global scale and on Antarctica. Top cartoon is based on Turney et al. (2020) and describes the evolution of those feedbacks as a consequence of Heinrich event 11 (~135 ka) and subsequent evolution until MIS 5e (time frame of few millennia). Numbers indicate the order of the sequence. Bottom cartoon shows similar feedback loops but as projected until 2100 for the RCP 8.5 high-emission scenario (time frame of few decades) based on Golledge et al. (2019). *AABW*, Antarctic Bottom Water; *CDW*, Circumpolar Deep Water; *ITCZ*, Inter-Tropical Convergence Zone; *NAIW*, North Atlantic Intermediate Water; *NADW*, North Atlantic Deep Water.

that the bipolar seesaw accumulated heat in the Southern Hemisphere, enhancing ocean warming on a millennial time scale during the last deglaciation. Similarly, Clark et al. (2020) suggested that the rate of global mean sea level changes during the LIG, as well as spatial sea level variations, could be explained by the responses of the Antarctic and Greenland ice sheets to Heinrich event 11 and associated climate feedbacks. The sequence of feedbacks in Turney et al. (2020) can be applied to other interglacials and is as follows (Fig. 12.7, top):

1. Northern high-latitude freshwater was released during the Heinrich 11 event ($\sim$135 and 130 ka);
2. Subsequently, a weakening of North Atlantic Deep Water (NADW) flow was observed, and heat was transferred gradually southward.
3. An increased meridional inter-hemispheric thermal gradient due to Northern high latitudes cooling induced a southward shift of the Inter-Tropical Convergence Zone (ITCZ) and of the Southern Hemisphere westerly winds (e.g. Shevenell et al., 2011).
4. The southward shift and strengthening of the westerlies (e.g. Dickens et al., 2019; Etourneau et al., 2019; Lamy et al., 2019; Hillenbrand et al., 2017) drove an enhanced northward Ekman transport and a stronger southward advection of CDW on the continental shelf (e.g. Hillenbrand et al., 2017; Minzoni et al., 2017).
5. Enhanced advection of CDW amplified the melting of the AIS and of the sea ice, triggering the AIS retreat. Northward transport of cool surface waters caused sea ice expansion and local atmospheric cooling.
6. Large freshwater discharge caused a reduction in Antarctic Bottom Water (AABW) formation and a subsequent increase in NADW formation. Increase in NADW formation led to heat transfer towards northern high latitudes, and thus a bipolar see-saw swing towards the north.

Golledge et al. (2019) simulated a similar ice-sheet-climate sequence of feedbacks by considering on-going and projected meltwater discharge from the Greenland and Antarctic ice sheets until CE 2100. Results show that a slow-down of the AMOC occurs in response to Greenland Ice Sheet melting, and that projected meltwater discharge from Antarctica can trap the heat of CDW at intermediate depths on the continental shelf (Bronselaer et al., 2018; Sadai et al., 2020; Silvano et al., 2019), establishing a positive feedback that further enhances AIS melting (Fig. 12.7, bottom), as follows:

1. Projected freshwater release at Northern and Southern high-latitudes;
2. A weakening of NADW formation is observed, and heat is transferred gradually southward. In the South, freshwater stratifies the continental shelf waters.
3. An increased meridional inter-hemispheric thermal gradient induces a weak southward shift of the ITCZ and of the Southern Hemisphere Westerly winds.

4. Southward shift of the westerly winds drives an enhanced northward Ekman transport compensated by a stronger southward advection of CDW on the continental shelves, which amplifies the melting of Antarctic ice shelves and sea ice.
5. Continental shelf water stratification fosters a northward Ekman transport of cool surface waters associated with sea ice expansion and local atmospheric cooling. This mechanism further amplifies the advection of CDW to the AIS grounding line and initiates its retreat.
6. Larger freshwater release further causes a reduction in AABW formation.

Compared to Turney et al. (2020), the sequence of processes and feedbacks in 2100 remains incomplete and stops before all the heat from the North is transferred to South. This suggests that additional decades to centuries are needed for the full effects of the bipolar see-saw on southern high latitudes to be felt.

12.7 The PAIS legacy: bridging the past and the future

12.7.1 The PAIS legacy

The PAIS legacy is clearly one of successfully addressing high-level scientific priorities. Beyond this, it is also the story of a long-lasting network of collaborations, among different nations and researchers, and striving to share scientific infrastructure and capabilities to investigate remote and challenging Antarctic regions. The multidisciplinary concept of the PAIS programme represented the key to its success. Eight years after the start of the programme, PAIS achievements are many, both in terms of field campaigns and in terms of scientific advances concerning Antarctic ice sheet dynamics. Several projects fostered by the PAIS programme, which contributed to major scientific advances in constraining AIS contribution to past sea level changes, are briefly summarised below. This list is far from being exhaustive and interested readers can refer to the other chapters of this book for more detailed descriptions of PAIS research outcomes and other time periods not discussed here.

12.7.1.1 Antarctic ice sheet sensitivity during past high-CO_2 worlds and its contribution to global sea-level change

Geological proxies from the Antarctic continental margin have improved reconstructions of ocean and land temperatures, sea-ice extent, ice sheet extent, subglacial hydrology, carbon cycle feedbacks and paleogeography for past warm climate states. This has provided improved boundary conditions for testing and developing ice sheet and climate models capabilities and performance, as well as evaluating model sensitivity. Significant outcomes include the following:

- Reconciling southern high-latitude meridional temperature gradients and polar amplification between model simulations and data during Greenhouse climates (e.g. DeConto et al., 2012; Pross et al., 2012) and new knowledge of Antarctic margins SSTs and SWTs during the MCO, the mPWP and MIS 31 (Beltran et al, 2020; Hartman et al., 2018; Levy et al., 2016; McKay et al., 2009; Sangiorgi et al., 2018). Polar amplification is much larger during the MCO, mPWP and MIS 31 than during the Pleistocene interglacials. Those findings allow an estimate of Earth's climate sensitivity to high atmospheric CO_2 concentrations.
- Constraining equilibrium and transient ice volumes (e.g. Clark et al., 1996; de Boer et al., 2015; DeConto and Pollard, 2016; DeConto et al., 2012; Dolan et al., 2018; Gasson et al., 2016; Goelzer et al., 2016; Golledge et al., 2017a, 2017b; Pollard et al., 2015; Stap et al., 2019), and the contribution to global sea-level under past 'warmer-than-present' climates (e.g. Dutton et al., 2015; Miller et al., 2012, 2020a, 2020b).
- Recognition of the importance of bed topography and paleobathymetry on past Antarctic ice volume reconstructions (e.g. Gasson et al., 2016, building on Hochmuth and Gohl, 2019; Hochmuth et al., 2020; Paxman et al., 2019, 2020; Wilson and Luyendyk, 2009) and sensitivity to ocean warming (e.g. Colleoni et al., 2018a; Paxman et al., 2020).
- Recognition of the sensitivity of marine-based sectors of the EAIS from models and data (e.g. Aitken et al., 2016; Bertram et al., 2018; Blackburn et al., 2020; Cook et al., 2013, 2014; Gasson et al., 2016; Golledge et al., 2017b; Gulick et al., 2017; Levy et al., 2016; Pierce et al., 2017; Reinardy et al., 2015; Scherer et al., 2016; Simkins et al., 2017; Wilson et al., 2018).
- Insights into the influence of mean climate state (CO_2) on the response of the AIS to orbital forcing (e.g. Dolan et al., 2011; Levy et al., 2019; Patterson et al., 2014; building on concepts in Naish et al., 2009a, 2009b; Stap et al., 2019, 2020; Sutter et al., 2019).

12.7.1.2 Geological evidence of ocean forcing and marine ice sheet instability

The potential for abrupt and non-linear 'runaway' retreat of the marine-based sectors of the AIS due to marine ice sheet instability (MISI) and potentially also marine ice cliff instability (MICI) up until recently had only been mathematically simulated in ice sheet models.

- Geological observations of the last deglaciation and recent observations coupled with models have now identified MISI during the Holocene after atmospheric forcing had weakened in the Ross Sea (e.g. Bart and Tulaczyk, 2020; Jones et al., 2015; McKay et al., 2016; Spector et al.,

2017), and potentially MICI in the Amundsen Sea sector (Wise et al., 2017) and Antarctic Peninsula (Rebesco et al., 2014).
- There are geological and modern oceanographic observations of oceanic warm waters reaching the grounding line of marine-based ice sheets (e.g. Joughin and Alley, 2011; Hansen and Passchier, 2017; Hillenbrand et al., 2017; Rintoul et al., 2016; Schmidtko et al., 2014; Smith et al., 2017).

12.7.1.3 Improved temporal and spatial patterns of AIS retreat and its contribution to global Melt-Water Pulse 1A

Improved geological and bathymetric constraints combined with ice sheet models have shown:

- An improved understanding of the extent and dynamics of the LGM ice sheet and deglaciation into the Holocene (e.g. Anderson et al., 2014; Golledge et al., 2013; Hillenbrand et al., 2014; Hodgson et al., 2014; Johnson et al., 2014; Larter et al., 2014; Lee et al 2017; Mackintosh et al., 2014; McKay et al., 2016; O'Cofaigh et al., 2014; The RAISED Consortium et al., 2014);
- The AIS contributed to melt-water pulse 1A (e.g. Golledge et al., 2014; Weber et al., 2014), though not from all sectors (e.g. Spector et al., 2017) and to other millennial scale fluctuations with estimated contributions to global mean sea level up to 6 m SLE (Blasco et al., 2019; Golledge et al., 2014), at a rate of about 1 m/century in the case of MWP-1A (e.g. Golledge et al., 2014).

12.7.1.4 A better understanding of ice-sheet-ocean interactions

- During the last deglaciation, proxy data and model simulations consistently find that ocean warming drove the ice sheet retreat in different sectors of Antarctica (e.g. Crosta et al., 2018; Hillenbrand et al., 2017; Wilson et al., 2018);
- Ocean warming is also thought to have accelerated the last deglaciation in the Ross Sea during MWP-1A (e.g. Golledge et al., 2014), although this finding is challenged by geological evidence from the Trans-Antarctic Mountains (e.g. Spector et al., 2017). Based on regional ice sheet simulations, atmospheric forcing can enhance, diminish or compensate for oceanic warming during the first half of the deglaciation, while during the second half, ocean warming clearly drove the end of the ice sheet retreat (Buizert et al., 2015; Blasco et al., 2019; Lowry et al., 2019);
- Strengthening of the subpolar jet during deglaciation (e.g. Lamy et al., 2019) enhanced advection of CDW towards the continental margins (Evangelinos et al., 2020; Hillenbrand et al., 2017; Minzoni et al., 2017; Salabarnada et al., 2018);
- Improved understanding of sedimentological facies indicative of subice shelf environments opens up new opportunities for quantifying the

influence of the ocean on the AIS evolution through time (e.g. Smith et al., 2019; Yokoyama et al., 2016);
- Freshwater release from the Northern high latitudes can induce a bipolar seesaw, transferring heat to the Southern Hemisphere and fostering AIS retreat a few thousands of years later (Blasco et al., 2019; Buizert et al., 2015; Clark et al., 2020; Turney et al., 2020). Likewise, freshwater release from Antarctica can stratify the ocean, reduce vertical mixing and the release of heat and gas to the surface, and increase heat transport at the grounding lines of marine-based ice sheets (e.g. Golledge et al., 2019; Silvano et al., 2019).

12.7.1.5 Antarctic ice–Earth interactions and their influence on regional sea-level variability and Antarctic Ice Sheet dynamics

The importance of departures in regional sea-level changes from eustatic sea-level due to rotational, visco-elastic and gravitational changes as water mass is transferred between the ice sheets and the ocean has been identified in the far and near-fields of the AIS from paleo-reconstructions (e.g. Clark et al., 2002; Milne and Mitrovica, 2008; Raymo and Mitrovica, 2012; Raymo et al., 2011; Rovere et al., 2014; Stocchi et al., 2013). This has been established through 1D and 3D glacio-isostatic adjustment models that couple (runtime or asynchronously) ice sheets and solid Earth processes constrained by both near-field and far-field geological reconstructions of sea-level changes. Important outcomes include the following:

- Role of Earth deformation processes (GIA and dynamic topography) on near-field sea-level changes and ice sheet dynamics (e.g. Austermann et al., 2015; Gomez et al., 2015, 2018; Kingslake et al., 2018; Pollard et al., 2017; Stocchi et al., 2013; Whitehouse et al., 2017, 2019);
- Impact of global gravitationally consistent sea level changes induced by Northern Hemisphere ice sheet fluctuations on the retreat of the AIS (e.g. Gomez et al., 2020);
- Impact of long-term global mean sea level change on the stability of EAIS (e.g. Jakob et al., 2020; Shakun et al., 2018).

12.7.1.6 Improved interpretation of subglacial processes from mapping seabed

- Multibeam campaigns in different sectors of Antarctica have mapped the geomorphological footprints of paleo ice streams and their associated paleo-drainage networks (e.g. Kirkham et al., 2019; Larter et al., 2019; Nitsche et al., 2013; Simkins et al., 2017; The RAISED Consortium et al., 2014) as well as other subglacial features (Bart et al., 2018; Dowdeswell et al., 2020; Kuhn et al., 2017; Stokes, 2018).

- Analysis of the characteristics of those geomorphological features inform the long-term mean and potential maximum rates of grounding line retreat (e.g. 1−10 km/yr, Bart et al., 2018; Dowdeswell et al., 2020) but also show that meltwater can enhance ice flow and cause ice surges and meltwater outbursts (e.g. Kuhn et al., 2017; Simkins et al., 2017). These reconstructions provide constraints on the ice flow regime during both advances and retreats and on the mechanics and dynamics of ice stream (Stokes, 2018).

12.7.1.7 Paleo-data calibrated ice sheets models provide revised global sea-level predictions for IPCC scenarios

A new generation of continental scale ice sheet models that simulate MISI and in one case MICI have been developed and tested by reconstructing past AIS volume and extent constrained by paleoclimate and paleo-ice extent data. These models have been used to simulate future Antarctic meltwater contribution to GMSL changes based on the Representative Concentration Pathways (RCPS). Implications include the following:

- The Antarctic contribution to global sea-level rise for the year CE 2100 and beyond may have been underestimated in IPCC AR5 projections especially for high emission scenarios (e.g. DeConto and Pollard, 2016; Edwards et al., 2019; Golledge et al., 2015, 2020; Siegert et al., 2020).
- These paleo-calibrated AIS models show that a threshold for marine ice sheet stability may exist at $\sim$1.5°C−2°C global warming above pre-industrial (e.g. around RCP 2.6, the target of the Paris Agreement) (e.g. Clark et al., 2016; DeConto and Pollard, 2016; Golledge et al., 2015).
- Recent paleo-studies have stressed that a moderate local oceanic warming, lower than the upper bound of 1.5°C−2°C for pan-Antarctic ocean warming can also trigger fast ice sheet retreat if applied for a few centuries: Bakker et al. (2017); Beltran et al. (2020); Golledge et al. (2017a); Turney et al. (2020). This highlights the importance of polar amplification for the fast response of polar areas under past and future global warming conditions.

12.7.2 Challenges for the next programmes

Gaps illustrated above highlight the necessity to assess whether or not the WAIS only partially retreated or totally disintegrated during past warm periods. Records of such massive ice sheet retreats are possibly located below the ice sheet. Locating subglacial drilling sites that could have recorded such extensive retreat represents a high priority challenge worthy of future field campaigns (e.g. Bradley et al., 2012; Spector et al., 2018). Similarly, it is urgent to assess the EAIS marine-based sectors sensitivity to oceanic and atmospheric warming during past warm periods (e.g. Aitken et al., 2016;

Blackburn et al., 2020; Cook et al., 2013, 2014; Gulick et al., 2017; Pierce et al., 2017; Reinardy et al, 2015; Wilson et al., 2018) and their potential contribution to global mean sea level change (e.g. DeConto and Pollard, 2016; Mas e Braga et al., 2021; Paxman et al., 2020) to refine their future contribution to ongoing sea level rise (e.g. Golledge et al., 2017b; Rignot et al., 2019).

Paradoxically, even though the Pleistocene interglacials are more recent and well documented in many places around the world, AIS fluctuations through time have destroyed most of the ice proximal geological evidence of these interglacials on the continental shelf, making direct records of the ice sheet's behaviour difficult to find. Only a few precious SST records are currently available from the Antarctic continental slope and rise and those records are indirect and cannot fill the gap of ice proximal ocean temperature records. This data gap directly impedes the validation of numerical paleoclimate and paleo-ice sheet numerical simulations. The interpretation of sedimentary facies and geomorphological features on the seafloor, however, does allow us to infer the type of sub-glacial environments and, thus, ice flow during past deglaciations to be reconstructed (e.g. Bart et al., 2018; Prothro et al., 2020; Simkins et al., 2017; Smith et al., 2019).

Another observational challenge is to recover records with sub-millennial temporal resolution for the different past warm periods. Such high-resolution archives can be recovered from the continental slope and rise by drilling levee deposits and contourite systems, or from the continental shelf in overdeepened basins and fjords (e.g. ODP Leg 178 The Palmer Deep, Domack et al., 2001; IODP Expedition 318, Ashley et al., 2021; IODP Expedition 374 Ross Sea, McKay et al., 2019; IODP Expedition 379 Amundsen Sea, Gohl et al., 2019; approved IODP proposal 732 Antarctic Peninsula). High-resolution data represent the bridge between the past and the future, in particular for centennial to millennial-scale climate oscillations (e.g. Bakker et al., 2017; Bracegirdle et al., 2019; Golledge et al., 2020; Noble et al., 2020; Weber et al., 2014). High-resolution sedimentary data are also important for correlating marine sediment records with ice core records of the past 8,000,000 years. The on-going Beyond EPICA: Oldest Ice project (e.g. Fischer et al., 2013; Parrenin et al., 2017; https://www.beyondepica.eu/) will allow correlation with expanded sediment records from the Ross Sea (IODP Exp. 374) (McKay et al., 2019) including the MIS-31 super-interglacial event, and from the Amundsen Sea (IODP Exp. 379) (Gohl et al., 2019) across the Mid-Pleistocene Transition and from future expeditions, for example the IODP proposal 732-Full2.

To maintain pace with advances of the observational ice sheet community, the paleoclimate modelling community will need to expand efforts in regional atmospheric and oceanic modelling for different past periods representing both glacial and interglacial contexts. Regional modelling is computationally expensive and also requires highly resolved boundary conditions at high frequency

to capture the local variability of processes. Improved large-scale global climate simulations will also be required to support regional modelling. Many on-going data-model comparison initiatives already exist, and some of them focus on the periods described in this chapter, as for example the paleoclimate Model Intercomparison Project (PMIP, now in phase 4) (Kageyama et al., 2018), the Pliocene Model Intercomparison Project (PLIOMIP, now in phase 2) (Haywood et al., 2020), the recently started Miocene Model Intercomparison Project (MIOMIP) (Steinthorsdottir et al., 2020 and related special issue) and the Deep-Time Model Intercomparison Project (DEEPMIP) (Lunt et al., 2017). PMIP focuses on the Late Pleistocene and now also includes transient simulations of entire interglacials using coupled atmosphere-ocean models. DEEPMIP focuses mainly on the EOT and the Eocene warmth. More refined global mean sea level records are also necessary to better assess Antarctic ice volume fluctuations over the past 34 Myrs. Both MCO and mPWP periods are of high interest to assess Earth climate sensitivity to high atmospheric CO_2 concentrations (similar to projected ones) and global mean sea level rise (e.g. Haywood et al., 2016; Steinthorsdottir et al., 2020). Sequence stratigraphy of the continental margins is a powerful approach and the key to fill this gap. However, improvements are needed, especially to correct those records from glacio-hydro-isostasy (e.g. Grant et al., 2019; Grant and Naish, 2021). Thus, coupled ice-sheet-GIA-sediment erosion and transport models are needed (e.g. Pollard and DeConto, 2003, 2020; Whitehouse et al., 2019).

Finally, while the climate and paleoclimate communities are currently putting efforts into the development of fully coupled Earth System Models, such models are too computationally demanding to allow for long-term transient simulations. With upcoming progress in scientific computing, and progress in the computing facilities themselves, using fully coupled Earth System Models now seems an achievable objective for paleo studies.

12.7.3 Long-term projections and role of PAIS and future programs

Future projections of AIS evolution have shown large improvements over the past few years (e.g. DeConto and Pollard, 2016; Edwards et al., 2019; Pattyn et al., 2018). However, related uncertainties remain large, indicating that fundamental knowledge gaps still persist about ice sheet dynamics, and interactions with the atmosphere, ocean and the solid earth (Whitehouse et al., 2019). Morlighem et al. (2020) released an updated subglacial topography map revealing the high-resolution bed morphology of some of the glacial troughs and their potential in causing AIS instability in the case of fast retreat of the grounding line. Many of them are still unexplored, despite their clear importance in understanding past, present and future AIS dynamics. The release of the IPCC Special Report 'The Ocean and Cryosphere in a Changing Climate' (SROCC) in September 2019 (IPCC, 2019) showed that our appreciation of the various contributions to GMSL

change has improved since the last IPCC Assessment Report 5 (AR5) in 2013. After the release of AR5, satellite observations revealed that Antarctic ice shelves were thinning faster than previously thought (Paolo et al., 2015), caused by observed warming in the surrounding ocean (Pritchard et al., 2012). Recent re-assessments of 20th century observations confirmed the AIS has been losing mass since the publication of IPCC AR5 and that this mass loss accelerated at the end of the 20th century (e.g. Rignot et al., 2019; Shepherd et al., 2018).

To precisely assess the AIS contributions to GMSL changes, the polar community has increased the monitoring and modelling of AIS evolution. Attention has been focused on ice shelf buttressing and on large partly marine-based drainage basins of the WAIS and EAIS (Fürst et al., 2016) (e.g. Pine Island Glacier, Thwaites glacier, Totten glacier, Recovery ice stream, Foundation ice stream) and ice−ocean interactions around Antarctica. The particularity of most of the marine-based sectors of the AIS is that they are grounded on a bed with retrograde slopes (Joughin and Alley, 2011; Morlighem et al., 2020) and/or that their buttressing ice shelves are pinned on a sill with a retrograde slope and are thus vulnerable to future MISI. New estimates of future GMSL rise from the IPCC SROCC (2019) amount to 0.43 m (0.29−0.59 likely range, RCP 2.6 scenario) and 0.84 m (0.61−1.10, likely range, RCP 8.5) in CE 2100, with the possibility of multi-metre sea level rise by CE 2300 (Clark et al., 2016; Golledge et al., 2015) but with 'deep uncertainty' (IPCC SROCC, 2019). Ice shelf loss is a key pre-requisite for the onset of marine ice shelf instabilities. The large uncertainties in the most recent estimates of sea level rise from Antarctica mostly result from our inability to assess the potentially unstable behaviour of the marine-based sectors of the AIS, and in particular: the sensitivity of ice shelves to sub-ice shelf melting from below and surface warming above. These gaps inevitably lead to model-dependent results, particularly for processes that are parameterised (Asay-Davis et al., 2017; Siegert et al., 2020). This is where the past can close those knowledge gaps and provide necessary observational constraints to model the past and the future evolution of the AIS (e.g. Gasson and Keisling, 2020).

The Earth's past provides a natural laboratory for testing realistic cases of ice-sheet-climate−solid earth interactions at different timescales (Bracegirdle et al., 2019). The research produced within the PAIS programme has shown that the AIS potentially crossed its tipping point for major ice loss many times since the onset of large-scale glaciation (~34 Ma) under climatic conditions warmer than today. Past periods have the potential to identify thresholds for instability (e.g. Cook et al., 2013; Naish et al., 2009a, 2009b; Weber et al., 2014; Wilson et al., 2018) or large retreat/re-advance events (e.g. Golledge et al., 2017a, 2017b; Kingslake et al., 2018; Scherer et al., 2016; Wilson et al., 2018) and thus to provide credibility to future scenarios. Paleo-records also have the potential to reveal new

mechanisms, such as for example the marine-ice cliff instability (MICI, DeConto and Pollard, 2016; Pollard et al., 2015). MICI involves the fast disintegration of ice shelves by surface-melt induced hydro-fracturing and rapid calving at thick, marine-terminating ice margins. This mechanism has been inferred to explain rapid major mass loss from the WAIS and EAIS during MIS 5e and the mPWP (DeConto and Pollard, 2016; Pollard et al., 2015) but many open questions about MICI and its possible role in past and future sea level rise remain (e.g., Edwards et al., 2019; Pattyn et al., 2018). Geological and glaciological evidence can also highlight feedbacks in the ice sheet-climate system (Turney et al., 2020) or processes that might not appear policy-relevant but are indeed determinant in understanding the future sensitivity of the AIS and sea level rise to ongoing and projected climate changes (Haywood et al., 2019).

12.8 Coauthors from the PAIS community

Aisling M. Dolan, University of Leeds, Leeds, UK

Alan K. Cooper, U.S. Geological Survey Emeritus, Menlo Park, USA

Alessandra Venuti, Istituto Nazionale di Geofisica e Vulcanologia, Rome, Italy

Amy Leventer, Colgate University, Hamilton, NY, USA

Andrea Bergamasco, C.N.R. (National Research Council) ISMAR, Venice, Italy

Carolina Acosta Hospitaleche, CONICET, División Paleontología Vertebrados, Museo de La Plata (Facultad de Ciencias Naturales y Museo, UNLP) La Plata, Argentina

Carolina Acosta Hospitaleche, CONICET – División Paleontología Vertebrados, Museo de La Plata, Facultad de Ciencias Naturales y Museo, UNLP; La Plata, Argentina

Catalina Gebhardt, Alfred Wegener Institute Helmholtz Centre of Polar and Marine Research, Bremerhaven, Germany

Christine S. Siddoway, Colorado College, Colorado Springs, USA

Christopher C. Sorlien, Earth Research Institute, University of California, Santa Barbara, Santa Barbara, California, USA

David Harwood, University of Nebraska-Lincoln, Lincoln, Nebraska, USA

David Pollard, Pennsylvania State University, University Park, Pennsylvania, USA

David J. Wilson, Department of Earth Sciences, University College London, London, UK

Denise K. Kulhanek, Texas A&M University, College Station, TX, United States

Dominic A. Hodgson, British Antarctic Survey, Cambridge, UK

Edward G.W. Gasson, University of Bristol, UK

Fausto Ferraccioli, NERC/British Antarctic Survey, Cambridge, UK

Fernando Bohoyo, Instituto Geológico y Minero de España, Madrid, Spain

Francesca Battaglia, University of Venice Cá Foscari, Italy

Frank O. Nitsche, Lamont-Doherty Earth Observatory of Columbia University, Palisades, USA

Georgia R. Grant, GNS Science Wellington, New Zealand

Gerhard Kuhn, Alfred-Wegener-Institut Helmholtz-Zentrum für Polar- und Meeresforschung, Bremerhaven, Germany

Guy J.G. Paxman, Lamont-Doherty Earth Observatory, Columbia University, New York, USA

Ian D. Goodwin, Climate Change Research Centre, University of New South Wales, Sydney, Australia

Isabel Sauermilch, University of Tasmania, Institute for Marine and Antarctic Studies, Australia

Jamey Stutz, Antarctic Research Centre at Victoria University of Wellington, New Zealand

Jan Sverre Laberg, Department of Geosciences, UiT The Arctic University of Norway, NO-9037 Tromsø, Norway

Javier N. Gelfo, CONICET – UNLP, División Paleontología Vertebrados, Museo de La Plata, Argentina

Johann P. Klages, Alfred Wegener Institute Helmholtz Center for Polar and Marine Research, Bremerhaven, Germany

Julia S. Wellner, University of Houston, Houston, USA

Karsten Gohl, Alfred Wegener Institute Helmholtz Centre for Polar and Marine Research, Bremerhaven, Germany

Laura Crispini, University of Genova (DISTAV, Genova, Italy)

Leanne K. Armand, Australian National University, Canberra, Australia.

Marcelo A. Reguero, Instituto Antártico Argentino, B1650HMK, San Martín, Buenos Aires, Argentina

Marcelo A. Reguero, Instituto Antártico Argentino, Buenos Aires, Argentina

Marco Taviani, Institute of Marine Sciences (ISMAR), National Research Council (CNR), 40129, Bologna, Italy and Biology Department, Woods Hole Oceanographic Institution, 02543, Woods Hole, USA

Martin J. Siegert, Imperial College London, London, UK

Marvin A. Speece, Montana Technological University, Butte, USA

Mathieu Casado, Alfred Wegener Institute Helmholtz Centre for Polar and Marine Research, Potsdam, Germany

Michele Rebesco, OGS, Trieste, Italy

Mike Weber, University of Bonn, Institute for Geosciences, Department of Geochemistry and Petrology, 53115 Bonn, Germany

Minoru Ikehara, Kochi University, Japan

Nicholas R. Golledge, Antarctic Research Centre Victoria University of Wellington, Wellington 6140, New Zealand

Nigel Wardell, OGS, Trieste, Italy

Paolo Montagna, Institute of Polar Sciences, National Research Council, Bologna, Italy

Peter J. Barrett, Antarctic Research Centre, Victoria University of Wellington, Wellington, New Zealand.

Peter K. Bijl, Utrecht University, Utrecht, The Netherlands

Philip E. O'Brien, Macquarie University, Sydney, Australia

Philip J. Bart, Louisiana State University, Baton Rouge, USA

Raffaella Tolotti, University of Genoa, Genoa, Italy

Reed P. Scherer, Northern Illinois University, DeKalb, IL, USA

Renata G. Lucchi, National Institute of Oceanography and Applied Geophysics (OGS), Sgonico-Trieste, Italy

Riccardo Geletti, National Institute of Oceanography and Applied Geophysics – OGS, Trieste, Italy

Richard C.A. Hindmarsh, British Antarctic Survey & Durham University, Cambridge & Durham, United Kingdom

Richard H. Levy, GNS Science and Victoria University of Wellington, Lower Hutt and Wellington, New Zealand

Robert B. Dunbar, Stanford University, Stanford, California, USA

Robert D. Larter, British Antarctic Survey, Cambridge, UK

Robert M. Mckay, Antarctic Research Centre, Victoria University of Wellington, Wellington, New Zealand

R. Selwyn Jones, Monash University (Melbourne, Australia)

Sandra Passchier, Montclair State University, Montclair, USA

Sean P.S. Gulick, University of Texas at Austin, Austin, Texas

Sidney R. Hemming, Columbia University, New York, USA

Stefanie Brachfeld, Montclair State University, New Jersey, USA

Suzanne OConnell, Wesleyan University, Middletown, CT, USA

Trevor Williams, International Ocean Discovery Program, Texas A&M University, College Station, USA

Ursula Röhl, MARUM, University of Bremen, Bremen, Germany

Yasmina M. Martos, NASA Goddard Space Flight Center, Greenbelt, MD, USA & University of Maryland College Park, MD, USA

Acknowledgements

TN acknowledges support from MBIE Antarctic Science Platform contract ANTA1801.

References

Aitken, A.R.A., Roberts, J.L., Van Ommen, T.D., Young, D.A., Golledge, N.R., Greenbaum, J. S., et al., 2016. Repeated large-scale retreat and advance of Totten Glacier indicated by inland bed erosion. Nature 533 (7603), 385–389.

Albrecht, T., Winkelmann, R., Levermann, A., 2020. Glacial-cycle simulations of the Antarctic Ice Sheet with the Parallel Ice Sheet Model (PISM) – part 1: boundary conditions and climatic forcing. The Cryosphere 14, 599–632. Available from: https://doi.org/10.5194/tc-14-599-2020.

Alley, R.B., Anandakrishnan, S., Dupont, T.K., Parizek, B.R., Pollard, D., 2007. Effect of sedimentation on ice-sheet grounding-line stability. Science 315 (5820), 1838–1841.

Anderson, J.B., Conway, H., Bart, P.J., Witus, A.E., Greenwood, S.L., McKay, R.M., et al., 2014. Ross Sea paleo-ice sheet drainage and deglacial history during and since the LGM. Quaternary Science Reviews 100, 31–54.

Anderson, J.B., Shipp, S.S., Lowe, A.L., Wellner, J.S., Mosola, A.B., 2002. The Antarctic Ice Sheet during the Last Glacial Maximum and its subsequent retreat history: a review. Quaternary Science Reviews 21 (1-3), 49–70.

Argus, D.F., Peltier, W.R., Drummond, R., Moore, A.W., 2014. The Antarctica component of postglacial rebound model ICE-6G_C (VM5a) based on GPS positioning, exposure age dating of ice thicknesses, and relative sea level histories. Geophysical Journal International 198 (1), 537–563.

Armand, L., O'Brien, P., Armbrecht, L., Barker, H., Caburlotto, A., Connell, T., et al., 2018. Interactions of the Totten Glacier with the Southern Ocean through multiple glacial cycles (IN2017-V01): Post-survey report. Australian Antarctic Science Grant Program (AAS# 4333). The grant title is "Interactions of the Totten Glacier with the Southern Ocean through multiple glacial cycles" and the PI's are: Armand, LK O'Brien, P., Post, A., Goodwin, I., Opdyke, B., Leventer, A., Domack, E., Escutia-Dotti, C. DeSantis, L.

Arndt, J.E., Hillenbrand, C.D., Grobe, H., Kuhn, G., Wacker, L., 2017. Evidence for a dynamic grounding line in outer Filchner Trough, Antarctica, until the early Holocene. Geology 45 (11), 1035–1038.

Asay-Davis, X.S., Jourdain, N.C., Nakayama, Y., 2017. Developments in simulating and parameterizing interactions between the Southern Ocean and the Antarctic Ice sheet. Current Climate Change Reports. 3, 316–329. Available from: https://doi.org/10.1007/s40641-017-0071-0.

Ashley, K.E., McKay, R., Etourneau, J., Jimenez-Espejo, F.J., Condron, A., Albot, A., et al., 2021. Mid-Holocene Antarctic sea-ice increase driven by marine ice sheet retreat. Climate of the Past 17 (1), 1–19.

Austermann, J., Pollard, D., Mitrovica, J.X., Moucha, R., Forte, A.M., DeConto, R.M., et al., 2015. The impact of dynamic topography change on Antarctic ice sheet stability during the mid-Pliocene warm period. Geology 43 (10), 927–930. Available from: https://doi.org/10.1130/G36988.1.

Badger, M.P.S., Lear, C.H., Pancost, R.D., Foster, G.L., Bailey, T., et al., 2013a. CO2 drawdown following the middle Miocene expansion of the Antarctic Ice Sheet. Paleoceanography 28, 42–53. Available from: https://doi.org/10.1002/palo.20015.

Badger, M.P.S., Schmidt, D.N., Mackensen, A., Pancost, R.D., 2013b. High resolution alkenone palaeobarometry indicates relatively stable pCO_2 during the Pliocene (3.3 to 2.8 Ma). Philosophical Transactions of the Royal Society A 347, 20130094. Available from: https://doi.org/10.1098/rsta.2013.0094.

Bakker, P., Clark, P.U., Golledge, N.R., Schmittner, A., Weber, M.E., 2017. Centennial-scale Holocene climate variations amplified by Antarctic Ice Sheet discharge. Nature 541 (7635), 72–76.

Bamber, J.L., Oppenheimer, M., Kopp, R.E., Aspinall, W.P., Cooke, R.M., 2019. Ice sheet contributions to future sea-level rise from structured expert judgment. Proceedings of the National Academy of Sciences 116 (23), 11195–11200.

Bard, E., Hamelin, B., Fairbanks, R.G., 1990. U-Th ages obtained by mass spectrometry in corals from Barbados: sea level during the past 130,000 years. Nature 346 (6283), 456–458.

Barrett, P., 1989. Antarctic Cenozoic history from the CIROS-1 drillhole, McMurdo Sound, Antarctica. NZ DSIR Bulletin 245, 254.

Barrett, P.J., 2007. Cenozoic climate and sea level history from glaciomarine strata off the Victoria Land coast, Cape Roberts Project, Antarctica. In: Hambrey, M.J., Christoffersen, P., Glasser, N.F., Hubbard, B., (Eds.), Glacial Sedimentary Processes and Products. International Association of Sedimentologists Special Publications 39, 259–287.

Bart, P.J., 2001. Did the Antarctic ice sheets expand during the early Pliocene? Geology 29 (1), 67–70. Available from: https://doi.org/10.1130/0091-7613(2001)029%3C0067:DTAISE%3E2.0.CO;2.

Bart, P.J., 2003. Were West Antarctic ice sheet grounding events in the Ross Sea a consequence of East Antarctic ice sheet expansion during the middle Miocene? Earth and Planetary Science Letters 216 (1–2), 93–107. Available from: https://doi.org/10.1016/S0012-821X(03)00509-0.

Bart, P.J., De Santis, L., 2012. Glacial intensification during the Neogene: a review of seismic stratigraphic evidence from the Ross Sea, Antarctica, continental shelf. Oceanography 25 (3), 166–183.

Bart, P.J., DeCesare, M., Rosenheim, B.E., Majewski, W., McGlannan, A., 2018. A centuries-long delay between a paleo-ice-shelf collapse and grounding-line retreat in the Whales Deep Basin, eastern Ross Sea, Antarctica. Scientific Reports 8 (1), 1–9. Available from: https://doi.org/10.1038/s41598-018-29911-8.

Bart, P.J., Iwai, M., 2012. The overdeepening hypothesis: how erosional modification of the marine-scape during the early Pliocene altered glacial dynamics on the Antarctic Peninsula's Pacific margin. Palaeogeography, Palaeoclimatology, Palaeoecology 335, 42–51.

Bart, P.J., Krogmeier, B.J., Bart, M.P., Tulaczyk, S., 2017. The paradox of a long grounding during West Antarctic Ice Sheet retreat in Ross Sea. Scientific Reports 7 (1), 1–8. Available from: https://doi.org/10.1038/s41598-017-01329-8.

Bart, P.J., Tulaczyk, S., 2020. A significant acceleration of ice volume discharge preceded a major retreat of a West Antarctic paleo–ice stream. Geology 48 (4), 313–317. Available from: https://doi.org/10.1130/G46916.1.

Bartoli, G., Hönisch, B., Zeebe, R.E., 2011. Atmospheric CO_2 decline during the Pliocene intensification of Northern Hemisphere glaciations. Paleoceanography 26 (4). Available from: https://doi.org/10.1029/2010PA002055.

Bassett, S.E., Milne, G.A., Bentley, M.J., Huybrechts, P., 2007. Modelling Antarctic sea-level data to explore the possibility of a dominant Antarctic contribution to meltwater pulse IA. Quaternary Science Reviews 26 (17–18), 2113–2127.

Becquey, S., Gersonde, R., 2002. Past hydrographic and climatic changes in the Subantarctic Zone of the South Atlantic–The Pleistocene record from ODP Site 1090. Palaeogeography, Palaeoclimatology, Palaeoecology 182 (3–4), 221–239.

Becquey, S., Gersonde, R., 2003a. A 0.55-Ma paleotemperature record from the Subantarctic zone: implications for Antarctic Circumpolar Current development. Paleoceanography 18 (1).

Becquey, S., Gersonde, R., 2003b. 14. Data Report: Early and Mid-Pleistocene (MIS 65-11) Summer Sea-Surface Temperature, Foraminiferal Fragmentation, and Ice-Rafted Debris Records from the Subantarctic (ODP Leg 177 Site 1090). Proceedings of Ocean Drilling Program Science Results 177, 1–23.

Beltran, C., Golledge, N.R., Ohneiser, C., Kowalewski, D.E., Sicre, M.A., Hageman, K.J., et al., 2020. Southern Ocean temperature records and ice-sheet models demonstrate rapid Antarctic ice sheet retreat under low atmospheric CO_2 during Marine Isotope Stage 31. Quaternary Science Reviews 228, 106069. Available from: https://doi.org/10.1016/j.quascirev.2019.106069.

Bentley, M.J., 1999. Volume of Antarctic ice at the Last Glacial Maximum, and its impact on global sea level change. Quaternary Science Reviews 18, 1569–1595.

Bentley, M.J., Fogwill, C.J., Le Brocq, A.M., Hubbard, A.L., Sugden, D.E., Dunai, T.J., et al., 2010. Deglacial history of the West Antarctic Ice Sheet in the Weddell Sea embayment: constraints on past ice volume change. Geology 38 (5), 411–414.

Benz, V., Esper, O., Gersonde, R., Lamy, F., Tiedemann, R., 2016. Last Glacial Maximum sea surface temperature and sea-ice extent in the Pacific sector of the Southern Ocean. Quaternary Science Reviews 146, 216–237.

Bereiter, B., Eggleston, S., Schmitt, J., Nehrbass-Ahles, C., Stocker, T.F., Fischer, H., et al., 2015. Revision of the EPICA Dome C CO_2 record from 800 to 600 kyr before present. Geophysical Research Letters 42 (2), 542–549. Available from: https://doi.org/10.1002/2014GL061957.

Bertram, R.A., Wilson, D.J., van de Flierdt, T., McKay, R.M., Patterson, M.O., Jimenez-Espejo, F.J., et al., 2018. Pliocene deglacial event timelines and the biogeochemical response off-shore Wilkes Subglacial Basin, East Antarctica. Earth and Planetary Science Letters 494, 109–116. Available from: https://doi.org/10.1016/j.epsl.2018.04.054.

Bijl, P.K., Bendle, J.A., Bohaty, S.M., Pross, J., Schouten, S., Tauxe, L., et al., 2013. Eocene cooling linked to early flow across the Tasmanian Gateway. Proceedings of the National Academy of Sciences 110 (24), 9645–9650.

Bintanja, R., Van De Wal, R.S., Oerlemans, J., 2005. Modelled atmospheric temperatures and global sea levels over the past million years. Nature 437 (7055), 125–128. Available from: https://doi.org/10.1038/nature03975.

Bjill, P.K., Houben, A.J.P., Hartman, J.D., Pross, J., Salabarnada, A., Escutia, C., et al., 2018. Paleoceanography and ice sheet variability off-shore Wilkes Land, Antarctica – Part 2: Insights from Oligocene–Miocene dinoflagellate cyst assemblages. Climate of the Past 14, 1015–1033. Available from: https://doi.org/10.5194/cp-14-1015-2018.

Blackburn, T., Edwards, G.H., Tulaczyk, S., Scudder, M., Piccione, G., Hallet, B., et al., 2020. Ice retreat in Wilkes Basin of East Antarctica during a warm interglacial. Nature 583 (7817), 554–559. Available from: https://doi.org/10.1038/s41586-020-2484-5.

Blasco, J., Tabone, I., Alvarez-Solas, J., Robinson, A., Montoya, M., 2019. The Antarctic Ice Sheet response to glacial millennial-scale variability. Climate of the Past 15 (1), 121–133.

Blunier, T., Chappellaz, J., Schwander, J., Dällenbach, A., Stauffer, B., Stocker, T.F., et al., 1998. Asynchrony of Antarctic and Greenland climate change during the last glacial period. Nature 394 (6695), 739–743.

Bohaty, S., Scherer, R., Harwood, D.M., 1998. Quaternary diatom biostratigraphy and palaeoenvironments of the CRP-1 drillcore, Ross Sea, Antarctica. Terra Antartica 5 (3), 431–453.

Bohaty, S.M., Zachos, J.C., Delaney, M.L., 2012. Foraminiferal Mg/Ca evidence for southern ocean cooling across the eocene–oligocene transition. Earth and Planetary Science Letters 317, 251–261. Available from: https://doi.org/10.1016/j.epsl.2011.11.037.

Böhme, M., 2003. The Miocene climatic optimum: evidence from ectothermic vertebrates of Central Europe. Palaeogeography, Palaeoclimatology, Palaeoecology 195 (3-4), 389–401.

Böhm, E., Lippold, J., Gutjahr, M., Frank, M., Blaser, P., Antz, B., et al., 2015. Strong and deep Atlantic meridional overturning circulation during the last glacial cycle. Nature 517 (7532), 73–76. Available from: https://doi.org/10.1038/nature14059.

Böning, C.W., Behrens, E., Biastoch, A., Getzlaff, K., Bamber, J.L., 2016. Emerging impact of Greenland meltwater on deepwater formation in the North Atlantic Ocean. Nature Geoscience 9 (7), 523–527. Available from: https://doi.org/10.1038/ngeo2740.

Bracegirdle, T.J., Colleoni, F., Abram, N.J., Bertler, N.A., Dixon, D.A., England, M., et al., 2019. Back to the future: Using long-term observational and paleo-proxy reconstructions to improve model projections of Antarctic climate. Geosciences 9 (6), 255.

Bradley, S.L., Hindmarsh, R.C., Whitehouse, P.L., Bentley, M.J., King, M.A., 2015. Low post-glacial rebound rates in the Weddell Sea due to Late Holocene ice-sheet readvance. Earth and Planetary Science Letters 413, 79–89.

Bradley, S.L., Siddall, M., Milne, G.A., Masson-Delmotte, V., Wolff, E., 2012. Where might we find evidence of a Last Interglacial West Antarctic Ice Sheet collapse in Antarctic ice core records? Global and Planetary Change 88, 64–75. Available from: https://doi.org/10.1016/j.gloplacha.2012.03.004.

Brancolini, G., Busetti, M., Marchetti, A., De Santis, L., Zanolla, C., Cooper, A.K., et al., 1995b. Descriptive text for the Seismic Stratigraphic Atlas of the Ross Sea. In: Cooper, A. K., Barker, P.F., Brancolini, G. (Eds.), Geology and Seismic Stratigraphy of the Antarctic Margin. Antarctic Research Series 68 AGU, Washington, DC, pp. A268–A271.

Brancolini, G., Cooper, A.K., Coren, F., 1995a. Seismic facies and glacial history in the Western Ross Sea Antarctica. In: Cooper, A.K., Barker, P.F., Brancolini, G. (Eds.), Geology and Seismic Stratigraphy of the Antarctic Margin. Antarctic Research Series 68. AGU, Washington, DC, pp. 209–233.

Brierley, C.M., Fedorov, A.V., Liu, Z., Herbert, T.D., Lawrence, K.T., LaRiviere, J.P., 2009. Greatly expanded tropical warm pool and weakened Hadley circulation in the early Pliocene. Science 323 (5922), 1714–1718. Available from: https://doi.org/10.1126/science.1167625.

Briggs, R.D., Pollard, D., Tarasov, L., 2014. A data-constrained large ensemble analysis of Antarctic evolution since the Eemian. Quaternary Science Reviews 103, 91–115.

Brigham-Grette, J., 1999. Marine isotope stage11 high sea level record from northwest Alaska. In: Poore, R.Z., et al., (Eds.), Marine Oxygen Isotope Stage 11 and Associated Terrestrial Records. U.S. Geological Survey, pp. 19–20. Open File Reports, 99–312.

Bronselaer, B., Winton, M., Griffies, S.M., Hurlin, W.J., Rodgers, K.B., Sergienko, O.V., et al., 2018. Change in future climate due to Antarctic meltwater. Nature 564 (7734), 53–58. Available from: https://doi.org/10.1038/s41586-018-0712-z.

Bueler, E., Brown, J., 2009. Shallow shelf approximation as a "sliding law" in a thermomechanically coupled ice sheet model. Journal of Geophysical Research: Earth Surface 114 (F3). Available from: https://doi.org/10.1029/2008JF001179.

Buono, M.R., Fordyce, R.E., Marx, F.G., Fernández, M.S., Reguero, M., 2019. Eocene Antarctica: a window into the earliest history of modern whales. *Advances in Polar*. Science 30 (3), 293–302.

Burckle, L.H., Gersonde, R., Abrams, N., 1990. Late Pliocene-Pleistocene Paleoclimate in the Jane Basin Region ODP Site 697 [Series].

Capron, E., Govin, A., Feng, R., Otto-Bliesner, B.L., Wolff, E.W., 2017. Critical evaluation of climate syntheses to benchmark CMIP6/PMIP4 127 ka Last Interglacial simulations in the high-latitude regions. Quaternary Science Reviews 168, 137–150. Available from: https://doi.org/10.1016/j.quascirev.2017.04.019.

Capron, E., Govin, A., Stone, E.J., Masson-Delmotte, V., Mulitza, S., Otto-Bliesner, B., et al., 2014. Temporal and spatial structure of multi-millennial temperature changes at high latitudes during the Last Interglacial. Quaternary Science Reviews 103, 116–133. Available from: https://doi.org/10.1016/j.quascirev.2014.08.018.

Carlson, A.E., Clark, P.U., 2012. Ice sheet sources of sea level rise and freshwater discharge during the last deglaciation. Reviews of Geophysics 50 (4), Available from: https://doi.org/10.1029/2011RG000371.

Chadwick, M., Allen, C.S., Sime, L.C., Hillenbrand, C.D., 2020. Analysing the timing of peak warming and minimum winter sea-ice extent in the Southern Ocean during MIS 5e. Quaternary Science Reviews 229, 106134.

Clark, P.U., Alley, R.B., Keigwin, L.D., Licciardi, J.M., Johnsen, S.J., Wang, H., 1996. Origin of the first global meltwater pulse following the last glacial maximum. Paleoceanography 11 (5), 563–577.

Clark, P.U., He, F., Golledge, N.R., Mitrovica, J.X., Dutton, A., Hoffman, J.S., et al., 2020. Oceanic forcing of penultimate deglacial and last interglacial sea-level rise. Nature 577 (7792), 660–664. Available from: https://doi.org/10.1038/s41586-020-1931-7.

Clark, P.U., Mitrovica, J.X., Milne, G.A., Tamisiea, M.E., 2002. Sea-level fingerprinting as a direct test for the source of global meltwater pulse IA. Science 295 (5564), 2438–2441.

Clark, P.U., Shakun, J.D., Marcott, S.A., Mix, A.C., Eby, M., Kulp, S., et al., 2016. Consequences of twenty-first-century policy for multi-millennial climate and sea-level change. Nature Climate Change 6 (4), 360–369. Available from: https://doi.org/10.1038/nclimate2923.

Clark, P.U., Tarasov, L., 2014. Closing the sea level budget at the Last Glacial Maximum. Proceedings of the National Academy of Sciences 111 (45), 15861–15862.

Colleoni, F., De Santis, L., Montoli, E., Olivo, E., Sorlien, C.C., Bart, P.J., et al., 2018b. Past continental shelf evolution increased Antarctic ice sheet sensitivity to climatic conditions. Scientific Reports 8 (1), 1–12. Available from: https://doi.org/10.1038/s41598-018-29718-7.

Colleoni, F., De Santis, L., Siddoway, C.S., Bergamasco, A., Golledge, N.R., Lohmann, G., et al., 2018a. Spatio-temporal variability of processes across Antarctic ice-bed–ocean interfaces. Nature Communications 9, 2289. Available from: https://doi.org/10.1038/s41467-018-04583-0.

Cook, C.P., Hill, D.J., van de Flierdt, T., Williams, T., Hemming, S.R., Dolan, A.M., et al., 2014. Sea surface temperature control on the distribution of far-traveled Southern Ocean ice-rafted detritus during the Pliocene. Paleoceanography 29 (6), 533–548. Available from: https://doi.org/10.1002/2014PA002625.

Cook, C.P., Van De Flierdt, T., Williams, T., Hemming, S.R., Iwai, M., Kobayashi, M., et al., 2013. Dynamic behaviour of the East Antarctic ice sheet during Pliocene warmth. Nature Geoscience 6 (9), 765–769. Available from: https://doi.org/10.1038/ngeo1889.

Cooper, A., Barker, P., Barrett, P., Behrendt, J., Brancolini, G., Childs, et al., 2011. The ANTOSTRAT legacy: science collaboration and international transparency in potential marine mineral resource exploitation of Antarctica. Science Diplomacy: Antarctica, Science, and the Governance of International Spaces.

Cooper, A.K., Barrett, P.J., Hinz, K., Traube, V., Letichenkov, G., Stagg, H.M., 1991. Cenozoic prograding sequences of the Antarctic continental margin: a record of glacio-eustatic and tectonic events. Marine Geology 102 (1–4), 175–213.

Cooper, A.K., P.E. O'Brien, C. Richter (Eds.), 2004. Proceedings of the Ocean Drilling Program, Scientific Results, vol. 188. College Station, TX. <https://doi.org/10.2973/odp.proc.sr.188.2004>.

Coxall, H.K., Wilson, P.A., Pälike, H., Lear, C.H., Backman, J., 2005. Rapid stepwise onset of Antarctic glaciation and deeper calcite compensation in the Pacific Ocean. Nature 433 (7021), 53–57.

Cramer, B.S., Miller, K.G., Barrett, P.J., Wright, J.D., 2011. Late Cretaceous–Neogene trends in deep ocean temperature and continental ice volume: Reconciling records of benthic foraminiferal geochemistry (δ18O and Mg/Ca) with sea level history. Journal of Geophysical Research: Oceans 116 (C12).

Crampton, J.S., Cody, R.D., Levy, R., Harwood, D., McKay, R., Naish, T.R., 2016. Southern Ocean phytoplankton turnover in response to stepwise Antarctic cooling over the past 15 million years. Proceedings of the National Academy of Sciences 113 (25), 6868–6873.

Crosta, X., Crespin, J., Swingedouw, D., Marti, O., Masson-Delmotte, V., Etourneau, J., et al., 2018. Ocean as the main driver of Antarctic ice sheet retreat during the Holocene. Global and Planetary Change 166, 62–74. Available from: https://doi.org/10.1016/j.gloplacha.2018.04.007.

Dahl-Jensen, D., Albert, M.R., Aldahan, A., Azuma, N., Balslev-Clausen, D., Baumgartner, M., et al., 2013. Eemian interglacial reconstructed from a Greenland folded ice core. Nature 493 (7433), 489.

de Boer, B., Colleoni, F., Golledge, N.R., DeConto, R.M., 2019. Paleo ice-sheet modeling to constrain past sea level. PAGES Magazine 27 (1), 20.

de Boer, B., Dolan, A.M., Bernales, J., Gasson, E., Golledge, N.R., Sutter, J., et al., 2015. Simulating the Antarctic ice sheet in the late-Pliocene warm period: PLISMIP-ANT, an ice-sheet model intercomparison project. The Cryosphere 9, 881–903. Available from: https://doi.org/10.5194/tc-9-881-2015.

de Boer, B., Haywood, A.M., Dolan, A.M., Hunter, S.J., Prescott, C.L., 2017a. The transient response of ice volume to orbital forcing during the warm late Pliocene. Geophysical Research Letters 44 (20), 10–486. Available from: https://doi.org/10.1002/2017GL073535.

de Boer, B., Haywood, A.M., Dolan, A.M., Hunter, S.J., Prescott, C.L., 2017. The transient response of ice volume to orbital forcing during the warm Late Pliocene. Geophysical Research Letters 44 (20), 10–486.

de Boer, B., Lourens, L.J., Van De Wal, R.S., 2014. Persistent 400,000-year variability of Antarctic ice volume and the carbon cycle is revealed throughout the Plio-Pleistocene. Nature Communications 5, 2999. Available from: https://doi.org/10.1038/ncomms3999.

de Boer, B., Stocchi, P., van de Wal, R.W.S., 2014b. A fully coupled 3-D ice-sheet – sea-level model: algorithm and applications. Geoscience Model Development Discussion 7, 2141–2156. Available from: http://doi.org/10.5194/gmd-7-2141-2014.

de Boer, B., Stocchi, P., Whitehouse, P., Van de Wal, R.S.W., 2017b. Current state and future perspectives on coupled ice-sheet – sea-level modelling. Quaternary Science Reviews 169, 13–28. Available from: https://doi.org/10.1016/j.quascirev.2017.05.013.

de Boer, B., Van de Wal, R.S.W., Lourens, L.J., Bintanja, R., Reerink, T.J., 2013. A continuous simulation of global ice volume over the past 1 million years with 3-D ice-sheet models. Climate Dynamics 41 (5-6), 1365–1384. Available from: https://doi.org/10.1007/s00382-012-1562-2.

DeConto, R.M., Pollard, D., 2003. Rapid Cenozoic glaciation of Antarctica induced by declining atmospheric CO_2. Nature 421 (6920), 245–249. Available from: https://doi.org/10.1038/nature01290.

DeConto, R.M., Pollard, D., Harwood, D., 2007. Sea ice feedback and Cenozoic evolution of Antarctic climate and ice sheets. Paleoceanography 22, PA3214. Available from: https://doi.org/10.1029/2006PA001350.

DeConto, R.M., Pollard, D., Kowalewski, D., 2012. Reprint of: Modeling Antarctic ice sheet and climate variations during Marine Isotope Stage 31. Global and Planetary Change 96, 181–188. Available from: https://doi.org/10.1016/j.gloplacha.2012.05.018.

DeConto, R.M., Pollard, D., Wilson, P.A., Pälike, H., Lear, C., Pagani, M., 2008. Thresholds for Cenozoic bipolar glaciation. Nature 455, 653–656.

DeConto, R.M., Pollard, D., 2016. Contribution of Antarctica to past and future sea level rise. Nature 531, 591–597. Available from: https://doi.org/10.1038/nature17145.

de La Vega, E., Chalk, T.B., Wilson, P.A., Bysani, R.P., Foster, G.L., 2020. Atmospheric CO 2 during the Mid-Piacenzian Warm Period and the M2 glaciation. Scientific reports 10 (1), 1–8.

Denton, G.H., Sugden, D.E., 2005. Meltwater features that suggest Miocene ice-sheet overriding of the Transantarctic Mountains in Victoria Land, Antarctica. Geografiska Annaler: Series A. Physical Geography 87 (1), 67–85.

Deschamps, P., Durand, N., Bard, E., Hamelin, B., Camoin, G., Thomas, A.L., et al., 2012. Ice-sheet collapse and sea-level rise at the Bølling warming 14,600 years ago. Nature 483 (7391), 559–564.

De Santis, L., Anderson, J.B., Brancolini, G., Zayatz, I., 1995. In: Cooper, A.K., et al., (Eds.), In Antarctic Research Series, vol. 71. Springer International.

De Santis, L., Brancolini, G., Donda, F., 2003. Seismo-stratigraphic analysis of the Wilkes Land continental margin (East Antarctica): influence of glacially driven processes on the Cenozoic deposition. Deep Sea Research Part II: Topical Studies in Oceanography 50 (8-9), 1563–1594. Available from: https://doi.org/10.1016/S0967-0645(03)00079-1.

De Santis, L., Prato, S., Brancolini, G., Lovo, M., Torelli, L., 1999. The Eastern Ross Sea continental shelf during the Cenozoic: implications for the West Antarctic ice sheet development. Global and Planetary Change 23 (1–4), 173–196. Available from: https://doi.org/10.1016/S0921-8181(99)00056-9.

De Schepper, S., Gibbard, P.L., Salzmann, U., Ehlers, J., 2014. A global synthesis of the marine and terrestrial evidence for glaciation during the Pliocene Epoch. Earth-Science Reviews 135, 83–102. Available from: https://doi.org/10.1016/j.earscirev.2014.04.003.

Detlef, H., Belt, S.T., Sosdian, S.M., Smik, L., Lear, C.H., Hall, I.R., et al., 2018. Sea ice dynamics across the Mid-Pleistocene transition in the Bering Sea. Nature Communications 9 (1), 1–11.

De Vleeschouwer, D., Vahlenkamp, M., Crucifix, M., Pälike, H., 2017. Alternating Southern and Northern Hemisphere climate response to astronomical forcing during the past 35 m.y. Geology 45 (4), 375–378. Available from: https://doi.org/10.1130/G38663.1.

Dickens, W.A., Kuhn, G., Leng, M.J., Graham, A.G.C., Dowdeswell, J.A., Meredith, M.P., et al., 2019. Enhanced glacial discharge from the eastern Antarctic Peninsula since the 1700s associated with a positive Southern Annular Mode. Scientific Reports 9 (1), 1–11.

Dolan, A.M., De Boer, B., Bernales, J., Hill, D.J., Haywood, A.M., 2018. High climate model dependency of Pliocene Antarctic ice-sheet predictions. Nature Communications 9 (1), 1–12. Available from: https://doi.org/10.1038/s41467-018-05179-4.

Dolan, A.M., Haywood, A.M., Hill, D.J., Dowsett, H.J., Hunter, S.J., Lunt, D.J., Pickering, S.J., 2011. Sensitivity of Pliocene ice sheets to orbital forcing. Palaeogeography, Palaeoclimatology, Palaeoecology 309 (1–2), 98–110.

Domack, E., Leventer, A., Dunbar, R., Taylor, F., Brachfeld, S., Sjunneskog, C., 2001. Chronology of the Palmer Deep site, Antarctic Peninsula: a Holocene palaeoenvironmental reference for the circum-Antarctic. The Holocene 11 (1), 1–9.

Donda, F., Brancolini, G., O'Brien, P.E., De Santis, L., Escutia, C., 2007. Sedimentary processes in the Wilkes Land margin: a record of the Cenozoic East Antarctic Ice Sheet evolution. Journal of the Geological Society of London 164, 243–256.

Dowdeswell, J.A., Batchelor, C.L., Montelli, A., Ottesen, D., Christie, F.D.W., Dowdeswell, E.K., et al., 2020. Delicate seafloor landforms reveal past Antarctic grounding-line retreat of kilometers per year. Science 368 (6494), 1020–1024. https://doi.org/10.1126/science.aaz3059.

Dowsett, H., Dolan, A., Rowley, D., Moucha, R., Forte, A.M., Mitrovica, J.X., et al., 2016. The PRISM4 (mid-Piacenzian) paleoenvironmental reconstruction. Climate of the Past 12 (7), 1519–1538.

Dowsett, H.J., Foley, K.M., Stoll, D.K., Chandler, M.A., Sohl, L.E., Bentsen, M., et al., 2013. Sea surface temperature of the mid-Piacenzian ocean: a data-model comparison. Scientific Reports 3. Available from: https://doi.org/10.1038/srep02013.

Dowsett, H.J., Robinson, M.M., Haywood, A.M., Hill, D.J., Dolan, A.M., Stoll, D.K., et al., 2012. Assessing confidence in Pliocene sea surface temperatures to evaluate predictive models. Nature Climate Change 2 (5), 365–371.

Dumitru, O.A., Austermann, J., Polyak, V.J., Fornós, J.J., Asmerom, Y., Ginés, J., et al., 2019. Constraints on global mean sea level during Pliocene warmth. Nature 574 (7777), 233–236. Available from: https://doi.org/10.1038/s41586-019-1543-2.

Dutton, A., Carlson, A.E., Long, A.J., Milne, G.A., Clark, P., DeConto, R., et al., 2015. Sea-level rise due to polar ice-sheet mass loss during past warm periods. Science 3491, 6244. https://doi.org/10.1126/science.aaa4019.

Dwyer, G.S., Chandler, M.A., 2009. Mid-Pliocene sea level and continental ice volume based on coupled benthic Mg/Ca palaeotemperatures and oxygen isotopes. Philosophical Transactions of the Royal Society A: Mathematical, Physical and Engineering Sciences 367 (1886), 157–168. Available from: https://doi.org/10.1098/rsta.2008.0222.

Edwards, T.L., Brandon, M.A., Durand, G., Edwards, N.R., Golledge, N.R., Holden, P.B., et al., 2019. Revisiting Antarctic ice loss due to marine ice-cliff instability. Nature 566 (7742), 58–64. Available from: https://doi.org/10.1038/s41586-019-0901-4.

Eittreim, S.L., Cooper, A.K., Wannesson, J., 1995. Seismic stratigraphic evidence of ice sheet advances on the Wilkes Land margin of Antarctica. Sedimentary Geology 96 (1–2), 131–156. Available from: https://doi.org/10.1016/0037-0738(94)00130-M.

Eldrett, J.S., Harding, I.C., Wilson, P.A., Butler, E., Roberts, A.P., 2007. Continental ice in Greenland during the Eocene and Oligocene. Nature 446 (7132), 176. Available from: https://doi.org/10.1038/nature05591.

EPICA Community Members, 2006. One-to-one coupling of glacial climate variability in Greenland and Antarctica. Nature 444, 195–198. Available from: https://doi.org/10.1038/nature05301.

Escutia, C., Bárcena, M.A., Lucchi, R.G., Romero, O., Ballegeer, M., Gonzalez, J.J., et al., 2009. Circum-Antarctic warming events between 4 and 3.5 Ma recorded in sediments from the Prydz Bay (ODP Leg 188) and the Antarctic Peninsula (ODP Leg 178) margins. Global and Planetary Change 69, 170–184. Available from: https://doi.org/10.1016/j.gloplacha.2009.09.003.

Escutia, C., H. Brinkhuis, A. Klaus, and the Expedition 318 Scientists, 2011. Wilkes Land Glacial History: Cenozoic East Antarctic Ice Sheet evolution from Wilkes Land margin sediments, in: Proceedings of the Integrated Ocean Drilling Program, vol. 318, Integrated Ocean Drilling Program Management International Inc., Tokyo. <https://doi.org/10.2204/iodp.proc.318.2011>.

Escutia, C., De Santis, L., Donda, F., Dunbar, R.B., Cooper, A.K., Brancolini, G., et al., 2005. Cenozoic ice sheet history from East Antarctic Wilkes Land continental margin sediments. Global and Planetary Change 45 (1–3), 51–81. Available from: https://doi.org/10.1016/j.gloplacha.2004.09.010.

Escutia, C., DeConto, R.M., Dunbar, R., Santis, L.D., Shevenell, A., Naish, T., 2019. Keeping an eye on Antarctic Ice Sheet stability. Oceanography 32 (1), 32–46.

Escutia, C., Eittreim, S.L., Cooper, A.K., 1997. Cenozoic glaciomarine sequences on the Wilkes Land continental rise, Antarctica. Proceedings Volume – VII International Symposium on Antarctic Earth Sciences 791–795.

Escutia, C., Warnke, D., Acton, G.D., Barcena, A., Burckle, L., Canals, M., et al., 2003. Sediment distribution and sedimentary processes across the Antarctic Wilkes Land margin

during the Quaternary. Deep Sea Research Part II: Topical Studies in Oceanography 50 (8–9), 1481–1508. Available from: https://doi.org/10.1016/S0967-0645(03)00073-0.

Etourneau, J., Sgubin, G., Crosta, L., Swingedouw, D., Willmott, V., Barbara, L., et al., 2019. Ocean temperature impact on ice shelf extent in the eastern Antarctic Peninsula. Nature Communications 10, 304. Available from: https://doi.org/10.1038/s41467-018-08195-6.

Evangelinos, D., Escutia, C., Etourneau, J., Hoem, F., Bijl, P., Boterblom, W., et al., 2020. Late Oligocene-Miocene proto-Antarctic Circumpolar Current dynamics off the Wilkes Land margin, East Antarctica. Global and Planetary Change 191, 103221. Available from: https://doi.org/10.1016/j.gloplacha.2020.103221.

Fischer, H., Severinghaus, J., Brook, E., Wolff, E., Albert, M., Alemany, O., et al., 2013. Where to find 1.5 million yr old ice for the IPICS "Oldest-Ice" ice core. Climate of the Past 9 (6), 2489–2505.

Flower, B.P., Kennett, J.P., 1993. Middle Miocene ocean-climate transition: High-resolution oxygen and carbon isotopic records from Deep Sea Drilling Project Site 588A, southwest Pacific. Paleoceanography 8 (6), 811–843.

Foster, G.L., Lear, C.H., Rae, J.W.B., 2012. The evolution of pCO_2, ice volume and climate during the middle Miocene. Earth and Planetary Science Letters 341–344, 243–254. Available from: https://doi.org/10.1016/j.epsl.2012.06.007.

Fretwell, P., Pritchard, H.D., Vaughan, D.G., Bamber, J.L., Barrand, N.E., Bell, R., et al., 2013. Bedmap2: improved ice bed, surface and thickness datasets for Antarctica. The Cryosphere 7 (1), 375–393. Available from: https://doi.org/10.5194/tc-7-375-2013.

Fürst, J.J., Durand, G., Gillet-Chaulet, F., Tavard, L., Rankl, M., Braun, M., et al., 2016. The safety band of Antarctic ice shelves. Nature Climate Change 6 (5), 479–482. Available from: https://doi.org/10.1038/nclimate2912.

Galeotti, S., DeConto, R.M., Naish, T.R., Stocchi, P., Florindo, F., Pagani, M., et al., 2016. Antarctic Ice Sheet variability across the Eocene-Oligocene boundary climate transition. Science 352, 76–80. Available from: https://doi.org/10.1126/science.aab0669.

Galeotti, S., et al., 2021. The Eocene-Oligocene boundary climate transition: an Antarctic perspective. In: Florindo, F., et al. (Eds.), Antarctic Climate Evolution, second ed. Elsevier (this volume).

Ganopolski, A., Robinson, A., 2011. The past is not the future. Nature Geoscience 4 (10), 661–663. Available from: https://doi.org/10.1038/ngeo1268.

Gasson, E., DeConto, R., Pollard, D., 2015. Antarctic bedrock topography uncertainty and ice sheet stability. Geophysical Research Letters 42 (13), 5372–5377.

Gasson, E., DeConto, R.M., Pollard, D., 2016. Dynamic Antarctic ice sheet during the early to mid-Miocene. Proceedings of the National Academy of Sciences of the United States of America 113 (13), 3459–3464. Available from: https://doi.org/10.1073/pnas.1516130113.

Gasson, E.G.W., Keisling, B.A., 2020. The Antarctic Ice Sheet: a paleoclimate modeling perspec-tive. Oceanography 33 (2). Available from: https://doi.org/10.5670/oceanog.2020.208.

Gasson, E., Lunt, D.J., DeConto, R., Goldner, A., Heinemann, M., Huber, M., et al., 2014. Uncertainties in the modelled CO_2 threshold for Antarctic glaciation. Climate of the Past. Available from: https://doi.org/10.5194/cp-10-451-2014.

Gersonde, R., Crosta, X., Abelmann, A., Armand, L., 2005. Sea-surface temperature and sea ice distribution of the Southern Ocean at the EPILOG Last Glacial Maximum—a circum-Antarctic view based on siliceous microfossil records. Quaternary Science Reviews 24 (7–9), 869–896.

Goelzer, H., Huybrechts, P., Loutre, M.-F., Fichefet, T., 2016. Last Interglacial climate and sea-level evolution from a coupled ice sheet−climate model. Climate of the Past 12, 2195−2213. Available from: https://doi.org/10.5194/cp-12-2195-2016.

Gohl, K., Uenzelmann-Neben, G., Larter, R.D., Hillenbrand, C.D., Hochmuth, K., Kalberg, T., et al., 2013. Seismic stratigraphic record of the Amundsen Sea Embayment shelf from pre-glacial to recent times: evidence for a dynamic West Antarctic ice sheet. Marine Geology 344, 115−131. Available from: https://doi.org/10.1016/j.margeo.2013.06.011.

Gohl, K., Wellner, J.S., Klaus, A.the Expedition 379 Scientists, 2019. Expedition 379 preliminary report: Amundsen Sea West Antarctic Ice Sheet history. International Ocean Discovery Program . Available from: https://doi.org/10.14379/iodp.pr.379.2019.

Goldner, A., Herold, N., Huber, M., 2014. The challenge of simulating the warmth of the Mid-Miocene Climatic Optimun in CESM1. Climate of the Past . Available from: https://doi.org/10.5194/cp-10-523-2014.

Golledge, N.R., Fogwill, C.J., Mackintosh, A.N., Buckley, K.M., 2012. Dynamics of the last glacial maximum Antarctic ice-sheet and its response to ocean forcing. Proceedings of the National Academy of Sciences of the United States of America 109, 16052−16056. Available from: https://doi.org/10.1073/.02pnas.1205385109.

Golledge, N.R., Keller, E.D., Gomez, N., Naughten, K.A., Bernales, J., Trusel, L.D., et al., 2019. Global environmental consequences of twenty-first-century ice-sheet melt. Nature 566 (7742), 65−72. Available from: https://doi.org/10.1038/s41586-019-0889-9.

Golledge, N.R., Kowalewski, D.E., Naish, T.R., Levy, R.H., Fogwill, C.J., Gasson, E.G., 2015. The multi-millennial Antarctic commitment to future sea-level rise. Nature 526 (7573), 421−425. Available from: https://doi.org/10.1038/nature15706.

Golledge, N.R., Levy, R.H., McKay, R.M., Fogwill, C.J., White, D.A., Graham, A.G., et al., 2013. Glaciology and geological signature of the Last Glacial Maximum Antarctic ice sheet. Quaternary Science Reviews 78, 225−247.

Golledge, N.R., Levy, R.H., McKay, R.M., Naish, T.R., 2017b. East Antarctic ice sheet most vulnerable to Weddell Sea warming. Geophysical Research Letters 44 (5), 2343−2351.

Golledge, N.R., Menviel, L., Carter, L., Fogwill, C.J., England, M.H., Cortese, G., et al., 2014. Antarctic contribution to meltwater pulse 1A from reduced Southern Ocean overturning. Nature Communications 5, 5107. Available from: https://doi.org/10.1038/ncomms6107.

Golledge, N.R., Thomas, Z.A., Levy, R.H., Gasson, E.G., Naish, T.R., McKay, R.M., et al., 2017a. Antarctic climate and ice-sheet configuration during the early Pliocene interglacial at 4.23 Ma. Climate of the Past 13 (7). Available from: https://doi.org/10.5194/cp-13-959-2017.

Golledge, N.R., 2020. Long-term projections of sea-level rise from ice sheets. Wiley Interdisciplinary Reviews: Climate Change 11 (2), e634.

Gomez, N., Latychev, K., Pollard, D., 2018. A coupled ice sheet−sea level model incorporating 3D earth structure: variations in Antarctica during the last deglacial retreat. Journal of Climate 31 (10), 4041−4054.

Gomez, N., Mitrovica, J.X., Huybers, P., Clark, P.U., 2010. Sea level as a stabilizing factor for marine-ice-sheet grounding lines. Nature Geoscience. 3, 850−853.

Gomez, N., Pollard, D., Holland, D., 2015. Sea-level feedback lowers projections of future Antarctic Ice-Sheet mass loss. Nature Communications 6 (1), 1−8. Available from: https://doi.org/10.1038/ncomms9798.

Gomez, N., Pollard, D., Mitrovica, J.X., 2013. A 3-D coupled ice sheet−sea level model applied to Antarctica through the last 40 ky. Earth and Planetary Science Letters 384, 88−99. Available from: https://doi.org/10.1016/j.epsl.2013.09.042.

Gomez, N., Weber, M.E., Clark, P.U., Mitrovica, J.X., Han, H.K., 2020. Antarctic ice dynamics amplified by Northern Hemisphere sea-level forcing. Nature 587 (7835), 600–604.

Graham, A.G., Dutrieux, P., Vaughan, D.G., Nitsche, F.O., Gyllencreutz, R., Greenwood, S.L., et al., 2013. Seabed corrugations beneath an Antarctic ice shelf revealed by autonomous underwater vehicle survey: origin and implications for the history of Pine Island Glacier. Journal of Geophysical Research: Earth Surface 118 (3), 1356–1366.

Grant, G.R., Naish, T.R., Dunbar, G.B., Stocchi, P., Kominz, M.A., Kamp, P.J., et al., 2019. The amplitude and origin of sea-level variability during the Pliocene epoch. Nature 574 (7777), 237–241. Available from: https://doi.org/10.1038/s41586-019-1619-z.

Grant G., Naish T., 2021. Pliocene sea-level revisited: Is there more than meets the eye? PAGES. Available from: https://doi.org/10.22498/pages.29.1.34.

Grant, K.M., Rohling, E.J., Ramsey, C.B., Cheng, H., Edwards, R.L., Florindo, F., et al., 2014. Sea-level variability over five glacial cycles. Nature communications 5 (1), 1–9. Available from: https://doi.org/10.1038/ncomms6076.

Green, R.A., et al., 2020. "Evaluating seasonal sea-ice cover over the Southern Ocean from the Last Glacial Maximum". Climate of the Past Discussions 1–23.

Greenop, R., Foster, G.L., Wilson, P.A., Lear, C.H., 2014. Middle Miocene climate instability associated with high-amplitude CO_2 variability. Paleoceanography 29. Available from: https://doi.org/10.1002/2014PA002653.

Gulick, S.P., Shevenell, A.E., Montelli, A., Fernandez, R., Smith, C., Warny, S., et al., 2017. Initiation and long-term instability of the East Antarctic Ice Sheet. Nature 552 (7684), 225–229. Available from: https://doi.org/10.1038/nature25026.

Halberstadt, A.R.W., Simkins, L.M., Greenwood, S.L., Anderson, J.B., 2016. Past ice-sheet behaviour: retreat scenarios and changing controls in the Ross Sea, Antarctica. The Cryosphere 10, 1003–1020. Available from: https://doi.org/10.5194/tc-10-1003-2016.

Hambrey, M.J., W.U. Ehrmann, B. Larsen, 1991. Cenozoic glacial record of the Prydz Bay continental shelf, East Antarctica. In: Barron, J., Larsen, B., et al. (Eds.), Proceedings of the Ocean Drilling Program Scientific Results, vol. 119. College Station, TX, pp. 77–132. <https://doi.org/10.2973/odp.proc.sr.119.200.1991>.

Hannah, M.J., 2006. The palynology of ODP site 1165, Prydz Bay, East Antarctica: a record of Miocene glacial advance and retreat. Palaeogeography, Palaeoclimatology, Palaeoecology 231 (1–2), 120–133. Available from: https://doi.org/10.1016/j.palaeo.2005.07.029.

Hansen, M.A., Passchier, S., Khim, B.-K., Song, B., Williams, T., 2015. Threshold behavior of a marine-based sector of the East Antarctic Ice Sheet in response to early Pliocene ocean warming. Paleoceanography 30. Available from: https://doi.org/10.1002/2014PA002704.

Hansen, M.A., Passchier, S., 2017. Oceanic circulation changes during early Pliocene marine ice-sheet instability in Wilkes Land, East Antarctica. Geo-Marine Letters. Available from: https://doi.org/10.1007/s00367-016-0489-8.

Hartman, J.D., Sangiorgi, F., Peterse, F., Barcena, M.A., Albertazzi, S., Asioli, A., et al., 2016. Phytoplankton assemblages and lipid biomarkers indicate sea-surface warming and sea-ice decline in the Ross Sea during Marine Isotope sub-Stage 5e. *EGUGA*, EPSC2016-2637.

Hartman, J.D., Sangiorgi, F., Salabarnada, A., Peterse, F., Houben, A.J., Schouten, S., et al., 2018. Paleoceanography and ice sheet variability offshore Wilkes Land, Antarctica-Part 3: insights from Oligocene-Miocene TEX86-based sea surface temperature reconstructions. Climate of the Past 14 (9), 1275–1297. Available from: https://doi.org/10.5194/cp-14-1275-2018.

Hauptvogel, D.W., Passchier, S., 2012. Early–Middle Miocene (17–14 Ma) Antarctic ice dynamics reconstructed from the heavy mineral provenance in the AND-2A drill core, Ross

Sea, Antarctica. Global and Planetary Change 82, 38–50. Available from: https://doi.org/10.1016/j.gloplacha.2011.11.003.

Haywood, A.M., Dowsett, H.J., Dolan, A.M., 2016. Integrating geological archives and climate models for the mid-Pliocene warm period. Nature Communications 7 (1), 1–14. Available from: https://doi.org/10.1038/ncomms10646.

Haywood, A.M., Hill, D.J., Dolan, A.M., Otto-Bliesner, B.L., Bragg, F., Chan, W.L., et al., 2013. Large-scale features of Pliocene climate: results from the Pliocene Model Intercomparison Project. Climate of the Past 9 (1), 191–209.

Haywood, A.M., Tindall, J.C., Dowsett, H.J., Dolan, A.M., Foley, K.M., Hunter, S.J., et al., 2020. A return to large-scale features of Pliocene climate: the Pliocene Model Intercomparison Project Phase 2, Climate of the Past Discussions, in review. <https://doi.org/10.5194/cp-2019-145>.

Haywood, A.M., Valdes, P.J., Aze, T., Barlow, N., Burke, A., Dolan, A.M., et al., 2019. What can Palaeoclimate Modelling do for you? Earth Systems and Environment 3 (1), 1–18. Available from: https://doi.org/10.1007/s41748-019-00093-1.

Hearty, P.J., Kindler, P., Cheng, H., Edwards, R.L., 1999. A +20 m middle Pleistocene sea-level highstand (Bermuda and the Bahamas) due to partial collapse of Antarctic ice. Geology 27 (4), 375–378.

Hearty, P.J., Rovere, A., Sandstrom, M.R., O'Leary, M.J., Roberts, D., Raymo, M.E., 2020. Pliocene-Pleistocene Stratigraphy and Sea-Level Estimates, Republic of South Africa With Implications for a 400 ppmv CO_2 World. Paleoceanography and Paleoclimatology 35 (7), e2019PA003835.

Herbert, T.D., Lawrence, K.T., Tzanova, A., Peterson, L.C., Caballero-Gill, R., Kelly, C.S., 2016. Late Miocene global cooling and the rise of modern ecosystems. Nature Geoscience 9 (11), 843–847. Available from: https://doi.org/10.1038/ngeo2813.

Herold, N., Seton, M., Müller, R.D., You, Y., Huber, M., 2008. Middle Miocene tectonic boundary conditions for use in climate models. Geochemistry, Geophysics, Geosystems 9, Q10009. Available from: https://doi.org/10.1029/2008GC002046.

Hillenbrand, C.-D., Bentley, M.J., Stolldorf, T.D., Hein, A.S., Kuhn, G., Graham, A.G.C., et al., 2014. Reconstruction of changes in the Weddell Sea sector of the Antarctic Ice Sheet since the Last Glacial Maximum. Quaternary Science Review. 100, 111–136. Available from: https://doi.org/10.1016/j.quascirev.2013.07.020.

Hillenbrand, C.D., Ehrmann, W., 2005. Late Neogene to Quaternary environmental changes in the Antarctic Peninsula region: evidence from drift sediments. Global and Planetary Change 45 (1–3), 165–191.

Hillenbrand, C.D., Kuhn, G., Frederichs, T., 2009. Record of a Mid-Pleistocene depositional anomaly in West Antarctic continental margin sediments: an indicator for ice-sheet collapse? Quaternary Science Reviews 28 (13–14), 1147–1159.

Hillenbrand, C.D., Melles, M., Kuhn, G., Larter, R.D., 2012. Marine geological constraints for the grounding-line position of the Antarctic Ice Sheet on the southern Weddell Sea shelf at the Last Glacial Maximum. Quaternary Science Reviews 32, 25–47.

Hillenbrand, C.D., Smith, J.A., Hodell, D.A., Greaves, M., Poole, C.R., Kender, S., et al., 2017. West Antarctic Ice Sheet retreat driven by Holocene warm water incursions. Nature 547 (7661), 43–48. Available from: https://doi.org/10.1038/nature22995.

Hochmuth, K., Gohl, K., 2019. "Seaward growth of Antarctic continental shelves since establishment of a continent-wide ice sheet: Patterns and mechanisms.". Palaeogeography, Palaeoclimatology, Palaeoecology 520, 44–54. Available from: https://doi.org/10.1016/j.palaeo.2019.01.025.

Hochmuth, K., Gohl, K., Leitchenkov, G., Sauermilch, I., Whittaker, J.M., Uenzelmann-Neben, G., et al., 2020. The evolving paleobathymetry of the circum-Antarctic Southern Ocean since 34 Ma – a key to understanding past cryosphere-ocean developments. Geochemistry, Geophysics, Geosystems. Available from: https://doi.org/10.1029/2020GC009122.

Hodell, D.A., Charles, C.D., Ninnemann, U.S., 2000. Comparison of interglacial stages in the South Atlantic sector of the southern ocean for the past 450 kyr: implifications for Marine Isotope Stage (MIS) 11. Global and Planetary Change 24 (1), 7–26.

Hodgson, D.A., Graham, A.G., Roberts, S.J., Bentley, M.J., Cofaigh, C.O., Verleyen, E., et al., 2014. Terrestrial and submarine evidence for the extent and timing of the Last Glacial Maximum and the onset of deglaciation on the maritime-Antarctic and sub-Antarctic islands. Quaternary Science Reviews 100, 137–158.

Hoffman, J.S., Clark, P.U., Parnell, A.C., He, F., 2017. Regional and global sea-surface temperatures during the last interglaciation. Science 355 (6322), 276–279. Available from: https://doi.org/10.1126/science.aai8464.

Holbourn, A., Kuhnt, W., Clemens, S., Prell, W., Andersen, N., 2013. Middle to late Miocene stepwise climate cooling: Evidence from a high-resolution deep water isotope curve spanning 8 million years. Paleoceanography 28 (4), 688–699.

Holbourn, A., Kuhnt, W., Lyle, M., Schneider, L., Romero, O., Andersen, N., 2014. Middle Miocene climate cooling linked to intensification of eastern equatorial Pacific upwelling. Geology 42 (1), 19–22. Available from: https://doi.org/10.1130/G34890.1.

Holbourn, A., Kuhnt, W., Schulz, M., Flores, J.A., Andersen, N., 2007. Orbitally-paced climate evolution during the middle Miocene "Monterey" carbon-isotope excursion. Earth and Planetary Science Letters 261 (3-4), 534–550.

Holloway, M.D., Sime, L.C., Singarayer, J.S., Tindall, J.C., Bunch, P., Valdes, P.J., 2016. Antarctic last interglacial isotope peak in response to sea ice retreat not ice-sheet collapse. Nature Communications 7 (1), 1–9. Available from: https://doi.org/10.1038/ncomms12293.

Honisch, B., Hemming, G., Archer, D., Siddal, M., McManus, J., 2009. Atmospheric carbon dioxide concentration across the Mid-Pleistocene Transition. Science 324, 1551–1554. Available from: https://doi.org/10.1126/science.1171477.

Horgan, H.J., Christianson, K., Jacobel, R.W., Anandakrishnan, S., Alley, R.B., 2013. Sediment deposition at the modern grounding zone of Whillans Ice Stream, West Antarctica. Geophysical Research Letters 40 (15), 3934–3939.

Huang, X., Gohl, K., Jokat, W., 2014. Variability in Cenozoic sedimentation and paleo-water depths of the Weddell Sea basin related to pre-glacial and glacial conditions of Antarctica. Global and Planetary Change 118, 25–41. Available from: https://doi.org/10.1016/j.gloplacha.2014.03.010.

Huang, X., Jokat, W., 2016. Middle Miocene to present sediment transport and deposits in the Southeastern Weddell Sea, Antarctica. Global and Planetary Change 139, 211–225.

Huang, X., Stärz, M., Gohl, K., Knorr, G., Lohmann, G., 2017. Impact of Weddell Sea shelf progradation on Antarctic bottom water formation during the Miocene. Paleoceanography 32 (3), 304–317. Available from: https://doi.org/10.1002/2016PA002987.

Huybrechts, P., 2002. Sea-level changes at the LGM from ice-dynamic reconstructions of the Greenland and Antarctic ice sheets during the glacial cycles. Quaternary Science Review 21, 203–231. Available from: https://doi.org/10.1016/S0277-3791(01)00082-8.

Imbrie J., Hays J.D., Martinson D.G., McIntyre A., Mix A.C., Morely J.J., et al., 1984. The orbital theory of Pleistocene climate: support from a revised chronology of the marined 18O record. In: Berger, A.L. (Ed.), Milankovitch and Climate, vol. 1. D. Reidel, Dordrecht, pp. 269–305.

IPCC A.R.5., 2013. Climate Change (2013): The Physical Science Basis. Contribution of Working Group I to the Fifth Assessment Report of the Intergovernmental Panel on Climate Change [T. F. Stocker, D. Qin, G.-K. Plattner, M. Tignor, S.K. Allen, J. Boschung, A. Nauels, Y. Xia, V. Bex, and P.M. Midgley (Eds.)]. Cambridge University Press, Cambridge, United Kingdom, and New York, pp. 1535. <https://doi.org/10.1017/CBO9781107415324>.

IPCC, S.R.O.C.C., 2019. IPCC Special Report on the Ocean and Cryosphere in a Changing Climate [H.-O. Pörtner, D.C. Roberts, V. Masson-Delmotte, P. Zhai, M. Tignor, E. Poloczanska, K. Mintenbeck, A. Alegría, M. Nicolai, A. Okem, J. Petzold, B. Rama, N.M. Weyer (Eds.)].

Ivins, E.R., James, T.S., 2005. Antarctic glacial isostatic adjustment: a new assessment. Antarctic Science 17 (4), 541. Available from: https://doi.org/10.1017/S0954102005002968.

Ivins, E.R., James, T.S., Wahr, J., O. Schrama, E.J., Landerer, F.W., Simon, K.M., 2013. Antarctic contribution to sea level rise observed by GRACE with improved GIA correction. Journal of Geophysical Research: Solid Earth 118 (6), 3126–3141. Available from: https://doi.org/10.1002/jgrb.50208.

Jakobsson, M., Anderson, J.B., Nitsche, F.O., Dowdeswell, J.A., Gyllencreutz, R., Kirchner, N., et al., 2011. Geological record of ice shelf break-up and grounding line retreat, Pine Island Bay, West Antarctica. Geology 39 (7), 691–694.

Jakobsson, M., Anderson, J.B., Nitsche, F.O., Gyllencreutz, R., Kirshner, A.E., Kirchner, N., et al., 2012. Ice sheet retreat dynamics inferred from glacial morphology of the central Pine Island Bay Trough, West Antarctica. Quaternary Science Reviews 38, 1–10.

Jakob, K.A., Wilson, P.A., Pross, J., Ezard, T.H., Fiebig, J., Repschläger, J., et al., 2020. A new sea-level record for the Neogene/Quaternary boundary reveals transition to a more stable East Antarctic Ice Sheet. Proceedings of the National Academy of Sciences 117 (49), 30980–30987.

Jamieson, S.S., Vieli, A., Cofaigh, C.Ó., Stokes, C.R., Livingstone, S.J., Hillenbrand, C.D., 2014. Understanding controls on rapid ice-stream retreat during the last deglaciation of Marguerite Bay, Antarctica, using a numerical model. Journal of Geophysical Research: Earth Surface 119 (2), 247–263.

Jamieson, S.S., Vieli, A., Livingstone, S.J., Cofaigh, C.Ó., Stokes, C., Hillenbrand, C.D., et al., 2012. Ice-stream stability on a reverse bed slope. Nature Geoscience 5 (11), 799–802. Available from: https://doi.org/10.1038/ngeo1600.

Jansen, E., Fronval, T., Rack, F., Channell, J.E., 2000. Pliocene-Pleistocene ice rafting history and cyclicity in the Nordic Seas during the last 3.5 Myr. Paleoceanography 15 (6), 709–721.

Jansen, E., et al., 2007. In: Solomon, S.D., et al., (Eds.), Climate Change 2007: The Physical Science Basis. Cambridge University Press, pp. 433–497.

Johnson, J.S., Bentley, M.J., Smith, J.A., Finkel, R.C., Rood, D.H., Gohl, K., et al., 2014. Rapid thinning of Pine Island Glacier in the early Holocene. Science 343 (6174), 999–1001.

Jones, R.S., Mackintosh, A.N., Norton, K.P., Golledge, N.R., Fogwill, C.J., Kubik, P.W., et al., 2015. Rapid Holocene thinning of an East Antarctic outlet glacier driven by marine ice sheet instability. Nature Communications 6 (1), 1–9.

Joughin, I., Alley, R.B., 2011. Stability of the West Antarctic ice sheet in a warming world. Nature Geoscience 4 (8), 506–513. Available from: https://doi.org/10.1038/ngeo1194.

Jouzel, J., Masson-Delmotte, V., Cattani, O., Dreyfus, G., Falourd, S., Hoffmann, G., et al., 2007. Orbital and millennial Antarctic climate variability over the past 800,000 years. Science 317 (5839), 793–796. Available from: https://doi.org/10.1126/science.1141038.

Justino, F., Kucharski, F., Lindemann, D., Wilson, A., Stordal, F., 2019. A modified seasonal cycle during MIS31 super-interglacial favors stronger interannual ENSO and monsoon

variability. Climate of the Past 15 (2), 735–749. Available from: https://doi.org/10.5194/cp-15-735-2019.

Justino, F., Lindemann, D., Kucharski, F., Wilson, A., Bromwich, D., Stordal, F., 2017. Oceanic response to changes in the WAIS and astronomical forcing during the MIS31 superinterglacial. Climate of the Past 13, 1081–1095. Available from: https://doi.org/10.5194/cp-13-1081-2017.

Kageyama, M., Braconnot, P., Harrison, S.P., Haywood, A.M., Jungclaus, J.H., Otto-Bliesner, B. L., et al., 2018. The PMIP4 contribution to CMIP6 – Part 1: overview and over-arching analysis plan. Geoscientific Model Development 11 (3), 1033–1057.

Karas, C., Khélifi, N., Bahr, A., Naafs, B.D.A., Nürnberg, D., Herrle, J.O., 2020. Did North Atlantic cooling and freshening from 3.65–3.5 Ma precondition Northern Hemisphere ice sheet growth? Global and Planetary Change 185, 103085.

Katz, M.E., Miller, K.G., Wright, J.D., Wade, B.S., Browning, J.V., Cramer, B.S., et al., 2008. Stepwise transition from the Eocene greenhouse to the Oligocene icehouse. Nature Geoscience 1 (5), 329–334. Available from: https://doi.org/10.1038/ngeo179.

Kemp, A.E.S., Grigorov, I., Pearce, R.B., Garabato, A.N., 2010. Migration of the Antarctic Polar Front through the mid-Pleistocene transition: evidence and climatic implications. Quaternary Science Reviews 29 (17–18), 1993–2009. Available from: https://doi.org/10.1016/j.quascirev.2010.04.027.

Kennedy, A.T., Farnsworth, A., Lunt, D.J., Lear, C.H., Markwick, P.J., 2015. Atmospheric and oceanic impacts of Antarctic glaciation across the Eocene–Oligocene transition. Philosophical Transactions of the Royal Society A 373. Available from: https://doi.org/10.1098/rsta.2014.041920140419.

Kennett, J.P., 1977. Cenozoic evolution of Antarctic glaciation, the circum-Antarctic Ocean, and their impact on global paleoceanography. Journal of Geophysical Research 82 (27), 3843–3860.

Kim, S., De Santis, L., Hong, J.K., Cottlerle, D., Petronio, L., Colizza, E., et al., 2018. Seismic stratigraphy of the Central Basin in northwestern Ross Sea slope and rise, Antarctica: clues to the late Cenozoic ice-sheet dynamics and bottom-current activity. Marine Geology 395, 363–379. Available from: https://doi.org/10.1016/j.margeo.2017.10.013.

Kindler, P., Hearty, P.J., 2000. Elevated marine terraces from Eleuthera (Bahamas) and Bermuda: sedimentological, petrographic and geochronological evidence for important deglaciation events during the middle Pleistocene. Global and Planetary Change 24 (1), 41–58.

Kingslake, J., Scherer, R.P., Albrecht, T., Coenen, J., Powell, R.D., Reese, R., et al., 2018. Extensive retreat and re-advance of the West Antarctic Ice Sheet during the Holocene. Nature 558 (7710), 430–434. Available from: https://doi.org/10.1038/s41586-018-0208-x.

King, A.L., Howard, W.R., 2000. Middle Pleistocene sea-surface temperature change in the southwest Pacific Ocean on orbital and suborbital time scales. Geology 28 (7), 659–662.

Kirkham, J.D., Hogan, K.A., Larter, R.D., Arnold, N.S., Nitsche, F.O., Golledge, N.R., et al., 2019. Past water flow beneath Pine Island and Thwaites glaciers, West Antarctica. The Cryosphere 13, 1959–1981. Available from: https://doi.org/10.5194/tc-13-1959-2019.

Klages, J.P., Kuhn, G., Graham, A.G., Hillenbrand, C.D., Smith, J.A., Nitsche, F.O., et al., 2015. Palaeo-ice stream pathways and retreat style in the easternmost Amundsen Sea Embayment, West Antarctica, revealed by combined multibeam bathymetric and seismic data. Geomorphology 245, 207–222.

Klages, J.P., Kuhn, G., Hillenbrand, C.D., Smith, J.A., Graham, A.G., Nitsche, F.O., et al., 2017. Limited grounding-line advance onto the West Antarctic continental shelf in the

easternmost Amundsen Sea Embayment during the last glacial period. PLoS One 12 (7), e0181593.

Kominz, M.A., Browning, J.V., Miller, K.G., Sugarman, P.J., Mizintseva, S., Scotese, C.R., 2008. Late Cretaceous to Miocene sea-level estimates from the New Jersey and Delaware coastal plain coreholes: an error analysis. Basin Research 20 (2), 211–226. Available from: https://doi.org/10.1111/j.1365-2117.2008.00354.x.

Konfirst, M.A., Scherer, R.P., Hillenbrand, C.D., Kuhn, G., 2012. A marine diatom record from the Amundsen Sea—insights into oceanographic and climatic response to the Mid-Pleistocene transition in the West Antarctic sector of the Southern Ocean. Marine Micropaleontology 92, 40–51.

Konrad, H., Thoma, M., Sasgen, I., Klemann, V., Grosfeld, K., Barbi, D., et al., 2014. The deformational response of a viscoelastic solid earth model coupled to a thermomechanical ice sheet model. Surveys in Geophysics. 35, 1441–1458. Available from: https://doi.org/10.1007/s10712-013-9257-8.

Kristoffersen, Y., Jokat, W., 2008. The Weddell Sea. In: Cooper et al., Cenozoic climate history from seismic-reflection and drilling studies on the Antarctic continental margin. In: Florindo, F., Siegert, M. (Eds.), Antarctic Climate Evolution, vol. 8. Elsevier, pp. 144–152.

Kriwet, J., Engelbrecht, A., Mörs, T., Reguero, M., Pfaff, C., 2016. Ultimate Eocene (Priabonian) chondrichthyans (Holocephali, Elasmobranchii) of Antarctica. Journal of Vertebrate Paleontology 36 (4), e1160911.

Kuhn, G., Hillenbrand, C.D., Kasten, S., Smith, J.A., Nitsche, F.O., Frederichs, T., et al., 2017. Evidence for a palaeo-subglacial lake on the Antarctic continental shelf. Nature Communications 8 (1), 1–10.

Kulpecz, A.A., Miller, K.G., Browning, J.V., Edwards, L.E., Powars, D.S., McLaughlin, P.P., Jr., et al., 2009. Post-impact deposition in the Chesapeake Bay impact structure: Variations in eustasy, compaction, sediment supply, and passive-aggressive tectonism. In: Gohn, G.S., et al. (Eds.), The ICDP-USGS Deep Drilling Project in the Chesapeake Bay Impact Structure: Results from the Eyreville Core Holes: Geological Society of America Special Paper 458, pp. 811–837. <https://doi.org/10.1130/2009.2458(34)>.

Kunz-Pirrung, M., Gersonde, R., Hodell, D.A., 2002. Mid-Brunhes century-scale diatom sea surface temperature and sea ice records from the Atlantic sector of the Southern Ocean (ODP Leg 177, sites 1093, 1094 and core PS2089-2). Palaeogeography, Palaeoclimatology, Palaeoecology 182 (3–4), 305–328. Available from: https://doi.org/10.1016/S0031-0182(01)00501-6.

Ladant, J.B., Donnadieu, Y., Lefebvre, V., Dumas, C., 2014. The respective role of atmospheric carbon dioxide and orbital parameters on ice sheet evolution at the Eocene-Oligocene transition. Paleoceanography 29 (8), 810–823. Available from: https://doi.org/10.1002/2013PA002593.

Lambeck, K., Chappell, J., 2001. Sea level change through the last glacial cycle. Science 292, 679–686. Available from: https://doi.org/10.1126/science.1059549.

Lambeck, K., Rouby, H., Purcell, A., Sun, Y., Sambridge, M., 2014. Sea level and global ice volumes from the Last Glacial Maximum to the Holocene. Proceedings of the National Academy of Sciences 111 (43), 15296–15303. Available from: https://doi.org/10.1073/pnas.1411762111.

Lambeck, K., Yokoyama, Y., Purcell, A., 2002. Into and out of the Last glacial Maximum sea level change during Oxygen Isotope Stages 3–2. Quaternary Science Reviews 21, 343–360.

Lamy, F., Chiang, J.C.H., Martínez-Méndez, G., Thierens, M., Arz, H.W., Bosmans, J., et al., 2019. Precession modulation of the South Pacific westerly wind belt over the past million

years. Proceedings of the National Academy of Sciences 116 (47), 23455–23460. Available from: https://doi.org/10.1073/pnas.1905847116.

Lamy, F., Gersonde, R., Winckler, G., Esper, O., Jaeschke, A., Kuhn, G., et al., 2014. Increased dust deposition in the Pacific Southern Ocean during glacial periods. Science 343 (6169), 403–407.

Langebroek, P.M., Paul, A., Schulz, M., 2009. Antarctic ice-sheet response to atmospheric CO_2 and insolation in the Middle Miocene. Climate of the Past 5 (4). Available from: https://doi.org/10.5194/cp-5-633-2009.

Lang, N., Wolff, E.W., 2011. Interglacial and glacial variability from the last 800 ka in marine, ice and terrestrial archives. Climate of the Past 7 (2), 361–380. Available from: https://doi.org/10.5194/cp-7-361-2011.

Larter, R.D., Anderson, J.B., Graham, A.G., Gohl, K., Hillenbrand, C.D., Jakobsson, M., et al., 2014. Reconstruction of changes in the Amundsen Sea and Bellingshausen sea sector of the West Antarctic ice sheet since the last glacial maximum. Quaternary Science Reviews 100, 55–86.

Larter, R.D., Hogan, K.A., Hillenbrand, C.D., Smith, J.A., Batchelor, C.L., Cartigny, M., et al., 2019. Subglacial hydrological control on flow of an Antarctic Peninsula palaeo-ice stream. Cryosphere 13 (6), 1583–1596. Available from: https://doi.org/10.5194/tc-13-1583-2019.

Larter, R.D., Rebesco, M., Vanneste, L.E., Gambôa, L.A.P., Barker, P.F., 1997. Cenozoic Tectonic, Sedimentary and Glacial History of the Continental Shelf West of Graham Land, Antarctic Peninsula. In: Barker, P.F., Cooper, A.K. (Eds.), Geology and Seismic Stratigraphy of the Antarctic Margin, vol. 2. American Geophysical Union, pp. 1–27.

Lear, C.H., Bailey, T.R., Pearson, P.N., Coxall, H.K., Rosenthal, Y., 2008. Cooling and ice growth across the Eocene-Oligocene transition. Geology 36 (3), 251–254. Available from: https://doi.org/10.1130/g24584a.1.

Lear, C.H., Coxall, H.K., Foster, G.L., Lunt, D.J., Mawbey, E.M., Rosenthal, Y., et al., 2015. Neogene ice volume and ocean temperatures: insights from infaunal foraminiferal Mg/Ca paleothermometry. Paleoceanography 30 (11), 1437–1454.

Lee, J.I., McKay, R.M., Golledge, N.R., Yoon, H.I., Yoo, K.C., Kim, H.J., et al., 2017. Widespread persistence of expanded East Antarctic glaciers in the southwest Ross Sea during the last deglaciation. Geology 45 (5), 403–406.

Levy, R., Harwood, D., Florindo, F., Sangiorgi, F., Tripati, R., von Eynatten, H., et al.,SMS Science Team 2016. Early to mid-Miocene Antarctic Ice Sheet dynamics. Proceedings of the National Academy of Sciences Mar 2016 113 (13), 3453–3458. Available from: https://doi.org/10.1073/pnas.1516030113.

Levy, R.H., Meyers, S.R., Naish, T.R., Golledge, N.R., McKay, R.M., Crampton, J.S., et al., 2019. Antarctic ice-sheet sensitivity to obliquity forcing enhanced through ocean connections. Nature Geoscience 12, 132–137. Available from: https://doi.org/10.1038/s41561-018-0284-4.

Levy, R.H., et al., 2021. Antarctic environmental change and ice sheet evolution through the Miocene to Pliocene - a perspective from the Ross Sea and George V to Wilkes Land Coasts. In: Florindo, F., et al. (Eds.), Antarctic Climate Evolution, second edition. Elsevier (this volume).

Lewis, A.R., Ashworth, A.C., 2016. An early to middle Miocene record of ice-sheet and landscape evolution from the Friis Hills, Antarctica. GSA Bulletin 128 (5–6), 719–738.

Lewis, A.R., Marchant, D.R., Ashworth, A.C., Hedenäs, L., Hemming, S.R., Johnson, J.V., et al., 2008. Mid-Miocene cooling and the extinction of tundra in continental Antarctica. Proceedings of the National Academy of Sciences 105 (31), 10676–10680.

Liakka, J., Colleoni, F., Ahrens, B., Hickler, T., 2014. The impact of climate-vegetation interactions on the onset of the Antarctic ice sheet. Geophysical Research Letters 41 (4), 1269–1276. Available from: https://doi.org/10.1002/2013GL058994.

Licht, K.J., 2004. The Ross Sea's contribution to eustatic sea level during meltwater pulse 1A. Sedimentary Geology 165 (3–4), 343–353.

Lindeque, A., Gohl, K., Henrys, S., Wobbe, F., Davy, B., 2016. Seismic stratigraphy along the Amundsen Sea to Ross Sea continental rise: A cross-regional record of pre-glacial to glacial processes of the West Antarctic margin. Palaeogeography, Palaeoclimatology, Palaeoecology 443, 183–202.

Lisiecki, L.E., Raymo, M.E., 2005. A Pliocene-Pleistocene stack of 57 globally distributed benthic $\delta^{18}O$ records. Paleoceanography 20 (1). Available from: https://doi.org/10.1029/2004PA001071.

Liu, Z., He, Y., Jiang, Y., Wang, H., Liu, W., Bohaty, S.M., et al., 2018. Transient temperature asymmetry between hemispheres in the Palaeogene Atlantic Ocean. Nature Geoscience 11 (9), 656–660. Available from: https://doi.org/10.1038/s41561-018-0182-9.

Liu, J., Milne, G.A., Kopp, R.E., Clark, P.U., Shennan, I., 2016. Sea-level constraints on the amplitude and source distribution of Meltwater Pulse 1A. Nature Geoscience 9 (2), 130–134.

Liu, Z., Pagani, M., Zinniker, D., DeConto, R., Huber, M., Brinkhuis, H., et al., 2009. Global cooling during the Eocene–Oligocene climate transition. Science 323, 1187–1190.

Livingstone, S.J., O'Cofaigh, C., Stokes, C.R., Hillenbrand, C.-D., Vieli, A., Jamieson, S.S.R., 2013. Glacial geomorphology of Marguerite Bay Palaeo-Ice stream, western Antarctic Peninsula. Journal of Maps 9, 558–572.

Loutre, M.F., Berger, A., 2003. Marine Isotope Stage 11 as an analogue for the present interglacial. Global and Planetary Change 36 (3), 209–217. Available from: https://doi.org/10.1016/S0921-8181(02)00186-8.

Lowry, D.P., Golledge, N.R., Bertler, N.A., Jones, R.S., McKay, R., 2019. Deglacial grounding-line retreat in the Ross Embayment, Antarctica, controlled by ocean and atmosphere forcing. Science Advances 5 (8), eaav8754. Available from: https://doi.org/10.1126/sciadv.aav8754.

Lunt, D.J., Haywood, A.M., Schmidt, G.A., Salzmann, U., Valdes, P.J., Dowsett, H.J., et al., 2012. On the causes of mid-Pliocene warmth and polar amplification. Earth and Planetary Science Letters 321, 128–138.

Lunt, D.J., Huber, M., Anagnostou, E., Baatsen, M.L., Caballero, R., DeConto, R., et al., 2017. The DeepMIP contribution to PMIP4: Experimental design for model simulations of the EECO, PETM, and pre-PETM (version 1.0). Geoscientific Model Development 10 (2), 889–901.

Lüthi, D., Le Floch, M., Bereiter, B., Blunier, T., Barnola, J.M., Siegenthaler, U., et al., 2008. High-resolution carbon dioxide concentration record 650,000–800,000 years before present. Nature 453 (7193), 379–382.

Lythe, M.B., Vaughan, D.G., 2001. BEDMAP: A new ice thickness and subglacial topographic model of Antarctica. Journal of Geophysical Research: Solid Earth 106 (B6), 11335–11351.

Mackintosh, A., Golledge, N., Domack, E., Dunbar, R., Leventer, A., White, D., et al., 2011. Retreat of the East Antarctic ice sheet during the last glacial termination. Nature Geoscience 4 (3), 195–202. Available from: https://doi.org/10.1038/ngeo1061.

Mackintosh, A.N., Verleyen, E., O'Brien, P.E., White, D.A., Jones, R.S., McKay, R., et al., 2014. Retreat history of the East Antarctic Ice Sheet since the last glacial maximum. Quaternary Science Reviews 100, 10–30.

Marino, G., Rohling, E.J., Rodríguez-Sanz, L., Grant, K.M., Heslop, D., Roberts, A.P., et al., 2015. Bipolar seesaw control on last interglacial sea level. Nature 522 (7555), 197–201. Available from: https://doi.org/10.1038/nature14499.

Maris, M.N.A., De Boer, B., Ligtenberg, S.R.M., Crucifix, M., Van de Berg, W.J., Oerlemans, J., 2014. Modelling the evolution of the Antarctic ice sheet since the last interglacial. The Cryosphere 8 (4), 1347–1360.

Martín-Español, A., King, M.A., Zammit-Mangion, A., Andrews, S.B., Moore, P., Bamber, J.L., 2016. An assessment of forward and inverse GIA solutions for Antarctica. Journal of Geophysical Research: Solid Earth 121 (9), 6947–6965.

Martinez-Boti, M.A., Foster, G.L., Chalk, T.B., Rohling, E.J., Sexton, P.F., et al., 2015. Plio-Pleistocene climate sensitivity evaluated using high-resolution CO_2 records. Nature 518, 49–54. Available from: https://doi.org/10.1038/nature14145.

Mas e Braga, M., Bernales, J., Prange, M., Stroeven, A.P., Rogozhina, I., 2021. Sensitivity of the Antarctic ice sheets to the peak warming of Marine Isotope Stage 11. The Cryosphere 15, 459–478. Available from: https://doi.org/10.5194/tc-2020-112.

Masson-Delmotte, V., Schulz, M., Abe-Ouchi, A., Beer, J., Ganopolski, A., Gonzáles Rouco, J.F., et al., 2013. Information from paleoclimate archives. In: Stocker, T.F., Qin, D., Plattner, G.K., Tignor, M., Allen, S.K., Boschung, J., Nauels, A., Xia, Y., Bex, V., Midgley, P.M. (Eds.), Climate Change 2013: The Physical Science Basis. Contribution of Working Group I to the Fifth Assessment Report of the Intergovernmental Panel on Climate Change. Cambridge University Press, Cambridge, United Kingdom and New York.

Matsuoka, K., Hindmarsh, R.C., Moholdt, G., Bentley, M.J., Pritchard, H.D., Brown, J., et al., 2015. Antarctic ice rises and rumples: Their properties and significance for ice-sheet dynamics and evolution. Earth-Science Reviews 150, 724–745.

McKay, R., Browne, G., Carter, L., Cowan, E., Dunbar, G., Krissek, L., et al., 2009. The stratigraphic signature of the late Cenozoic Antarctic Ice Sheets in the Ross Embayment. GSA Bulletin 121 (11–12), 1537–1561. Available from: https://doi.org/10.1130/B26540.1.

McKay, R.M., De Santis, L., Kulhanek, D.K.the Expedition 374 Scientists, 2019. Ross Sea West Antarctic Ice Sheet History. Proceedings of the International Ocean Discovery Program, 374:. International Ocean Discovery Program, College Station, TX, https://doi.org/10.14379/iodp.proc.374.2019.

McKay, R., Golledge, N.R., Maas, S., Naish, T., Levy, R., Dunbar, G., et al., 2016. Antarctic marine ice-sheet retreat in the Ross Sea during the early Holocene. Geology 44 (1), 7–10.

McKay, R.M., Naish, T., Carter, L., Riesselman, C., Dunbar, R., Sjunneskog, C., et al., 2012a. Antarctic and Southern Ocean influences on Late Pliocene global cooling. Proceedings of the National Academy of Sciences of the United States of America 109 (17), 6423–6428. Available from: https://doi.org/10.1073/pnas.1112248109.

McKay, R.M., Naish, T., Powell, R., Barrett, P., Talarico, F., Kyle, P., et al., 2012b. Pleistocene variability of Antarctic Ice Sheet extent in the Ross Embayment. Quaternary Science Reviews 34, 93–112. Available from: https://doi.org/10.1016/j.quascirev.2011.12.012.

McKay, R.M., et al., 2021. Cenozoic History of Antarctic Glaciation and Climate from onshore and offshore studies. In: Florindo, F., et al. (Eds.), Antarctic Climate Evolution, second edition. Elsevier (this volume).

Melles, M., Brigham-Grette, J., Minyuk, P.S., Nowaczyk, N.R., Wennrich, V., DeConto, R.M., et al., 2012. 2.8 million years of Arctic climate change from Lake El'gygytgyn, NE Russia. Science 337 (6092), 315–320. Available from: https://doi.org/10.1126/science.1222135.

Mengel, M., Levermann, A., 2014. Ice plug prevents irreversible discharge from East Antarctica. Nature Climate Change 4 (6), 451–455. Available from: https://doi.org/10.1038/nclimate2226.

Menviel, L., Timmermann, A., Timm, O.E., Mouchet, A., 2011. Deconstructing the Last Glacial termination: the role of millennial and orbital-scale forcings. Quaternary Science Reviews 30 (9–10), 1155–1172.

Miller, K.G., Browning, J.V., Schmelz, W.J., Kopp, R.E., Mountain, G.S., Wright, J.D., 2020a. Cenozoic sea-level and cryospheric evolution from deep-sea geochemical and continental margin records. Science Advances, 6 (20), eaaz1346. Available from: https://doi.org/10.1126/sciadv.aaz1346.

Miller, K.G., Kominz, M.A., Browning, J.V., Wright, J.D., Mountain, G.S., Katz, M.E., et al., 2005. The Phanerozoic record of global sea-level change. Science 310 (5752), 1293–1298. Available from: https://doi.org/10.1126/science.1116412.

Miller, K.G., Schmelz, W.J., Browning, J.V., Kopp, R.E., Mountain, G.S., Wright, J.D., 2020b. Ancient sea level as key to the future. Oceanography 33 (2), 32–41. Available from: https://doi.org/10.5670/oceanog.2020.224.

Miller, K.G., Wright, J.D., Browning, J.V., Kulpecz, A., Kominz, M., Naish, T.R., et al., 2012. High tide of the warm Pliocene: Implications of global sea level for Antarctic deglaciation. Geology 40 (5), 407–410. Available from: https://doi.org/10.1130/G32869.1.

Miller, K.G., Wright, J.D., Fairbanks, R.G., 1991. Unlocking the ice house: Oligocene-Miocene oxygen isotopes, eustasy, and margin erosion. Journal of Geophysical Research: Solid Earth 96 (B4), 6829–6848. Available from: https://doi.org/10.1029/90JB02015.

Miller, K.G., Wright, J.D., Katz, M.E., Browning, J.V., Cramer, B.S., Wade, B.S., et al., 2008. A view of Antarctic ice-sheet evolution from sea-level and deep-sea isotope changes during the Late Cretaceous–Cenozoic. Antarctica: A Keystone in a Changing World 55–70.

Miller, K.G., Wright, J.D., Katz, M.E., Wade, B.S., Browning, J.V., Cramer, B.S., et al., 2009. Climate threshold at the Eocene-Oligocene transition: Antarctic ice sheet influence on ocean circulation. Geological Society of America Special Paper 452, 169–178. Available from: https://doi.org/10.1130/2009.2452(11).

Milne, G.A., Mitrovica, J.X., 2008. Searching for eustasy in deglacial sea-level histories. Quaternary Science Reviews 27 (25–26), 2292–2302.

Minzoni, R.T., Majewski, W., Anderson, J.B., Yokoyama, Y., Fernandez, R., Jakobsson, M., 2017. Oceanographic influences on the stability of the Cosgrove Ice Shelf. Antarctica. The Holocene 27 (11), 1645–1658.

Morlighem, M., Rignot, E., Binder, T., Blankenship, D., Drews, R., Eagles, G., et al., 2020. Deep glacial troughs and stabilizing ridges unveiled beneath the margins of the Antarctic ice sheet. Nature Geoscience 13 (2), 132–137. Available from: https://doi.org/10.1038/s41561-019-0510-8.

Naish, T.R., et al., 2001. "Orbitally induced oscillations in the East Antarctic ice sheet at the Oligocene/Miocene boundary.". Nature 413 (6857), 719–723.

Naish, T., Powell, R., Levy, R., Wilson, G., Scherer, R., Talarico, F., et al., 2009a. Obliquity-paced Pliocene West Antarctic Ice Sheet oscillations. Nature 458, 322–328. Available from: https://doi.org/10.1038/nature07867.

Naish, T.R., Wilson, G.S., 2009b. Constraints on the amplitude of Mid-Pliocene (3.6–2.4 Ma) eustatic sea-level fluctuations from the New Zealand shallow-marine sediment record. Philosophical Transactions of the Royal Society A: Mathematical, Physical and Engineering Sciences 367 (1886), 169–187. Available from: https://doi.org/10.1098/rsta.2008.0223.

Naish, T., Zwartz, D., 2012. Looking back to the future. Nature Climate Change 2 (5), 317–318.

Naish, T., Duncan, B., Levy., R., McKay, R., Escutia, C., De Santis, L., et al., 2021. Antarctic Ice Sheet dynamics during the Late Oligocene and Early Miocene: Climatic conundrums

revisited. In: Florindo, F., et al. (Eds.), Antarctic Climate Evolution, second edition. Elsevier (this volume).

Nakada, M., Kimura, R., Okuno, J., Moriwaki, K., Miura, H., Maemoku, H., 2000. Late Pleistocene and Holocene melting history of the Antarctic ice sheet derived from sea-level variations. Marine Geology 167 (1–2), 85–103.

Nichols, K.A., Goehring, B.M., Balco, G., Johnson, J.S., Hein, A.A., Todd, C., 2019. New Last Glacial Maximum Ice Thickness constraints for the Weddell Sea sector, Antarctica. The Cryosphere Discussions . Available from: https://doi.org/10.5194/tc-2019-64.

Nitsche, F.O., Gohl, K., Larter, R.D., Hillenbrand, C.D., Kuhn, G., Smith, J.A., et al., 2013. Paleo ice flow and subglacial meltwater dynamics in Pine Island Bay, West Antarctica. The Cryosphere 7, 249–262.

Noble, T.L., Rohling, E.J., Aitken, A.R.A., Bostock, H.C., Chase, Z., Gomez, N., et al., 2020. The sensitivity of the Antarctic Ice Sheet to a changing climate: Past, present and future. Reviews of Geophysics 58 (4). Available from: https://doi.org/10.1029/2019RG000663.

O'Brien, P.E., Cooper, A.K., Florindo, F., Handwerger, D.A., Lavelle, M., Passchier, S., et al., 2004. Prydz channel fan and the history of extreme ice advances in Prydz Bay. Proceedings of the Ocean Drilling Program, Scientific Results 188, 1–32. ISSN 0884-5891.

O'Brien, P.E., Goodwin, I., Forsberg, C.F., Cooper, A.K., Whitehead, J., 2007. Late Neogene ice drainage changes in Prydz Bay, East Antarctica and the interaction of Antarctic ice sheet evolution and climate. Palaeogeography, Palaeoclimatology, Palaeoecology 245 (3–4), 390–410. Available from: https://doi.org/10.1016/j.palaeo.2006.09.002.

O'Brien, P., Opdyke, B., Post, A., Armand, L., 2020. Sabrina Sea Floor Survey (IN2017-V01) Piston Core Images, Visual Logs and Grain Size DATA Summaries IN2017-V01-A005-PC01.

Otto-Bliesner, B.L., Jahn, A., Feng, R., Brady, E.C., Hu, A., Löfverström, M., 2017. Amplified North Atlantic warming in the late Pliocene by changes in Arctic gateways. Geophysical Research Letters 44 (2), 957–964. Available from: https://doi.org/10.1002/2016GL071805.

O'Cofaigh, C., Davies, B.J., Livingstone, S.J., Smith, J.A., Johnson, J.S., Hocking, E.P., et al., 2014. Reconstruction of ice-sheet changes in the Antarctic Peninsula since the Last Glacial Maximum. Quaternary Science Reviews 100, 87–110.

Pagani, M., Huber, M., Liu, Z., Bohaty, S., Henderiks, J., et al., 2011. The role of carbon dioxide during the onset of Antarctic Glaciation. Science 334, 1261–1264. Available from: https://doi.org/10.1126/science.1203909.

Pagani, M., Liu, Z., LaRiviere, J., Ravelo, A.C., 2010. High Earth-system climate sensitivity determined from Pliocene carbon dioxide concentrations. Nature Geoscience 3, 27–30. Available from: https://doi.org/10.1038/ngeo724.

Pagani, M., Zachos, J.C., Freeman, K.H., Tipple, B., Bohaty, S., 2005. Carbon dioxide concentrations during the Paleogene. Science 309, 600–603. Available from: https://doi.org/10.1126/science.1110063.

Pälike, H., Norris, R.D., Herrle, J.O., Wilson, P.A., Coxall, H.K., Lear, C.H., et al., 2006. The heartbeat of the Oligocene climate system. Science 314, 1894–1897.

Paolo, F.S., Fricker, H.A., Padman, L., 2015. Volume loss from Antarctic ice shelves is accelerating. Science 348 (6232), 327–331. Available from: https://doi.org/10.1126/science.aaa0940.

Parrenin, F., Cavitte, M.G., Blankenship, D.D., Chappellaz, J., Fischer, H., Gagliardini, O., et al., 2017. Is there 1.5-million-year-old ice near Dome C, Antarctica? The Cryosphere 11 (6), 2427–2437.

Passchier, S., Bohaty, S.M., Jiménez-Espejo, F., Pross, J., Röhl, U., van de Flierdt, T., et al., 2013. Early Eocene − to − middle Miocene cooling and aridification of East Antarctica. Geochemistry, Geophysics, Geosystems 14 (5), 1399−1410. Available from: https://doi.org/10.1002/ggge.20106.

Passchier, S., Browne, G., Field, B., Fielding, C.R., Krissek, L.A., Panter, K.ANDRILL-SMS Science Team, 2011. Early and middle Miocene Antarctic glacial history from the sedimentary facies distribution in the AND-2A drill hole, Ross Sea, Antarctica. GSA Bulletin 123 (11−12), 2352−2365. Available from: https://doi.org/10.1130/B30334.1.

Passchier, S., Ciarletta, D., Miriagos, T., Bijl, P., Bohaty, S., 2016. An Antarctic stratigraphic record of step-wise ice growth through the Eocene-Oligocene Transition. Geological Society of America Bulletin 129 (3−4), 318−330. Available from: https://doi.org/10.1130/B31482.

Patterson, M.O., McKay, R., Naish, T., Escutia, C., Jimenez-Espejo, F.J., Raymo, M.E., et al., 2014. Orbital forcing of the East Antarctic ice sheet during the Pliocene and Early Pleistocene. Nature Geoscience 7, 841−847. Available from: https://doi.org/10.1038/ngeo2273.

Pattyn, F., Ritz, C., Hanna, E., Asay-Davis, X., DeConto, R., Durand, G., et al., 2018. The Greenland and Antarctic ice sheets under 1.5 C global warming. Nature Climate Change 8 (12), 1053−1061. Available from: https://doi.org/10.1038/s41558-018-0305-8.

Paxman, G.J.G., Gasson, E.G.W., Jamieson, S.S.R., Bentley, M.J., Ferraccioli, F., 2020. Long-term increase in Antarctic Ice Sheet vulnerability driven by bed topography evolution. Geophysical Research Letters 47. Available from: https://doi.org/10.1029/2020GL090003.

Paxman, G.J., Jamieson, S.S., Hochmuth, K., Gohl, K., Bentley, M.J., Leitchenkov, G., et al., 2019. Reconstructions of Antarctic topography since the Eocene−Oligocene boundary. Palaeogeography, Palaeoclimatology, Palaeoecology 535, 109346. Available from: https://doi.org/10.1016/j.palaeo.2019.109346.

Pedro, J.B., Jochum, M., Buizert, C., He, F., Barker, S., Rasmussen, S.O., 2018. Beyond the bipolar seesaw: Toward a process understanding of interhemispheric coupling. Quaternary Science Reviews 192, 27−46. Available from: https://doi.org/10.1016/j.quascirev.2018.05.005.

Pekar, S.F., Christie-Blick, N., Kominz, M.A., Miller, K.G., 2002. Calibration between eustatic estimates from backstripping and oxygen isotopic records for the Oligocene. Geology 30 (10), 903−906. Available from: https://doi.org/10.1130/0091-7613.

Pekar, S.F., Christie-Blick, N., 2008. Resolving apparent conflicts between oceanographic and Antarctic climate records and evidence for a decrease in pCO_2 during the Oligocene through early Miocene (34−16 Ma). Palaeogeography, Palaeoclimatology, Palaeoecology 260 (1−2), 41−49. Available from: https://doi.org/10.1016/j.palaeo.2007.08.019.

Peltier, W.R., Argus, D.F., Drummond, R., 2015. Space geodesy constrains ice age terminal deglaciation: The global ICE-6G_C (VM5a) model. Journal of Geophysical Research: Solid Earth 120 (1), 450−487.

Peltier, W.R., Fairbanks, R.G., 2006. Global glacial ice volume and Last Glacial Maximum duration from an extended Barbados sea level record. Quaternary Science Reviews 25 (23−24), 3322−3337.

Peltier, W.R., 2004. Global glacial isostasy and the surface of the ice-age Earth: the ICE-5G (VM2) model and GRACE. Annual Review of Earth and Planetary Sciences 32, 111−149.

Peltier, W.R., 2005. On the hemispheric origins of meltwater pulse 1a. Quaternary Science Reviews 24 (14−15), 1655−1671.

Petit, J.R., Jouzel, J., Raynaud, D., Barkov, N.I., Barnola, J.M., Basile, I., et al., 1999. Climate and atmospheric history of the past 420,000 years from the Vostok ice core, Antarctica. Nature 399 (6735), 429. Available from: https://doi.org/10.1038/20859.

Petrini, M., Colleoni, F., Kirchner, N., Hughes, A.L., Camerlenghi, A., Rebesco, M., et al., 2018. Interplay of grounding-line dynamics and sub-shelf melting during retreat of the Bjørnøyrenna Ice Stream. Scientific Reports 8 (1), 1−-9.

Philippon, G., Ramstein, G., Charbit, S., Kageyama, M., Ritz, C., Dumas, C., 2006. Evolution of the Antarctic ice sheet throughout the last deglaciation: A study with a new coupled climate—north and south hemisphere ice sheet model. Earth and Planetary Science Letters 248 (3−4), 750−758. Available from: https://doi.org/10.1016/j.epsl.2006.06.017.

Pierce, E.L., van de Flierdt, T., Williams, T., Hemming, S.R., Cook, C.P., Passchier, S., 2017. Evidence for a dynamic East Antarctic ice sheet during the mid-Miocene climate transition. Earth and Planetary Science Letters 478, 1−13.

Pollard, D., Chang, W., Haran, M., Applegate, P., DeConto, R., 2016. Large ensemble modeling of the last deglacial retreat of the West Antarctic Ice Sheet: comparison of simple and advanced statistical techniques. Geoscientific Model Development . Available from: https://doi.org/10.5194/gmd-9-1697-2016.

Pollard, D., DeConto, R.M., 2003. Antarctic ice and sediment flux in the Oligocene simulated by a climate−ice sheet−sediment model. Palaeogeography, Palaeoclimatology, Palaeoecology 198 (1−2), 53−67. Available from: https://doi.org/10.1016/S0031-0182(03)00394-8.

Pollard, D., DeConto, R.M., 2005. Hysteresis in Cenozoic Antarctic ice-sheet variations. Global and Planetary Change 45 (1−3), 9−21. Available from: https://doi.org/10.1016/j.gloplacha.2004.09.011.

Pollard, D., DeConto, R.M., 2009. Modelling West Antarctic ice sheet growth and collapse through the past five million years. Nature 458 (7236), 329−332. Available from: https://doi.org/10.1038/nature07809.

Pollard, D., DeConto, R.M., 2012. Description of a hybrid ice sheet-shelf model, and application to Antarctica. Geoscientific Model Development 5 (5), 1273−1295. Available from: https://doi.org/10.5194/gmd-5-1273-2012.

Pollard, D., DeConto, R.M., Alley, R.B., 2015. Potential Antarctic Ice Sheet retreat driven by hydrofracturing and ice cliff failure. Earth and Planetary Science Letters 412, 112−121. Available from: https://doi.org/10.1016/j.epsl.2014.12.035.

Pollard, D., Gomez, N., Deconto, R.M., 2017. Variations of the Antarctic ice sheet in a coupled ice sheet-Earth-sea level model: sensitivity to viscoelastic Earth properties. Journal of Geophysical Research: Earth Surface 122 (11), 2124−2138. Available from: https://doi.org/10.1002/2017JF004371.

Pollard, D., DeConto, R.M., 2020. Continuous simulations over the last 40 million years with a coupled Antarctic ice sheet-sediment model. Palaeogeography, Palaeoclimatology, Palaeoecology 537, 109374. Available from: https://doi.org/10.1016/j.palaeo.2019.109374.

Presti, M., Barbara, L., Denis, D., Schmidt, S., De Santis, L., Crosta, X., 2011. Sediment delivery and depositional patterns off Adélie Land (East Antarctica) in relation to late Quaternary climatic cycles. Marine Geology 284 (1−4), 96−113.

Pritchard, H., Ligtenberg, S.R., Fricker, H.A., Vaughan, D.G., van den Broeke, M.R., Padman, L., 2012. Antarctic ice-sheet loss driven by basal melting of ice shelves. Nature 484 (7395), 502−505. Available from: https://doi.org/10.1038/nature10968.

Pross, J., Contreras, L., Bijl, P.K., Greenwood, D.R., Bohaty, S.M., Schouten, S., et al., 2012. Persistent near-tropical warmth on the Antarctic continent during the early Eocene epoch. Nature 488 (7409), 73−77.

Prothro, L.O., Majewski, W., Yokoyama, Y., Simkins, L.M., Anderson, J.B., Yamane, M., et al., 2020. Timing and pathways of East Antarctic Ice Sheet retreat. Quaternary Science Reviews 230, 106166.

Prothro, L.O., Simkins, L.M., Majewski, W., Anderson, J.B., 2018. Glacial retreat patterns and processes determined from integrated sedimentology and geomorphology records. Marine Geology 395, 104–119.

Quiquet, A., Dumas, C., Ritz, C., Peyaud, V., Roche, D.M., 2018. The GRISLI ice sheet model (version 2.0): calibration and validation for multi-millennial changes of the Antarctic ice sheet. Geoscientific Model Development 11 (12), 5003. Available from: https://doi.org/10.5194/gmd-11-5003-2018.

Raymo, M.E., Kozdon, R., Evans, D., Lisiecki, L., Ford, H.L., 2018. The accuracy of mid-Pliocene $\delta^{18}O$-based ice volume and sea level reconstructions. Earth-Science Reviews 177, 291–302.

Raymo, M.E., Lisiecki, L.E., Nisancioglu, K.H., 2006. Plio-Pleistocene ice volume, Antarctic climate, and the global δ18O record. Science 313 (5786), 492–495. Available from: https://doi.org/10.1126/science.1123296.

Raymo, M.E., Mitrovica, J.X., O'Leary, M.J., DeConto, R.M., Hearty, P.J., 2011. Departures from eustasy in Pliocene sea-level records. Nature Geoscience 4 (5), 328–332.

Raymo, M.E., Mitrovica, J.X., 2012. Collapse of polar ice sheets during the stage 11 interglacial. Nature 483 (7390), 453–456. Available from: https://doi.org/10.1038/nature10891.

Rayner, N., Parker, D.E., Horton, E., Folland, C., Alexander, L., Rowell, D., et al., 2003. Global analyses of sea surface temperature, sea ice, and night marine air temperature since the late nineteenth century. Journal of Geophysical Research 108 (D14), 4407. Available from: https://doi.org/10.1029/2002JD002670.

Rebesco, M., Camerlenghi, A., Geletti, R., Canals, M., 2006. Margin architecture reveals the transition to the modern Antarctic ice sheet ca. 3 Ma. Geology 34 (4), 301–304. Available from: https://doi.org/10.1130/G22000.1.

Rebesco, M., Domack, E., Zgur, F., Lavoie, C., Leventer, A., Brachfeld, S., Pettit, E., 2014. Boundary condition of grounding lines prior to collapse, Larsen-B Ice Shelf, Antarctica. Science 345 (6202), 1354–1358.

Reinardy, B.T.I., Escutia, C., Iwai, M., Jimenez-Espejo, F.J., Cook, C., van de Flierdt, T., et al., 2015. Repeated advance and retreat of the East Antarctic Ice Sheet on the continental shelf during the early Pliocene warm period. Palaeogeography, Palaeoclimatology, Palaeoecology 422, 65–84.

Retallack, G.J., 2009. Refining a pedogenic-carbonate CO_2 paleobarometer to quantify a middle Miocene greenhouse spike. Palaeogeography, Palaeoclimatology, Palaeoecology 281 (1-2), 57–65.

Reyes, A.V., Carlson, A.E., Beard, B.L., Hatfield, R.G., Stoner, J.S., Winsor, K., et al., 2014. South Greenland ice-sheet collapse during marine isotope stage 11. Nature 510 (7506), 525–528. Available from: https://doi.org/10.1038/nature13456.

Rignot, E., Mouginot, J., Scheuchl, B., van den Broeke, M., van Wessem, M.J., Morlighem, M., 2019. Four decades of Antarctic Ice Sheet mass balance from 1979–2017. Proceedings of the National Academy of Sciences 116 (4), 1095–1103. Available from: https://doi.org/10.1073/pnas.1812883116.

Rintoul, S.R., Silvano, A., Pena-Molino, B., van Wijk, E., Rosenberg, M., Greenbaum, J.S., et al., 2016. Ocean heat drives rapid basal melt of the Totten Ice Shelf. Science Advances 2 (12), e1601610.

Roberts, D.L., Karkanas, P., Jacobs, Z., Marean, C.W., Roberts, R.G., 2012. Melting ice sheets 400,000 yr ago raised sea level by 13 m: past analogue for future trends. Earth and Planetary Science Letters 357, 226–237. Available from: https://doi.org/10.1016/j.epsl.2012.09.006.

Roche, D.M., Paillard, D., Caley, T., Waelbroeck, C., 2014. LGM hosing approach to Heinrich Event 1: results and perspectives from data–model integration using water isotopes. Quaternary Science Reviews 106, 247–261. Available from: https://doi.org/10.1016/j.quascirev.2014.07.020.

Rohling, E.J., Grant, K., Bolshaw, M., Roberts, A.P., Siddall, M., Hemleben, C., et al., 2009. Antarctic temperature and global sea level closely coupled over the past five glacial cycles. Nature Geoscience 2 (7), 500–504. Available from: https://doi.org/10.1038/ngeo557.

Rovere, A., Antonioli, F., Bianchi, C.N., 2015. Fixed biological indicators. Handbook of Sea-Level Research. Wiley, pp. 268–280.

Rovere, A., Raymo, M.E., Mitrovica, J.X., Hearty, P.J., O'Leary, M.J., Inglis, J.D., 2014. The Mid-Pliocene sea-level conundrum: glacial isostasy, eustasy and dynamic topography. Earth and Planetary Science Letters 387, 27–33.

Roy, K., Peltier, W., 2018. Relative sea level in the Western Mediterranean Basin: a regional test of the ICE-7G NA (VM7) model and a constraint on Late Holocene Antarctic Deglaciation. Quaternary Science Reviews 183, 76–87.

Sadai, S., Condron, A., DeConto, R., Pollard, D., 2020. Future climate response to Antarctic Ice Sheet melt caused by anthropogenic warming. Science Advances 6 (39), eaaz1169.

Salabarnada, A., Escutia, C., Röhl, U., Nelson, C.H., McKay, R., Jiménez-Espejo, F.J., et al., 2018. Paleoceanography and ice sheet variability offshore Wilkes Land, Antarctica—part 1: insights from late Oligocene astronomically paced contourite sedimentation. Climate of the Past 14 (7), 991–1014. Available from: https://doi.org/10.5194/cp-14-991-2018.

Sandstrom, M.R., O'Leary, M.J., Barham, M., Cai, Y., Rasbury, E.T., Wooton, K.M., et al., 2021. Age constraints on surface deformation recorded by fossil shorelines at Cape Range, Western Australia. GSA Bulletin 133.

Sangiorgi, F., Bijl, P.K., Passchier, S., Salzmann, U., Schouten, S., McKay, R., et al., 2018. Southern Ocean warming and Wilkes Land ice sheet retreat during the mid-Miocene. Nature Communications 9 (1), 1–11. Available from: https://doi.org/10.1038/s41467-017-02609-7.

Scherer, R.P., Bohaty, S.M., Dunbar, R.B., Esper, O., Flores, J.A., Gersonde, R., et al., 2008. Antarctic records of precession-paced insolation-driven warming during early Pleistocene Marine Isotope Stage 31. Geophysical Research Letters 35 (3), Available from: https://doi.org/10.1029/2007GL032254.

Scherer, R., Bohaty, S., Harwood, D., Roberts, A., Taviani, M., 2003. Marine Isotope Stage 31 (1.07 Ma): an extreme interglacial in the Antarctic nearshore zone. Geophysical Research Abstracts 5, 11710.

Scherer, R.P., DeConto, R.M., Pollard, D., Alley, R.B., 2016. Windblown Pliocene diatoms and East Antarctic Ice Sheet retreat. Nature Communications 7 (1), 1–9. Available from: https://doi.org/10.1038/ncomms12957.

Schmidtko, S., Heywood, K.J., Thompson, A.F., Aoki, S., 2014. Multidecadal warming of Antarctic waters. Science 346 (6214), 1227–1231.

Schneider von Deimling, T., Ganopolski, A., Held, H., Rahmstorf, S., 2006. How cold was the last glacial maximum? Geophysical Research Letters 33, 14.

Schüpbach, S., Federer, U., Kaufmann, P., Albani, S., Barbante, C., Stocker, T., et al., 2013. High-resolution mineral dust and sea ice proxy records from the Talos Dome ice core. Climate of the Past 9 (6), 2789–2807. Available from: https://doi.org/10.5194/cp-9-2789-2013.

Seki, O., Foster, G.L., Schmidt, D.N., Mackensen, A., Kawamura, K., Pancost, R.D., 2010. Alkenone and boron based Plio-Pleistocene pCO2 records. Earth and Planetary Science Letters 292, 201–211. Available from: https://doi.org/10.1016/j.epsl.2010.01.037.

Shackleton, N.J., 2000. The 100,000-year Ice-Age cycle identified and found to lag temperature, carbon dioxide, and orbital eccentricity. Science 289, 1897–1902.

Shakun, J.D., Corbett, L.B., Bierman, P.R., Underwood, K., Rizzo, D.M., Zimmerman, S.R., et al., 2018. Minimal East Antarctic Ice Sheet retreat onto land during the past eight million years. Nature 558 (7709), 284–287. Available from: https://doi.org/10.1038/s41586-018-0155-6.

Shepherd, A., Ivins, E., Rignot, E., Smith, B., Van Den Broeke, M., Velicogna, I., et al., 2018. Mass balance of the Antarctic Ice Sheet from 1992 to 2017. Nature 558, 219–222. Available from: https://doi.org/10.1038/s41586-018-0179-y.

Shevenell, A.E., Ingalls, A.E., Domack, E.W., Kelly, C., 2011. Holocene Southern Ocean surface temperature variability west of the Antarctic Peninsula. Nature 470 (7333), 250–254.

Shevenell, A.E., Kennett, J.P., Lea, D.W., 2008. Middle Miocene ice sheet dynamics, deep-sea temperatures, and carbon cycling: a Southern Ocean perspective. Geochemistry, Geophysics, Geosystems 9 (2).

Siegert, M.J., Alley, R.B., Rignot, E., Englander, J., Corell, R., 2020. 21st Century sea-level rise could exceed IPCC predictions for strong-warming futures. One Earth 3, 691–703. Available from: https://doi.org/10.1016/j.oneear.2020.11.002.

Siegert, M.J., Hein, A.S., White, D.A., Gore, D.B., De Santis, L., Hillenbrand, C.D., 2021. Antarctic ice sheet changes since the Last Glacial Maximum. In: Florindo, F., et al. (Eds.), Antarctic Climate Evolution, second edition. Elsevier (this volume).

Silvano, A., Rintoul, S.R., Kusahara, K., Peña-Molino, B., van Wijk, E., Gwyther, D.E., et al., 2019. Seasonality of warm water intrusions onto the continental shelf near the Totten Glacier. Journal of Geophysical Research: Oceans 124 (6), 4272–4289.

Sime, L.C., Hodgson, D., Bracegirdle, T.J., Allen, C., Perren, B., Roberts, S., et al., 2016. Sea ice led to poleward-shifted windsat the Last Glacial Maximum: the influence of state dependency on CMIP5 and PMIP3 models. Climate of the Past 12 (12), 2241–2253. Available from: https://doi.org/10.5194/cp-12-2241-2016.

Simkins, L.M., Greenwood, S.L., Anderson, J.B., 2018. Diagnosing ice sheet grounding line stability from landform morphology. The Cryosphere 12, 2707–2726. Available from: https://doi.org/10.5194/tc-12-2707-2018.

Simkins, L.M., Anderson, J.B., Greenwood, S.L., Gonnermann, H.M., Prothro, L.O., Halberstadt, A.R.W., et al., 2017. Anatomy of a meltwater drainage system beneath the ancestral East Antarctic ice sheet. Nature Geoscience 10 (9), 691–697. Available from: https://doi.org/10.1038/ngeo3012.

Simms, A.R., Lisiecki, L., Gebbie, G., Whitehouse, P.L., Clark, J.F., 2019. Balancing the last glacial maximum (LGM) sea-level budget. Quaternary Science Reviews 205, 143–153.

Small, D., Bentley, M.J., Jones, R.S., Pittard, M.L., Whitehouse, P.L., 2019. Antarctic ice sheet palaeo-thinning rates from vertical transects of cosmogenic exposure ages. Quaternary Science Reviews 206, 65–80.

Smith, J.A., Andersen, T.J., Shortt, M., Gaffney, A.M., Truffer, M., Stanton, T.P., et al., 2017. Sub-ice-shelf sediments record history of twentieth-century retreat of Pine Island Glacier. Nature 541 (7635), 77–80.

Smith, J.A., Graham, A.G., Post, A.L., Hillenbrand, C.D., Bart, P.J., Powell, R.D., 2019. The marine geological imprint of Antarctic ice shelves. Nature Communications 10 (1), 1–16. Available from: https://doi.org/10.1038/s41467-019-13496-5.

Sosdian, S., Rosenthal, Y., 2009. Deep-sea temperature and ice volume changes across the Pliocene-Pleistocene climate transitions. Science 325, 306–310. Available from: https://doi.org/10.1126/science.1169938.

Spector, P., Stone, J., Cowdery, S.G., Hall, B., Conway, H., Bromley, G., 2017. Rapid early-Holocene deglaciation in the Ross Sea, Antarctica. Geophysical Research Letters 44 (15), 7817–7825.

Spector, P., Stone, J., Pollard, D., Hillebrand, T., Lewis, C., Gombiner, J., 2018. West Antarctic sites for subglacial drilling to test for past ice-sheet collapse. The Cryosphere 12 (8), 2741–2757. Available from: https://doi.org/10.5194/tc-12-2741-2018.

Stammer, D., 2008. Response of the global ocean to Greenland and Antarctic ice melting. Journal of Geophysical Research: Oceans 113 (C6). Available from: https://doi.org/10.1029/2006JC004079.

Stap, L.B., Knorr, G., Lohmann, G., 2020. Anti-phased Miocene ice volume and CO_2 changes by transient antarctic ice sheet variability. Paleoceanography and Paleoclimatology 35 (11), e2020PA003971.

Stap, L.B., Sutter, J., Knorr, G., Stärz, M., Lohmann, G., 2019. Transient variability of the Miocene Antarctic ice sheet smaller than equilibrium differences. Geophysical Research Letters 46 (8), 4288–4298.

Stap, L.B., Van De Wal, R.S., De Boer, B., Bintanja, R., Lourens, L.J., 2017. The influence of ice sheets on temperature during the past 38 million years inferred from a one-dimensional ice sheet-climate model. Climate of the Past 13 (9), 1243–1257. Available from: https://doi.org/10.5194/cp-13-1243-2017.

Steinhauff, D.M., Webb, P.-N., 1987. Miocene foraminifera from DSDP site 272, Ross Sea. Geology 11, 578–582.

Steinthorsdottir, M., Coxall, H.K., de Boer, A.M., Huber, M., Barbolini, N., Bradshaw, C.D., et al., 2020. The Miocene: the future of the past. Paleoceanography and Paleoclimatology 35. Available from: https://doi.org/10.1029/2020PA004037e2020PA004037.

Stenni, B., Buiron, D., Frezzotti, M., Albani, S., Barbante, C., Bard, E., et al., 2011. Expression of the bipolar see-saw in Antarctic climate records during the last deglaciation. Nature Geoscience 4 (1), 46–49. Available from: https://doi.org/10.1038/ngeo1026.

Stocchi, P., et al., 2013. Relative sea-level rise around East Antarctica during Oligocene glaciation. Nature Geoscience 6, 380–384. Available from: https://doi.org/10.1038/ngeo1783.

Stocchi, P., Antonioli, F., Montagna, P., Pepe, F., Lo Presti, V., Caruso, A., et al., 2017. A stalactite record of four relative sea-level highstands during the Middle Pleistocene Transition. Quaternary Science Reviews 173, 92–100.

Stocker, T.F., 1998. The seesaw effect. Science 282 (5386), 61–62.

Stocker, T.F., Johnsen, S.J., 2003. A minimum thermodynamic model for the bipolar seesaw. Paleoceanography 18, 1087. Available from: https://doi.org/10.1029/2003PA000920.

Stokes, C.R., 2018. Geomorphology under ice streams: Moving from form to process. Earth Surface Processes and Landforms 43 (1), 85–123. Available from: https://doi.org/10.1002/esp.4259.

Struve, T., Pahnke, K., Lamy, F., Wengler, M., Böning, P., Winckler, G., 2020. A circumpolar dust conveyor in the glacial Southern Ocean. Nature Communications 11 (1), 1–11.

Sugden, D., Denton, G., 2004. Cenozoic landscape evolution of the Convoy Range to Mackay Glacier area, Transantarctic Mountains: onshore to offshore synthesis. Geological Society of America Bulletin 116 (7–8), 840–857.

Super, J.R., Thomas, E., Pagani, M., Huber, M., O'Brien, C., Hull, P.M., 2018. North Atlantic temperature and pCO_2 coupling in the early-middle Miocene. Geology 46 (6), 519–522. Available from: https://doi.org/10.1130/G40228.1.

Sutter, J., Fischer, H., Grosfeld, K., Karlsson, N.B., Kleiner, T., Van Liefferinge, B., et al., 2019. Modelling the Antarctic Ice Sheet across the mid-Pleistocene transition–implications for

Oldest Ice. The Cryosphere 13 (7), 2023–2041. Available from: https://doi.org/10.5194/tc-13-2023-2019.

Sutter, J., Gierz, P., Grosfeld, K., Thoma, M., Lohmann, G., 2016. Ocean temperature thresholds for last interglacial West Antarctic Ice Sheet collapse. Geophysical Research Letters 43 (6), 2675–2682. Available from: https://doi.org/10.1002/2016GL067818.

Tan, N., Ramstein, G., Dumas, C., Contoux, C., Ladant, J.B., Sepulchre, P., et al., 2017. Exploring the MIS M2 glaciation occurring during a warm and high atmospheric CO2 Pliocene background climate. Earth and Planetary Science Letters 472, 266–276. Available from: https://doi.org/10.1016/j.epsl.2017.04.050.

Tarasov, L., Peltier, W.R., 2002. Greenland glacial history and local geodynamic consequences. Geophysical Journal International 150, 198–229. Available from: https://doi.org/10.1046/j.1365-246X.2002.01702.x.

Tarasov, L., Peltier, W.R., 2003. Greenland glacial history, borehole constraints, and Eemian extent. Journal of Geophysical Research. 108, 1–20. Available from: https://doi.org/10.1029/2001JB001731.

Taylor-Silva, B.I., Riesselman, C.R., 2018. Polar frontal migration in the warm late Pliocene: Diatom evidence from the Wilkes Land margin, East Antarctica. Paleoceanography and Paleoclimatology 33 (1), 76–92. Available from: https://doi.org/10.1002/2017PA003225.

Teitler, L., Florindo, F., Warnke, D.A., Filippelli, G.M., Kupp, G., Taylor, B., 2015. Antarctic Ice Sheet response to a long warm interval across Marine Isotope Stage 31: a cross-latitudinal study of iceberg-rafted debris. Earth and Planetary Science Letters 409, 109–119.

The RAISED ConsortiumBentley, M.J., Cofaigh, C.O., Anderson, J.B., Conway, H., Davies, B., Graham, A.G., et al., 2014. A community-based geological reconstruction of Antarctic Ice Sheet deglaciation since the Last Glacial Maximum. Quaternary Science Reviews 100, 1–9. Available from: https://doi.org/10.1016/j.quascirev.2014.06.025.

Thiede, J., Jessen, C., Knutz, P., Kuijpers, A., Mikkelsen, N., Spielhagen, R.F., 2011. Millions of years of Greenland Ice Sheet history recorded in ocean sediments. Polarforschung 80 (3), 141–159.

Tierney, J.E., Zhu, J., King, J., Malevich, S.B., Hakim, G.J., Poulsen, C.J., 2020. Glacial cooling and climate sensitivity revisited. Nature 584, 569–573.

Tigchelaar, M., Timmermann, A., Pollard, D., Friedrich, T., Heinemann, M., 2018. Local insolation changes enhance Antarctic interglacials: Insights from an 800,000-year ice sheet simulation with transient climate forcing. Earth and Planetary Science Letters 495, 69–78. Available from: https://doi.org/10.1016/j.epsl.2018.05.004.

Tripati, A., Darby, D., 2018. Evidence for ephemeral middle Eocene to early Oligocene Greenland glacial ice and pan-Arctic sea ice. Nature Communications 9 (1), 1–11.

Turney, C.S., Fogwill, C.J., Golledge, N.R., McKay, N.P., van Sebille, E., Jones, R.T., et al., 2020. Early Last Interglacial ocean warming drove substantial ice mass loss from Antarctica. Proceedings of the National Academy of Sciences 117 (8), 3996–4006.

Turney, C.S., Jones, R.T., 2010. Does the Agulhas Current amplify global temperatures during super-interglacials? Journal of Quaternary Science 25 (6), 839–843. Available from: https://doi.org/10.1002/jqs.1423.

Tzedakis, P.C., Wolff, E.W., Skinner, L.C., Brovkin, V., Hodell, D.A., McManus, J.F., et al., 2012. Can we predict the duration of an interglacial? Climate of the Past 8, 1473–1485. Available from: https://doi.org/10.5194/cp-8-1473-2012.

Uemura, R., Motoyama, H., Masson-Delmotte, V., et al., 2018. Asynchrony between Antarctic temperature and CO_2 associated with obliquity over the past 720,000 years. Nature Communications 9, 96. Available from: https://doi.org/10.1038/s41467-018-03328-3.

Uenzelmann-Neben, G., 2006. Depositional patterns at Drift 7, Antarctic Peninsula: Along-slope versus down-slope sediment transport as indicators for oceanic currents and climatic conditions. Marine Geology 233 (1–4), 49–62.

Uenzelmann-Neben, G., Gohl, K., Larter, R., Schlüter, P., 2007. Differences in ice retreat across Pine Island Bay, West Antarctica, since the Last Glacial Maximum: Indications from multichannel seismic reflection data. US Geological Survey Open-File Report, 2007, srp084. <http://pubs.usgs.gov/of/2007/1047/srp/srp084/>. https://doi.org/10.3133/of2007-1047.srp084.

Uenzelmann-Neben, G., Gohl, K., 2012. Amundsen Sea sediment drifts: archives of modifications in oceanographic and climatic conditions. Marine Geology 299, 51–62.

Uenzelmann-Neben, G., Gohl, K., 2014. Early glaciation already during the Early Miocene in the Amundsen Sea, Southern Pacific: indications from the distribution of sedimentary sequences. Global and Planetary Change 120, 92–104.

Uenzelmann-Neben, G., 2019. Variations in ice-sheet dynamics along the Amundsen Sea and Bellingshausen Sea West Antarctic Ice Sheet margin. GSA Bulletin 131 (3–4), 479–498.

Villa, G., Lupi, C., Cobianchi, M., Florindo, F., Pekar, S.F., 2008. A Pleistocene warming event at 1 Ma in Prydz Bay, East Antarctica: evidence from ODP site 1165. Palaeogeography, Palaeoclimatology, Palaeoecology 260 (1–2), 230–244. Available from: https://doi.org/10.1016/j.palaeo.2007.08.017.

Villa, G., Persico, D., Wise, S.W., Gadaleta, A., 2012. Calcareous nanofossil evidence for Marine Isotope Stage 31 (1 Ma) in core AND-1B, ANDRILL McMurdo ice shelf project (Antarctica). Global and Planetary Change 96, 75–86.

von der Heydt, A.S., Dijkstra, H.A., van de Wal, R.S., Caballero, R., Crucifix, M., Foster, G.L., et al., 2016. Lessons on climate sensitivity from past climate changes. Current Climate Change Reports 2 (4), 148–158. Available from: https://doi.org/10.1007/s40641-016-0049-3.

Waelbroeck, C., Labeyrie, L., Michel, E., Duplessy, J.C., McManus, J.F., Lambeck, K., et al., 2002. Sea-level and deep water temperature changes derived from benthic foraminifera isotopic records. Quaternary Science Reviews 21 (1–3), 295–305. Available from: https://doi.org/10.1016/S0277-3791(01)00101-9.

WAIS Divide Project Members, 2015. Precise interpolar phasing of abrupt climate change during the last ice age. Nature 520 (7549), 661–665.

Wardlaw, B.R., Quinn, T.M., 1991. The record of Pliocene sea-level change at Enewetak atoll. Quaternary Science Reviews 10, 247–258. Available from: https://doi.org/10.1016/0277-3791(91)90023-N.

Warny, S., Askin, R.A., Hannah, M.J., Mohr, B.A., Raine, J.I., Harwood, D.M.SMS Science Team, 2009. Palynomorphs from a sediment core reveal a sudden remarkably warm Antarctica during the middle Miocene. Geology 37 (10), 955–958. Available from: https://doi.org/10.1130/G30139A.1.

Warrick, R.A., Le Provost, C., Meier, M.F., Oerlemans, J., Woodworth, P.L., 1996. In: Houghton, J.T., et al., (Eds.), Changes in sea level, in Climate Change1995: the science of climate change. Cambridge University Press, New York, pp. 361–405.

Watanabe, O., Jouzel, J., Johnsen, S., Parrenin, F., Shoji, H., Yoshida, N., 2003. Homogeneous climate variability across East Antarctica over the past three glacial cycles. Nature 422 (6931), 509–512. Available from: https://doi.org/10.1038/nature01525.

Weaver, A.J., Saenko, O.A., Clark, P.U., Mitrovica, J.X., 2003. Meltwater pulse 1A from Antarctica as a trigger of the Bølling-Allerød warm interval. Science 299 (5613), 1709–1713.

Weber, M.E., Clark, P.U., Kuhn, G., Timmermann, A., Sprenk, D., Gladstone, R., et al., 2014. Millennial-scale variability in Antarctic ice-sheet discharge during the last deglaciation. Nature 510 (7503), 134–138. Available from: https://doi.org/10.1038/nature13397.

Werner, M., Jouzel, J., Masson-Delmotte, V., Lohmann, G., 2018. Reconciling glacial Antarctic water stable isotopes with ice sheet topography and the isotopic paleothermometer. Nature Communications 9 (1), 1–10.

Westerhold, T., Marwan, N., Drury, A.J., Liebrand, D., Agnini, C., Anagnostou, E., et al., 2020. An astronomically dated record of Earth's climate and its predictability over the last 66 million years. Science 369 (6509), 1383–1387. Available from: https://doi.org/10.1126/science.aba6853.

Whitehead, J.M., Bohaty, S.M., 2003. Pliocene summer sea surface temperature reconstruction using silicoflagellates from Southern Ocean ODP Site 1165. Paleoceanography 18 (3).

Whitehead, J.M., Quilty, P.G., McKelvey, B.C., O'brien, P.E., 2006. A review of the Cenozoic stratigraphy and glacial history of the Lambert Graben-Prydz Bay region, East Antarctica. Antarctic Science . Available from: https://doi.org/10.1017/S0954102006000083.

Whitehead, J.M., Wotherspoon, S., Bohaty, S.M., 2005. Minimal Antarctic sea ice during the Pliocene. Geology 33 (2), 137–140. Available from: https://doi.org/10.1130/G21013.1.

Whitehouse, P.L., Bentley, M.J., Le Brocq, A.M., 2012b. A deglacial model for Antarctica: geological constraints and glaciological modelling as a basis for a new model of Antarctic glacial isostatic adjustment. Quaternary Science Reviews 32, 1–24. Available from: https://doi.org/10.1016/j.quascirev.2011.11.016.

Whitehouse, P.L., Bentley, M.J., Milne, G.A., King, M.A., Thomas, I.D., 2012a. A new glacial isostatic adjustment model for Antarctica: calibrated and tested using observations of relative sea-level change and present-day uplift rates. Geophysical Journal International 190 (3), 1464–1482.

Whitehouse, P.L., Bentley, M.J., Vieli, A., Jamieson, S.S., Hein, A.S., Sugden, D.E., 2017. Controls on last glacial maximum ice extent in the Weddell Sea embayment, Antarctica. Journal of Geophysical Research: Earth Surface 122 (1), 371–397. Available from: https://doi.org/10.1002/2016JF004121.

Whitehouse, P.L., 2018. Glacial isostatic adjustment modelling: historical perspectives, recent advances, and future directions. Earth Surface Dynamics 6 (2), 401–429.

Whitehouse, P.L., Gomez, N., King, M.A., Wiens, D.A., 2019. Solid Earth change and the evolution of the Antarctic Ice Sheet. Nature Communications 10 (1), 1–14. Available from: https://doi.org/10.1038/s41467-018-08068-y.

Wilson, D.J., Bertram, R.A., Needham, E.F., van de Flierdt, T., Welsh, K.J., McKay, R.M., et al., 2018. Ice loss from the East Antarctic Ice Sheet during late Pleistocene interglacials. Nature 561 (7723), 383–386. Available from: https://doi.org/10.1038/s41586-018-0501-8.

Wilson, D.J., et al., 2021. Pleistocene Antarctic climate variability: ice sheet–ocean–climate interactions. In: Florindo, F., et al. (Eds.), Antarctic Climate Evolution, second edition, Elsevier (this volume).

Wilson, D.S., Jamieson, S.S., Barrett, P.J., Leitchenkov, G., Gohl, K., Larter, R.D., 2012. Antarctic topography at the Eocene–Oligocene boundary. Palaeogeography, Palaeoclimatology, Palaeoecology 335, 24–34. Available from: https://doi.org/10.1016/j.palaeo.2011.05.028.

Wilson, D.S., Luyendyk, B.P., 2009. West Antarctic paleotopography estimated at the Eocene-Oligocene climate transition. Geophysical Research Letters 36, 16.

Wilson, D.S., Pollard, D., DeConto, R.M., Jamieson, S.S., Luyendyk, B.P., 2013. Initiation of the West Antarctic Ice Sheet and estimates of total Antarctic ice volume in the earliest Oligocene. Geophysical Research Letters 40 (16), 4305–4309. Available from: https://doi.org/10.1002/grl.50797.

Winnick, M.J., Caves, J.K., 2015. Oxygen isotope mass-balance constraints on Pliocene sea level and East Antarctic Ice Sheet stability. Geology 43 (10), 879–882. Available from: https://doi.org/10.1130/G36999.1.

Wise, M.G., Dowdeswell, J.A., Jakobsson, M., Larter, R.D., 2017. Evidence of marine ice-cliff instability in Pine Island Bay from iceberg-keel plough marks. Nature 550 (7677), 506–510.

Wise Jr., S.W., Schlich, R., et al., 1992. Proceedings of ODP, Science Results, Part 2, vol. 120. Ocean Drilling Program, College Station, TX, pp. 451–1155.

Wolff, E.W., Fischer, H., Fundel, F., Ruth, U., Twarloh, B., Littot, G.C., et al., 2006. Southern Ocean sea-ice extent, productivity and iron flux over the past eight glacial cycles. Nature 440 (7083), 491–496. Available from: https://doi.org/10.1038/nature04614.

Wu, L., Wilson, D.J., Wang, R., Passchier, S., Krijgsman, W., Yu, X., et al., 2021. Late Quaternary dynamics of the Lambert Glacier-Amery Ice Shelf system, East Antarctica. Quaternary Science Reviews 252, 106738.

Yan, Q., Zhang, Z., Wang, H., 2016. Investigating uncertainty in the simulation of the Antarctic ice sheet during the mid-Piacenzian. Journal of Geophysical Research: Atmospheres 121 (4), 1559–1574. Available from: https://doi.org/10.1002/2015JD023900.

Yokoyama, Y., Anderson, J.B., Yamane, M., Simkins, L.M., Miyairi, Y., Yamazaki, T., et al., 2016. Widespread collapse of the Ross Ice Shelf during the late Holocene. Proceedings of the National Academy of Sciences 113 (9), 2354–2359.

Zachos, J.C., Breza, J.R., Wise, S.W., 1992. Early Oligocene ice-sheet expansion on Antarctica: Stable isotope and sedimentological evidence from Kerguelen Plateau, southern Indian Ocean. Geology 20 (6), 569–573.

Zachos, J.C., Dickens, G.R., Zeebe, R.E., 2008. An early Cenozoic perspective on greenhouse warming and carbon-cycle dynamics. Nature 451 (7176), 279–283. Available from: https://doi.org/10.1038/nature06588.

Zachos, J.C., Kump, L.R., 2005. Carbon cycle feedbacks and the initiation of Antarctic glaciation in the earliest Oligocene. Global and Planetary Change 47 (1), 51–66.

Zachos, J., Pagani, M., Sloan, L., Thomas, E., Billups, K., 2001. Trends, rhythms, and aberrations in global climate 65 Ma to present. Science 292 (5517), 686–693. Available from: https://doi.org/10.1126/science.1059412.

Zhang, L., Hay, W.W., Wang, C., Gu, X., 2019. The evolution of latitudinal temperature gradients from the latest Cretaceous through the Present. Earth-Science Reviews 189, 147–158. Available from: https://doi.org/10.1016/j.earscirev.2019.01.025.

Zhang, Y.G., Pagani, M., Liu, Z., Bohaty, S.M., DeConto, R.M., 2013. A 40-million-year history of atmospheric CO_2. Philosophical Transactions of the Royal Society. A 371. Available from: https://doi.org/10.1098/rsta.2013.0096.

Further reading

Briggs, R.D., Tarasov, L., 2013. How to evaluate model-derived deglaciation chronologies: a case study using Antarctica. Quaternary Science Reviews 63, 109–127. Available from: https://doi.org/10.1016/j.quascirev.2012.11.021.

Holden, P.B., Edwards, N.R., Wolff, E.W., Valdes, P.J., Singarayer, J.S., 2011. The Mid-Brunhes event and West Antarctic ice sheet stability. Journal of Quaternary Science 26 (5), 474–477. Available from: https://doi.org/10.1002/jqs.1525.

Irvalı, N., Galaasen, E.V., Ninnemann, U.S., Rosenthal, Y., Born, A., Kleiven, H.F., 2020. A low climate threshold for south Greenland Ice Sheet demise during the Late Pleistocene. Proceedings of the National Academy of Sciences 117, 190–195.

Jacobs, S.S., Hellmer, H.H., Doake, C.S.M., Jenkins, A., Frolich, R.M., 1992. Melting of ice shelves and the mass balance of Antarctica. Journal of Glaciology 38 (130), 375–387. Available from: https://doi.org/10.3189/S0022143000002252.

Kageyama, M., Paul, A., Roche, D.M., Van Meerbeeck, C.J., 2010. Modelling glacial climatic millennial-scale variability related to changes in the Atlantic meridional overturning circulation: a review. Quaternary Science Reviews 29 (21–22), 2931–2956. Available from: https://doi.org/10.1016/j.quascirev.2010.05.029.

Kohfeld, K.E., Graham, R.M., De Boer, A.M., Sime, L.C., Wolff, E.W., Le Quéré, C., et al., 2013. Southern Hemisphere westerly wind changes during the Last Glacial Maximum: paleo-data synthesis. Quaternary Science Reviews 68, 76–95.

Masson-Delmotte, V., Buiron, D., Ekaykin, A., Frezzotti, M., Gallée, H., Jouzel, J., et al., 2011. A comparison of the present and last interglacial periods in six Antarctic ice cores. Climate of the Past 7, 397–423. Available from: https://doi.org/10.5194/cp-7-397-2011.

Milker, Y., Rachmayani, R., Weinkauf, M., Prange, M., Raitzsch, M., Schulz, M., et al., 2013. Global and regional sea surface temperature trends during Marine Isotope Stage 11. Climate of the Past 9 (5), 2231–2252. Available from: https://doi.org/10.5194/cp-9-2231-2013.

Miller, K.G., Mountain, G.S., Wright, J.D., Browning, J.V., 2011. A 180-million-year record of sea level and ice volume variations from continental margin and deep-sea isotopic records. Oceanography 24 (2), 40–53. Available from: https://www.jstor.org/stable/24861267.

Miller, K.G., Fairbanks, R.G., Mountain, G.S., 1987. Tertiary oxygen isotope synthesis, sea level history, and continental margin erosion. Paleoceanography 2 (1), 1–19. Available from: https://doi.org/10.1029/PA002i001p00001.

Passchier, S., 2011. Linkages between East Antarctic Ice Sheet extent and Southern Ocean temperatures based on a Pliocene high-resolution record of ice-rafted debris off Prydz Bay, East Antarctica. Paleoceanography 26 (4). Available from: https://doi.org/10.1029/2010PA002061.

Passchier, S., Ciarletta, D.J., Miriagos, T.E., Bijl, P.K., Bohaty, S.M., 2017. An Antarctic stratigraphic record of stepwise ice growth through the Eocene-Oligocene transition. GSA Bulletin 129 (3–4), 318–330.

Peltier, W.R., 2004. Global glacial isostasy and the surface of the ice-age Earth: the ICE-5G (VM2) model and GRACE. Annual Review of Earth and Planetary Sciences 32, 111–149. Available from: https://doi.org/10.1146/annurev.earth.32.082503.144359.

Rohling, E.J., Hibbert, F.D., Grant, K.M., Galaasen, E.V., Irvalı, N., Kleiven, H.F., et al., 2019. Asynchronous Antarctic and Greenland ice-volume contributions to the last interglacial sea-level highstand. Nature Communications 10 (1), 1–9. Available from: https://doi.org/10.1038/s41467-019-12874-3.

Shevenell, A.E., Kennett, J.P., Lea, D.W., 2004. Middle Miocene southern ocean cooling and Antarctic cryosphere expansion. Science 305 (5691), 1766–1770.

Smith, B., Fricker, H.A., Gardner, A.S., Medley, B., Nilsson, J., Paolo, F.S., et al., 2020. Pervasive ice sheet mass loss reflects competing ocean and atmosphere processes. Science 368 (6496), 1239–1242. Available from: https://doi.org/10.1126/science.aaz5845.

Stap, L.B., de Boer, B., Ziegler, M., Bintanja, R., Lourens, L.J., van de Wal, R.S., 2016. CO_2 over the past 5 million years: continuous simulation and new δ11B-based proxy data. Earth and Planetary Science Letters 439, 1–10. Available from: https://doi.org/10.1016/j.epsl.2016.01.022.

Strugnell, J.M., Pedro, J.B., Wilson, N.G., 2018. Dating Antarctic ice sheet collapse: Proposing a molecular genetic approach. Quaternary Science Reviews 179, 153–157. Available from: https://doi.org/10.1016/j.quascirev.2017.11.014.

Taviani, M., Reid, D.E., Anderson, J.B., 1993. Skeletal and isotopic composition and paleoclimatic significance of Late Pleistocene carbonates, Ross Sea, Antarctica. Journal of Sedimentary Research 63 (1), 84–90. Available from: https://doi.org/10.1306/D4267A96-2B26-11D7-8648000102C1865D.

Turney, C.S., Jones, R.T., Phipps, S.J., Thomas, Z., Hogg, A., Kershaw, A.P., et al., 2017. Rapid global ocean-atmosphere response to Southern Ocean freshening during the last glacial. Nature Communications 8 (1), 1–9. Available from: https://doi.org/10.1038/s41467-017-00577-6.

Vautravers, M.J., Hillenbrand, C.D., 2008. Deposition of planktonic forminifera on the Pacific margin of the Antarctic Peninsula (ODP Site 1101) during the last 1 Myr. Geophysical Research Abstracts 10.

Zecchin, M., Catuneanu, O., Rebesco, M., 2015. High-resolution sequence stratigraphy of clastic shelves IV: high-latitude settings. Marine and Petroleum Geology 68, 427–437. Available from: https://doi.org/10.1016/j.marpetgeo.2015.09.004.